IMPACT ASSESSMENT AND EVALUATION OF CLIMATOLOGICAL VARIATION ON VEGETATION COVER OF NAGALAND USING GEOSPATIAL TECHNIQUES

THESIS SUBMITTED IN PARTIAL FULFILLMENT OF THE REQUIREMENTS FOR THE DEGREE OF DOCTOR OF PHILOSOPHY

By TINTOLI A KUHO

PHD/GEO/00512

DEPARTMENT OF GEOGRAPHY
SCHOOL OF SCIENCES
NAGALAND UNIVERSITY, LUMAMI -798627
NAGALAND

OCTOBER 2025

IMPACT ASSESSMENT AND EVALUATION OF CLIMATOLOGICAL VARIATION ON VEGETATION COVER OF NAGALAND USING GEOSPATIAL TECHNIQUES

BY

TINTOLI A KUHO and

DR. KEDOVIKHO YHOSHÜ

Submitted

In partial fulfillment of the requirements for the

Degree of Doctor of Philosophy in Geography

of Nagaland University

NAGALAND UNIVERSITY

Dr. Kedovikho Yhoshü
Assistant Professor
Department of Geography
Nagaland University
Lumami-798627

Mobile: 8731896565
Email: kedovikho@nagalanduniversity.ac.in

CERTIFICATE

The thesis titled "Impact assessment and evaluation of climatological variation on vegetation cover of Nagaland using geospatial techniques" presented by Ms. Tintoli A Kuho, Ph.D. Research Scholar of the Department of Geography, Nagaland University bearing Registration No. Ph.D./GEO/00512, dated 26th October, 2021 embodies the results of investigations carried out by her under my supervision and guidance.

I certify that this work has not been presented for any degree elsewhere and that the candidate has fulfilled all conditions laid down by the University.

09/10/25

(Dr. Kedovikho Yhoshü)
(Supervisor)

Dr. Kedovikho Yhoshü
Asst. Professor
Department of Geography
Nagaland University, Lumami

Department of Geography
School of Sciences
(A Central University established by an Act of Parliament No. 35 of 1989)
(संसद द्वारा पाररत अधधधनयम 1989, क्रमांक 35 के अंतर्गत स्थाधपत केंद्रीय धिश्वधिद्यालय)
मुख्यालय : लुमामी | Headquarters : Lumami - 798627

DECLARATION BY THE CANDIDATE

NAGALAND UNIVERSITY
October, 2025

I, **TINTOLI A KUHO**, hereby declare that the subject matter of this Thesis is the record of work done by me, that the contents of this Thesis did not form basis of the award of any previous degree to me or to the best of my knowledge to anybody else, and that the thesis has not been submitted by me for any research degree in any other University/Institute.

This is being submitted to the Nagaland University for the degree of Doctor of Philosophy in Geography.

(TINTOLI A KUHO)

09/10/25

(DR. KEDOVIKHO YHOSHÜ)

Dr. Kedovikho Yhoshü
Asst. Professor
Department of Geography
Nagaland University, Lumami

09/10/2025

(Head of the Department)

HEAD
Department of Geography
Nagaland University, Lumami

Department of Geography
School of Sciences
(A Central University established by an Act of Parliament No. 35 of 1989)
(संसद द्वारा पाररत अधधधनयम 1989, क्रमांक 35 के अंतर्गत स्थाधपत केंद्रीय धिश्वधिद्यालय)
मुख्यालय : लुमामी | Headquarters : Lumami - 798627

PLAGIARISM SELF DECLARATION UNDERTAKING

Name of Research Scholar	TINTOLI A KUHO
Ph.D. Registration Number	PhD/GEO/00512
Title of Ph.D. thesis	Impact assessment and evaluation of climatological variation on vegetation cover of Nagaland using geospatial techniques
Name & Institutional Address of the Supervisor	Dr. Kedovikho Yhoshü Department of Geography, Nagaland University, Lumami Campus: 798627
Name of the Department & School	Department of Geography, School of Sciences, Nagaland University, Lumami Campus: 798627
Date of submission	09.10.2025
Date of plagiarism check	09.10.2025
Percentage of similarity detected	6%

I hereby declare / certify that the Ph.D. thesis submitted by me is complete in all respects, as per the guidelines of the Nagaland University for this purpose. I also certify that the thesis (soft copy) has been checked for plagiarism using DrillBit plagiarism detection software. It is also certified that the contents of the electronic version of the thesis are the same as the final hard copy of the thesis. A copy of the report generated by the DrillBit plagiarism detection software is also enclosed.

Date:

Place: (Name & Signature of the Scholar)

Name & Signature of the Supervisor with seal

Kedovikho 9/10/25
Dr. Kedovikho Yhoshü
Asst. Professor
Department of Geography
Nagaland University, Lumami

Department of Geography
School of Sciences
(A Central University established by an Act of Parliament No. 35 of 1989)
(संसद द्वारा पाररत अधधधनयम 1989, क्रमांक 35 के अंतर्गत स्थाधपत केंद्रीय धिश्वधिद्यालय)
मुख्यालय : लुमामी | Headquarters : Lumami - 798627

PLAGIARISM VERIFICATION CERTIFICATE

NAGALAND UNIVERSITY
October, 2025

This is to certify that the plagiarism check has been performed for Ph.D. Thesis "Impact assessment and evaluation of climatological variation on vegetation cover of Nagaland using geospatial techniques" submitted by Ms. TINTOLI A KUHO, under the Supervision of Dr. Kedovikho Yhoshü, Department of Geography, School of Sciences, Nagaland University. The check performed by the Scholar is found correct and authentic software DrillBit Plagiarism Detection Software has been used for the similarity check.

09/10/25

Name Signature & Seal of the Dean of the School

Dean
School of Sciences
Nagaland University
Hqrs. Lumami Nagaland

DrillBit

The Report is Generated by DrillBit Plagiarism Detection Software

Submission Information

Author Name	Tintoli A Kuho
Title	Impact Assessment and Evaluation of Climatological Variation on Vegetation Cover of Nagaland using Geospatial Techniques
Paper/Submission ID	4497293
Submitted by	kedovikho@nagalanduniversity.ac.in
Submission Date	2025-10-09 15:00:15
Total Pages, Total Words	180, 32037
Document type	Thesis

Result Information

Similarity **6 %**

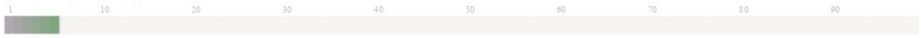

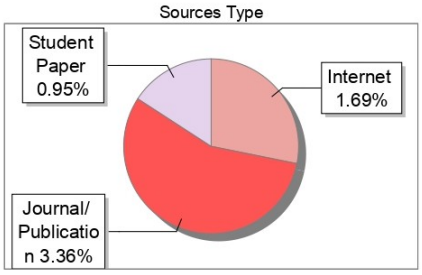

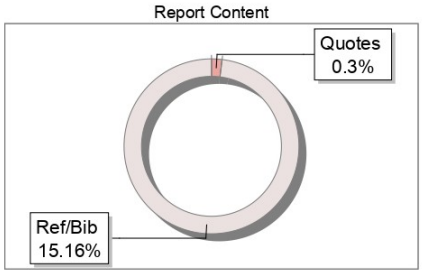

Exclude Information

Quotes	Excluded
References/Bibliography	Excluded
Source: Excluded < 4 Words	Excluded
Excluded Source	**0 %**
Excluded Phrases	Not Excluded

Database Selection

Language	English
Student Papers	Yes
Journals & publishers	Yes
Internet or Web	Yes
Institution Repository	Yes

A Unique QR Code use to View/Download/Share Pdf File

ACKNOWLEDGEMENT

First and foremost, I offer my deepest gratitude and glory to The Almighty God for His boundless grace, guidance, and strength throughout this journey. Without His blessings, none of this would have been possible.

This thesis is the result of the collective support, encouragement, and generosity of many individuals, to whom I am profoundly grateful.

I extend my heartfelt thanks to my parents for their unwavering love, sacrifices, and steadfast encouragement. Their support has been the cornerstone of my academic journey, and I remain forever indebted to them.

I am equally thankful to my siblings, Villy, Sushikali, and Limitoli, along with my extended family, Ajay and Azro, and my close friends. Their quiet strength and belief in me have carried me through moments of challenge and doubt.

A special note of gratitude goes to my relatives, Imkongmar Bethel and family, for their continuous and gracious support. By providing me a home throughout the duration of my research, they created a space of comfort, peace, and belonging. Their generosity made a profound difference in my ability to focus and persevere.

To my colleagues and peers, thank you for the shared knowledge, stimulating conversations, and camaraderie that enriched this journey. I am especially grateful to my fellow scholars, Rokovotso Nagi, Midlerthanglian Leivon, Sentinungba, Yoh Veswu, and Langsuanpao (Reuben) Seldou, for their readiness to assist and for making my research experience more manageable and collaborative. Their camaraderie and practical support not only eased the demands of this journey but also enriched it with shared purpose and friendship.

I sincerely thank the faculty of the Department of Geography for their invaluable guidance, encouragement, and support at every stage of my research. Their insights have been instrumental in shaping this work.

I extend my sincere appreciation to all the staff of the Forest and Biodiversity Management in the Himalaya (Nagaland) Project for their consistent encouragement and support which have greatly enriched my research experience and contributed meaningfully to the progress of this work.

I also acknowledge the Department of Soil and Water Conservation, Kohima, Nagaland, for providing the meteorological data used in this study. Their contribution was vital to the completion of this research.

Above all, I am especially grateful to my supervisor, Dr. Kedovikho Yhoshü, for his unwavering mentorship, insightful feedback, and steady guidance. His support has been pivotal in shaping both this thesis and my growth as a researcher. I believe that his thoughtful supervision not only strengthened the academic rigor of this work but also nurtured my confidence, independence, and clarity of purpose. I am particularly thankful for the trust he placed in me, which empowered me to undertake fieldwork in unfamiliar terrains and contexts. His encouragement created a space for growth, allowing me to explore new landscapes, develop practical skills, and deepen my understanding of ecological research beyond my research topic. I am truly fortunate to have had the opportunity to learn under his guidance, and I carry forward his example of integrity, humility, and dedication to knowledge.

Finally, I extend my sincere appreciation to all those who, in ways both big and small, contributed to this journey. Your kindness and generosity have left an enduring impact.

(TINTOLI A KUHO)

TABLE OF CONTENTS

LIST OF FIGURES

LIST OF TABLES

CHAPTER 1

IMPACT ASSESSMENT AND EVALUATION OF CLIMATOLOGICAL VARIATION ON VEGETATION COVER OF NAGALAND USING GEOSPATIAL TECHNIQUES

Chapter 1: Introduction

1.1. Climatological Variations and Its Impacts on Vegetation Cover

Vegetation cover is typically described as the percentage of ground surface that is occupied by the vertical projection of aboveground plant parts. This measure excludes roots and other belowground components, and it does not consider overlaps among individuals of the same species. Within ecological and applied studies, vegetation cover is widely recognized as a practical parameter for assessing the dominance of species, the prevalence of plant functional groups, or the overall extent of canopy closure. Compared to indicators such as plant density or productivity, cover is often more reliable. Density does not capture the variability in plant size, while productivity can be difficult to estimate, particularly in species that grow clonally or in colonies where individual plants are hard to distinguish (Dietz & Steinlein, 2002).

Vegetation cover represents a vital element of terrestrial ecosystems and is often regarded as a key indicator of ecological health and stability. It performs multiple functions, including regulating local and global climates, sustaining biodiversity, and driving essential ecological processes such as carbon storage, nutrient cycling, and soil protection. In addition, vegetation provides food and shelter for a wide range of species, underscoring its importance for biodiversity conservation. Because of these interconnected roles, alterations in vegetation cover can trigger cascading effects on regional climate systems, water cycles, and overall ecosystem balance. This makes vegetation dynamics a crucial subject of investigation within the broader framework of global environmental change. To promote sustainable resource management and effective conservation strategies, it is necessary to examine the underlying drivers of vegetation change, with particular attention to the influence of climate variability, anthropogenic pressures, and their combined impacts (Sun & Zhang, 2024). Vegetation also mirrors the environment in which it grows. The health, structure, and distribution

of plant communities reflect local conditions and can be tracked across landscapes using modern observation tools, including remote sensing (Liang *et al.*, 2024). Over time, however, vegetation has been profoundly altered by human activities such as land-use change, deforestation, altered fire regimes, and the spread of invasive species, alongside the growing pressures of climate change (Franklin *et al.*, 2016).

Unlike the slower impacts of climate change, shifts caused by land use and disturbance can occur more immediately and often leave long-lasting effects on ecosystems. The transformation of natural habitat into agriculture, infrastructure and urban areas is considered as one of the main drivers of the decline in vegetation cover and its associated biodiversity with approximately three-quarters of the terrestrial biosphere altered by human activities and the impact of these alterations on biodiversity expected to increase this century (Pan *et al.*, 2021). Human activities such as mining, deforestation, urban expansion, and agriculture have significantly reshaped Earth's physical and biological systems, producing visible changes across the biosphere, hydrosphere, lithosphere, and atmosphere. These alterations not only transform landforms but also disrupt ecological processes and contribute to regional climate variability (Vishvendra Raj Singh *et al.*, 2024). At the same time, climate change has intensified shifts in vegetation cover, undermining its critical role in regulating the exchange of energy, water, and carbon between the land surface and the atmosphere (Dastour & Hassan, 2024).

To understand these processes more clearly, it is necessary to quantify how climatic factors, such as temperature, rainfall, and humidity, shape vegetation attributes including composition, distribution, and seasonal dynamics. Establishing these empirical relationships provides valuable insight into ecosystem functioning (Dastour & Hassan, 2024). Changes in vegetation are widely regarded as indicators of environmental change, influenced by both natural climatic variability and human disturbance. Recent studies highlight that depending on the level of human intervention, vegetation has either degraded or

shown signs of recovery, with significant implications for biodiversity (Yin *et al.*, 2023).

The distribution and functioning of terrestrial ecosystems are closely tied to climate, though moderated by additional factors such as soil quality, water availability, nutrient status, and faunal interactions (Kalisa *et al.*, 2019). Vegetation itself is a fragile yet dynamic component of these systems, simultaneously shaped by and exerting influence on surrounding environmental factors, creating a feedback loop. It plays a pivotal role in regulating local climates, enhancing soil development, and providing essential habitat for wildlife. Consequently, vegetation dynamics are often viewed as reliable indicators of ecosystem condition (Debinski *et al.*, 2000). With the progression of climate change, the frequency of extreme weather events and the intensity of rainfall have already risen worldwide, a trend projected to intensify further in the coming decades. These climatic fluctuations are continuously reshaping terrestrial ecosystems, bringing about structural and functional changes (Chen, 2020).

1.2. Vegetation Response to Climatological Factors in India

India, the most populous country in the world, represents a critical region for assessing vegetation change and its drivers, with such knowledge being essential for developing policies that ensure long-term sustainability (Banerjee *et al.*, 2024). Forests, which cover nearly 20% of India's geographical area, constitute a significant portion of its vegetation. Modeling studies suggest that climate change may drive major shifts in vegetation distribution, with the BIOME4 model predicting that 77% and 68% of forested grids in India could undergo transformations in forest type due to changing climatic conditions. These shifts pose serious risks not only to ecosystems but also to communities that rely on forests for food, fuel, and livelihoods (Gopalakrishnan *et al.*, 2011).

Ecologically, India's forests are highly diverse, ranging from temperate needle-leaf and broadleaf forests of the Himalayas to the tropical evergreen forests of the

Western Ghats. Much of central India is dominated by dry deciduous teak and sal forests, while other areas support scrub-thorn vegetation, grasslands such as those surrounding the Nilgiri shola, and anthropogenic grasslands shaped by shifting cultivation and land management. The drier regions of central and western India also contain savannas, while large-scale single-species plantations of teak, eucalyptus, and pine, many established during colonial and post-colonial periods, add to the mosaic of forest types across the subcontinent (Lele & Krishnaswamy, 2019).

In the North Eastern Region (NER) of India, variations in monsoon rainfall attributed to changing climatological conditions have led to unusual drought occurrences. Despite being categorized as a humid zone with historically rare drought events (one in 15 years), the region experienced consecutive drought years in 2005 and 2006, with the probability of drought occurrence estimated at 54% compared to 27% in Western India between 2000 and 2014. Climate variability in Northeast India biodiversity hotspot has been shown to affect both vegetation and agricultural productivity, with implications for livelihoods and food security (Saitluanga *et al.*, 2021). In 2009, all seven northeastern states, including Nagaland, faced severe drought impacts (Parida & Oinam, 2015). Records from the Nagaland State Disaster Management Authority (NSDMA) further highlight deficient rainfall during 2009 and 2013, with deficits of 32%, 60%, 30%, and 58% in monsoon rainfall recorded for the years 2012, 2013, 2014, and 2015, respectively (GoI, 2015; Nongbri *et al.*, 2019).

Long-term analyses of rainfall patterns conducted by the Indian Meteorological Department (IMD) for the period 1989–2017 reveal a statistically significant declining trend in both seasonal and annual rainfall (Guhathakurta *et al.*, 2020). This suggests an increasing likelihood of drought conditions in the future. For Nagaland, such negative climatic shifts have become recurrent, with several districts reporting severe monsoon deficits over the past decade, a situation expected to intensify in the coming years (Jamir *et al.*, 2013). With the projected rise in global average temperatures, extreme climate-driven events such as

droughts and floods are anticipated to become more frequent. Moreover, recent studies confirm that southwest monsoon rainfall over the NER has steadily declined compared to the 1980s and 1990s, causing the region to experience frequent and unprecedented drought episodes, surpassing even those observed in Western India (Parida & Oinam, 2015).

1.3. Remote Sensing and GIS in Climate-Vegetation Studies

The magnitude of the impact of the extreme climatic events on vegetation cover can be quantified using different indices with the help of parameters like rainfall, streamflow, evaporation, soil-moisture, groundwater level, vegetation health, etc., depending on the nature of the investigation (Krishnan & Ct, 2016; Khetwani & Singh, 2019). However, traditional methods are not fully capable to assess and monitor them as the methods are limited to a region, often gives inaccurate measures and it is hard to get the near real-time data to predict and quantify them (Arun Kumar *et al.*, 2021). Thus, satellite remote sensing has become fundamentally essential in timely detection and monitoring of spatial variations in vegetation cover due to timely availability of spatio-temporal data. Assessment and management can also be done more accurately with the help of innovations in geospatial techniques (Parida & Oinam, 2015; Krishnan & Ct, 2016). In the recent years, monitoring has improved significantly using satellite vegetation health products, ground-based and satellite precipitation observations, soil moisture data, and other numerical model simulations (Hosseini-Moghari *et al.*, 2020). This can help in timely assessment and monitoring of vegetation condition that will benefit in preparedness, relief and mitigation and reduce the damage of climatological impacts to the environment, economy and society (Su *et al.*, 2017).

Sánchez *et al.*, 2018 stated that among remote sensing-based methods, several studies are based on the condition indices, versions of them or a synthetic integration of them. These indices have normalized the remotely sensed variable based on its absolute minimum and maximum temporal values for each pixel. The following indices are often used for describing drought events: Normalised Difference Vegetation Index (NDVI), Anomaly Vegetation Index (AVI),

Vegetation Condition Index (VCI), Normalised Difference Water Index (NDWI), Standardised Precipitation Index (SPI), Palmer Drought Severity Index (PDSI), Evapotranspiration Deficit Index (ETDI), Standardised Precipitation and Evaporation Index (SPEI) and Vegetation Supplication Water Index based on visible, near infrared, shortwave reflectance data for partly and fully covered surface, Temperature Vegetation Dryness Index, Temperature Condition Index, Crop Water Stress Index and Water Deficit Index based on thermal infrared remote sensing data.

Dunham *et al.*, 2005 used multi-temporal satellite imagery to monitor the response of vegetation to drought in the Great Lakes Region. In this study, the relationship between the Palmer Drought Severity Index (PDSI) and different vegetation types through the derivation of vegetation indices from Landsat 7 ETM+ data (NDVI, Tasseled Cap, and SAVI) was studied. Although NDVI was found to be a robust indicator of vegetation greenness and vigour, it was not the best index to use for the study, depending on the type of vegetation studied and the scale of analysis used. The study further recommended a combination of NDVI and other prominent vegetation indices that can be used to detect subtle drought conditions by specifically identifying various time lags between climate condition and vegetation response.

Pei *et al.*, 2021 used NDVI for the study in MLR-YR (middle and lower reaches of Yangtze River). This study was performed to detect of extreme precipitation change impact on the vegetation. On terrestrial vegetation, it was found that changes in extreme precipitation intensity coincided with that of the vegetation activity, which was well represented by the maximum and the minimum NDVIs, especially the maximum NDVI.

Li *et al.*, 2021 studied Vegetation Changes in response to climatic factors and human activities in Jilin Province, China, 2000–2019. This study found that the NDVI of different vegetation cover types is increasing, indicating that the vegetation is continuously greening. Precipitation was found to be the main positive controlling climatic factor of NDVI in the western regions of the study area, while average temperature was found to be the main factor in the eastern regions. Precipitation was found to be the main climatic control factor for

grassland and cropland, while forest land was limited by precipitation and average temperature. Barren land and permanent wetland showed slightly negatively correlation with precipitation. Overall, from 2000 to 2019, the residual values for NDVI increased from −0.0121 to 0.0116, and the impact of human activities on vegetation changed from negative to positive and by 2019, the proportion of positively affected zones was as high as 94.01%, and the negatively affected zones were mainly distributed across transitional areas of cropland and grassland, and urban and built-up land and forest land.

Nabizada *et al.*, 2022 for their study on vegetation for the eastern basins of Afghanistan for the period from 2000 to 2021 used data from the Moderate Resolution Imaging Spectroradiometer (MODIS), Global Precipitation Measurement Mission (GPM), and Land Data Assimilation System (GLDAS) to examine the impact of meteorological parameters. The study utilized several indices, such as Precipitation Condition Index (PCI), Temperature Condition Index (TCI), Soil Moisture Condition Index (SMCI), and Microwave Integrated Drought Index (MIDI). The relationships between meteorological quantities, drought conditions, and vegetation variations were examined by analysing the anomalies and using regression method. The results showed that the years 2000, 2001, and 2008 had the lowest vegetation coverage (VC), 2010, 2013, 2016, and 2020 had the highest VC.High correlations between VC, soil moisture and precipitation were found, whereas no significant correlation was found between VC and drought index MIDI.

Dikici, 2022 used Normalized Difference Vegetation Index (NDVI) and the Vegetation Condition Index (VCI) for Drought Analysis of the Seyhan Basin which revealed that climate change and drought showed increasing linear uptrend which was due to the decline of forestland and agricultural areas in the study area basin.

Rousta *et al.*, 2022 used NDVI, ET, and LST satellite images collected by moderate resolution imaging spectro-radiometer and tropical rainfall measuring mission sensors to investigate seasonal and yearly vegetation dynamics, and also the influence of climatological factors on it, in the area of the Caspian Sea Watersheds for 2001-2019. The indices retrieved from remote sensing for the

period 2001-2019 indicated a considerable inter-seasonal and inter-annual variability, but no significant increasing/ decreasing trends were found in the studied indices during 2001-2019. ET, precipitation and LST explained about 75% of the yearly and spring vegetation coverage variation.

Vegetation monitoring through satellite based information has been widely acknowledged in recent years for its low cost, synoptic view, repeated data acquisition and reliability. Additionally, remote sensing has a tremendous ability to provide comprehensive data coverage over a large region with a varied spatial resolution from a few centimetres to a few kilometres (Arun Kumar *et al.*, 2021). Due to these advantages, Remote Sensing/Geospatial approach has been widely encouraged by various researches, time and again, while developing and formulating new methods to overcome the drawbacks or improve the setbacks that are faced with the use of this approach. Thus, this study aims to study the impact of climatological impact on vegetation cover of Nagaland incorporating the integration of remotely sensed data and other geospatial ground data. The result in turn can help in various mitigation measures and ultimately assist in sustainable management of land.

1.4. Problem Statement

Nagaland, situated in the Indo-Burma biodiversity hotspot, is a part of the Eastern Himalaya which is vulnerable to climate change (Chatterjee *et al.*, 2006; Meru & Pandey, 2024). It is one such state where human-induced land transformations which have led to significant ecological stress. The hotspot harbors rich vegetation cover that is ecologically and socioeconomically vital. However, it is increasingly vulnerable to irregular monsoons, rising temperatures, forest fires, and unsustainable land-use practices such as shifting cultivation and urban expansion (Sinha & Modak, 2023). Although studies from other Indian states have integrated geospatial approaches to analyze climate–vegetation interactions (Kumar *et al.*, 2025), similar assessments are scarce for Nagaland, where ecosystems are both fragile and highly sensitive to change.

This lack of comprehensive, geospatially based studies creates a critical knowledge gap. Without a clear understanding of how climate variability influences vegetation cover in Nagaland, policy makers and local stakeholders face challenges in developing effective conservation, land management, and climate adaptation strategies. Therefore, the problem addressed in this study is the absence of integrated assessments that evaluate vegetation cover dynamics in response to climatic variations using remote sensing and geospatial techniques in Nagaland.

1.5.Research Gap

Existing studies have shown that vegetation dynamics are highly sensitive to climatic drivers such as precipitation and temperature (Franklin *et al.*, 2016; Pan *et al.*, 2021; Dastour & Hassan, 2024), as well as to anthropogenic pressures including deforestation, shifting cultivation, and land-use change (Vishvendra Raj Singh *et al.*, 2024). Remote sensing and geospatial techniques have been widely employed across India and other regions to assess vegetation responses to climate variability and land-use change, particularly in states such as Jharkhand, Rajasthan, and parts of Western India (Kumar *et al.*, 2025). These studies have effectively demonstrated how climate variability influences vegetation health, productivity, and distribution at regional scales.

Despite Nagaland's ecological significance as part of the Indo-Burma biodiversity hotspot and its position within one of Northeast India's most sensitive landscapes, there is a notable lack of integrated research linking vegetation cover dynamics with climate variability in the state. Earlier studies in Northeast India have largely concentrated on agricultural productivity and biodiversity conservation (Saitluanga *et al.*, 2021; Sinha & Modak, 2023), but few have systematically applied geospatial approaches to examine long-term vegetation patterns in Nagaland. This gap is particularly pressing as the state, with its diverse topography and socio-ecological systems, has been undergoing rapid land cover transformations. Accelerated urbanization, unplanned land-use practices, resource extraction, deforestation, and recurrent natural hazards such as

landslides, forest fires, and flash floods have further exacerbated ecosystem pressures in recent decades (Ritse *et al.*, 2020; Ayemi & Kar, 2020; Yhoshu & Krishnaiah, 2020; Mao & Gogoi, 2010).

Moreover, the combined impacts of climatic variability and human-induced land-use changes on vegetation cover in Nagaland remain insufficiently quantified. This knowledge gap generates uncertainty in identifying the key drivers of vegetation degradation or recovery, thereby constraining the capacity of policymakers and stakeholders to design effective conservation, adaptation, and land-use management strategies.

Therefore, the research gap lies in the absence of comprehensive, geospatially driven studies that explicitly assess the interactions between climate variability and human activities in shaping vegetation cover in Nagaland. To address this gap, the present study focuses on assessing the impact of climatological variations on vegetation dynamics in Nagaland, using an integrated approach that combines remotely sensed data with geospatial ground-based information. Filling this gap is essential for generating actionable insights that can enhance ecosystem resilience, guide effective conservation planning, and support sustainable land and resource management in the region. The findings of this study are expected to inform mitigation strategies and contribute to the sustainable management of vegetation and land resources, ensuring both ecological and socio-economic benefits.

1.6.Objectives of the Study

The following objectives were planned for the study:

A. To study the rainfall variation and its impact on the vegetation cover in the study area.
B. To identify and perform vegetation analysis using the recent trends in geospatial indices by integration of remotely sensed data.
C. To evaluate the change in vegetation cover in response to climatological factors.

1.7.Data and Methodology

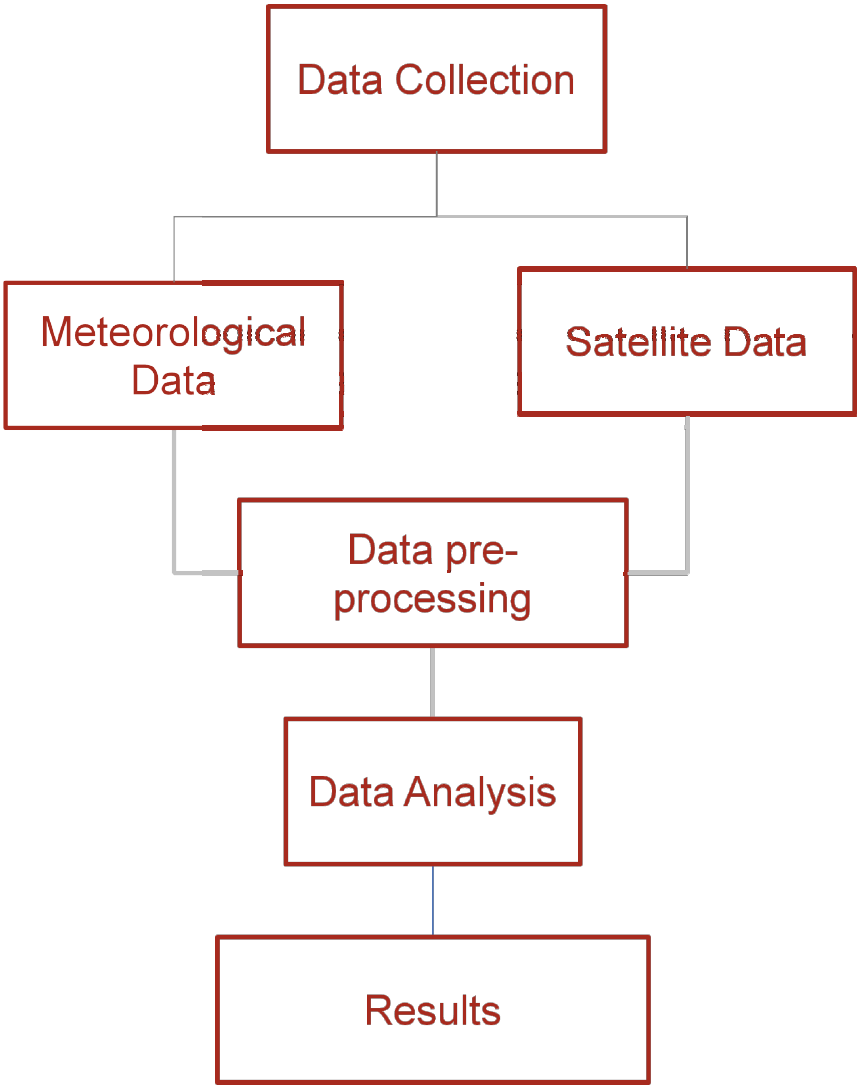

Figure 1 Overall Methodology flowchart.

1.7.1. Climate Data (Rainfall, Temperature)

In the present study, two climatological parameters, i.e., rainfall (precipitation) and temperature were analyzed. The climate data were obtained from the Department of Soil and Water Conservation, Nagaland, covering 17 meteorological stations across the state. Details of these stations are provided in the following table.

Table 1 Details for the Meteorological Stations across Nagaland.

Sl. No.	Location of the Observatory	Latitude (Approx)	Longitude (Approx.)	Altitude in m (M.S.L.)	Year of Installation
1	Kohima	25° 39' 00"	94° 07' 00"	1420	1981
2	Mon	26° 42' 00"	95° 01' 30"	734	1993
3	Wokha	26° 05' 45"	94° 15' 45"	1360	1995
4	Jalukie	25° 39' 00"	93° 40' 10"	415	1995
5	Meluri	25° 41' 30"	94° 38' 00"	1350	1995
6	Phek	25° 43' 30"	94° 28' 00"	1360	1996
7	Kiphire	25° 58' 00"	94° 47' 00"	1195	1998
8	Sechü	25° 43' 15"	94° 05' 30"	1094	1998
9	Bhandari	26°16' 45"	94° 07' 30"	703	1998
10	Zunheboto	26° 34' 00"	94° 31' 25"	1780	2001
11	Dimapur	25° 49' 40"	93° 41' 15"	160	2002
12	Mokokchung	26°19' 30"	94° 31' 00"	1180	2004
13	Tseminyu	25° 55' 20"	94° 13' 15"	1200	2005
14	Mangkolemba	26° 29' 45"	94° 38' 10"	661	2005
15	Tuensang	26° 13' 84"	94° 48' 71"	1633	2006
16	Shamator	26° 02' 23"	94° 52' 34"	1768	2014
17	Longleng	26° 29' 20"	94° 46' 10"	1200	2016

Data such as Average Bar Temperature, Average Max Temperature, Average Minimum Temperature, Average Minimum Temperature, Average Dew Point, Average R/H %, Rainfall in mm, Number of Days of Precipitation (>0mm), Number of rainy days (>2.5mm) were also provided. Rainfall data were recorded in millimeters (mm), while temperature data were recorded in degrees Celsius (°C) in monthly averages, spanning from the year of each station's installation up to 2021. All these data were formatted in Microsoft Excel for further analysis. It was noted that there were days when the Weather Station data was lacking for certain years/months post installation and those records were given as not available (NA) but the values were averaged out for further analysis.

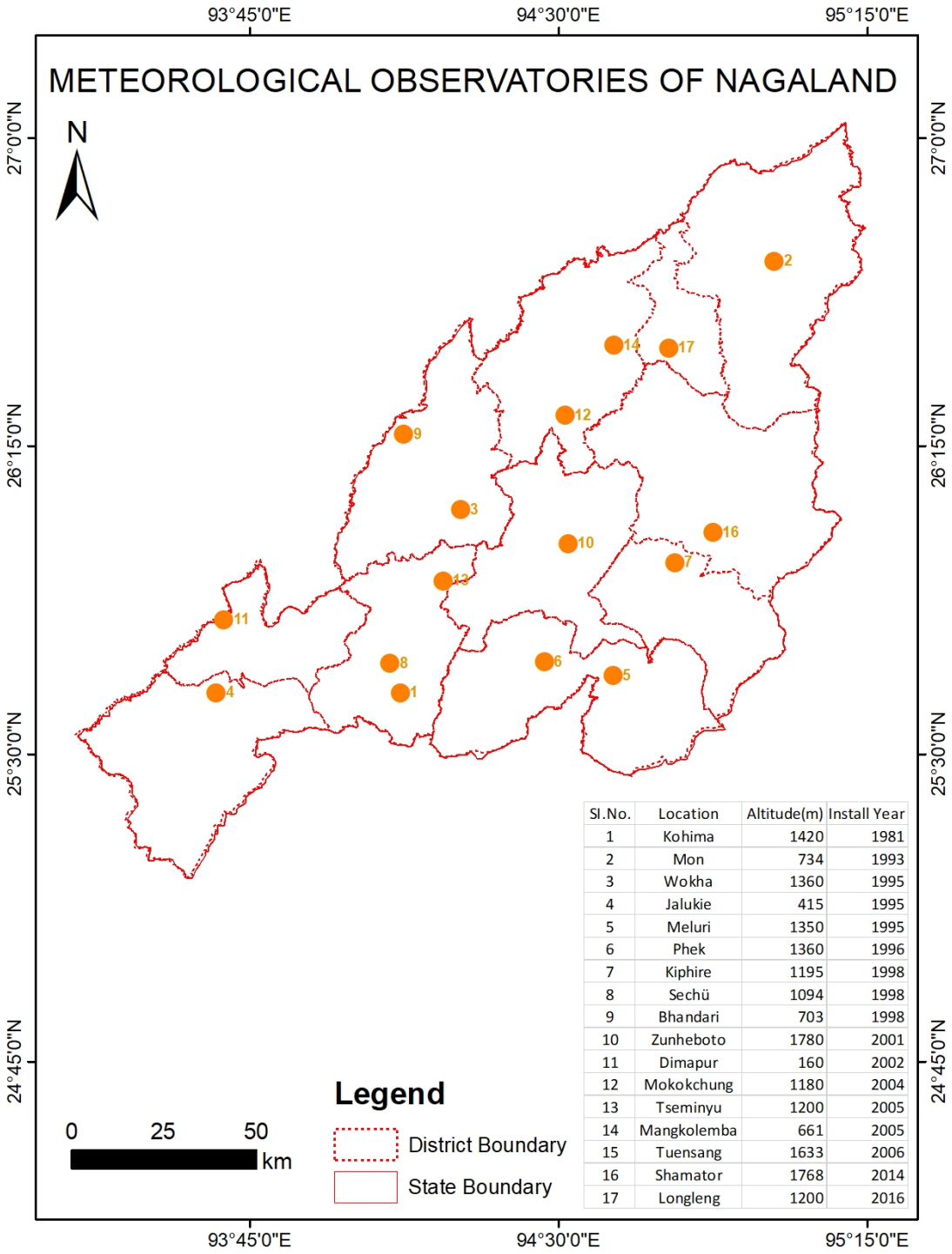

Figure 2 Meteorological Observatories in the study area.

1.7.2 Remote Sensing Data (Landsat 5TM, Landsat 8 OLI)

This study utilized satellite-based remote sensing data to assess the vegetation condition across selected landscapes in Nagaland. Specifically, passive remote sensing sensors with optical multispectral imagery viz. Landsat 5 Thematic Mapper (TM) and Landsat 8 Operational Land Imager (OLI) datasets were downloaded from United States Geological Survey (USGS) website, https://earthexplorer.usgs.gov/ employed to derive the geospatial indices and other ecological parameters relevant to long-term monitoring. To ensure that there was a consistent season of analysis, the data was acquired during the cloud-free months of November to February. However, in years where no cloud-free data available, cloud removal was done using cloud masking through image thresholding. The data was obtained for the following years. In order to obtain data for the whole state, data for four scenes viz. 135/041, 135/042,134/042,135/043 were downloaded for entire coverage.

Table: Details for the dates of satellite pass used in the present study

Year	Date of Pass	Data
2000	22-Feb-2000	Landsat 5TM
2006	06-Feb-2006	Landsat 5TM
2011	04-Feb-2011	Landsat 5TM
2013	24-Nov-2013	Landsat 8OLI
2018	08-Dec-2018	Landsat 8OLI
2023	20-Jan-2023	Landsat 8OLI

- **Landsat 5 TM**: Acquired from the USGS Earth Explorer platform, Landsat 5 TM data were used to represent historical conditions, particularly for the years prior to 2013, from 2000 onwards. The sensor provides seven spectral bands with a spatial resolution of 30 meters for visible, near-infrared, and shortwave infrared bands, and 120 meters for the thermal band (resampled to 30 meters) as detailed in the following table. These data were instrumental in establishing baseline data and detecting long-term changes of the study area.

Table 2 Details of specifications of Landsat 5TM bands

Bands	Wavelength (micrometers)	Resolution (meters)
Band 1 - Blue	0.45-0.52	30
Band 2 - Green	0.52-0.60	30
Band 3 - Red	0.63-0.69	30
Band 4 - Near Infrared (NIR)	0.76-0.90	30
Band 5 - Shortwave Infrared (SWIR) 1	1.55-1.75	30
Band 6 - Thermal	10.40-12.50	120 (resampled to 30)*
Band 7 - Shortwave Infrared (SWIR) 2	2.08-2.35	30

* Indicates that acquired data are resampled for Level-1 product processing

- **Landsat 8 OLI**: For more recent assessments, Landsat 8 OLI data were utilized, also sourced from USGS Earth Explorer. The OLI sensor offers improved radiometric resolution and includes nine spectral bands, with a 30-meter spatial resolution for multispectral bands and 15 meters for the panchromatic band. These datasets were selected for their consistency, cloud-free coverage, and suitability for vegetation health analysis.

Table 3 Details of specifications of Landsat 8 OLI bands.

Bands	Wavelength (micrometers)	Resolution (meters)
Band 1 - Coastal aerosol	0.43-0.45	30
Band 2 - Blue	0.45-0.51	30
Band 3 - Green	0.53-0.59	30
Band 4 - Red	0.64-0.67	30
Band 5 - Near Infrared (NIR)	0.85-0.88	30
Band 6 - Shortwave Infrared (SWIR) 1	1.57-1.65	30
Band 7 - Shortwave Infrared (SWIR) 2	2.11-2.29	30
Band 8 - Panchromatic	0.50-0.68	15
Band 9 - Cirrus	1.36-1.38	30
Band 10 - Thermal Infrared (TIRS) 1	10.6-11.19	100 (resampled to 30)*
Band 11 - Thermal Infrared (TIRS) 2	11.50-12.51	100 (resampled to 30)*

* Indicates that acquired data are resampled for Level-1 product processing

1.7.3 Ancillary Data (LULC)

The Land-use Land-cover (LULC) data was prepared using imagery from the Indian Remote Sensing (IRS) satellite series, specifically the Linear Imaging Self-Scanning Sensors, LISS-III (Green, Red, NIR, SWIR) and LISS-IV (Green, Red, NIR). LISS-III data have been available since 1995, beginning with IRS-1C, and were extensively used from 2008 onward via the National Remote Sensing Centre (NRSC). LISS-III provides multispectral imagery at a spatial resolution of 23.5 meters, suitable for regional-scale vegetation and land-use analysis. LISS-IV, operational since 2003 onboard IRS-P6 (Resourcesat-1), offers higher-resolution imagery at 5.8 meters, ideal for fine-scale mapping of ecological features. Both datasets were sourced from NRSC's Bhuvan portal (https://bhoonidhi.nrsc.gov.in/bhoonidhi/index.html) and selected based on seasonal relevance and cloud-free conditions. Preprocessing included geometric correction, radiometric normalization, and resampling to ensure compatibility with Landsat imagery and consistency across temporal analyses. For the more recent LULC data, this study also utilized imagery from the Sentinel-2A satellite, equipped with the Multispectral Instrument (MSI). Sentinel-2A is part of the European Space Agency's Copernicus Programme and has been operational since June 2015. The MSI sensor captures data across 13 spectral bands, ranging from visible and near-infrared (VNIR) to shortwave infrared (SWIR), with spatial resolutions of 10 m, 20 m, and 60 m**,** depending on the band as shown in the following table. Sentinel-2A MSI data were sourced from the Copernicus Open Access Hub (), selected based on cloud-free conditions and seasonal relevance. Preprocessing steps included atmospheric correction**,** cloud masking**,** and resampling to harmonize with other datasets used in the study. The high revisit frequency of (when 5 days) ensured timely and consistent coverage, especially valuable in regions prone to cloud cover during monsoon months.

Table 4 Details of specifications of Sentinel 2A MSI bands.

Band	Center wavelength (nm)	Native resolution
B1 Coastal aerosol	443	60 m
B2 Blue	490	10 m
B3 Green	560	10 m
B4 Red	665	10 m
B5 Red-edge 1	705	20 m
B6 Red-edge 2	740	20 m
B7 Red-edge 3	783	20 m
B8 NIR (wide)	842	10 m
B8A NIR (narrow)	865	20 m
B9 Water vapour	945	60 m
B10 Cirrus	1375	60 m
B11 SWIR 1	1610	20 m
B12 SWIR 2	2190	20 m

For maintaining high accuracy, the classified LULC data was converted into vector data and then corrected using WFS layer of SISDP LULC data 50k and 10k data obtained from Bhuvan portal (https://bhuvan-app3.nrsc.gov.in/data/download/index.php)

1.7.4. Primary Data Collection

Primary data were collected from selected sites across Nagaland to support ecological assessment and validate satellite-derived classifications. The study was done across key seasons on key locations including Doyang Reservoir in Wokha District, Nsonji Lake in Tseminyu District, Green Park and Dima Raja Pond in Chümoukedima and Dimapur Districts, and Shilloi Lake in Phek (now Meluri) District.

Geo-tagged photographs were captured at randomly selected locations to visually document site conditions and support validation of Land Use and Land Cover (LULC) classifications derived from satellite imagery. These field observations provided critical ground-truth data for interpreting remote sensing outputs and validating ecological indices.

1.7.5. Other satellite data used

To enhance visual interpretation and understand the elevation of various locations, this study utilized Advanced Land Observing Satellite (ALOS) Phased Array type L-band Synthetic Aperture Radar (PALSAR) data for deriving topographic parameters. ALOS PALSAR provides high-resolution Digital Elevation Models (DEMs) generated from L-band radar, which are particularly effective in densely vegetated and cloud-prone regions such as Nagaland. The DEM used in this study was sourced from the ALOS PALSAR RTC (Radiometrically Terrain-Corrected) dataset, available at a spatial resolution of 12.5 meters, and downloaded via the Alaska Satellite Facility (ASF) DAAC, https://search.asf.alaska.edu/.

Using QGIS and ArcGIS, the DEM was processed to extract key terrain attributes:

- **Elevation**: Directly derived from the DEM to represent surface height above mean sea level.
- **Slope**: Calculated using the first derivative of elevation, indicating the steepness of terrain and its influence on hydrological flow and vegetation patterns.
- **Aspect**: Derived to determine the directional orientation of slopes, which affects microclimatic conditions and species distribution.
- **Hillshade and Contours**: Generated to enhance visual interpretation

1.7.6. Software and Applications used

A combination of proprietary and open-source software tools was employed to support data processing, analysis, and visualization throughout the study.

Applications from Microsoft Office were largely used in for the documentation of the works carried out during the research period and compiling of the thesis. Microsoft Excel was used for formatting, organizing, and performing preliminary statistical analysis of data including field data and climatological data, which comprises of rainfall and temperature records across 17 meteorological stations in Nagaland. Microsoft Word was used for compiling, sorting and drafting, editing, and formatting the thesis manuscript.

Python 3.10 was used to automate the download of meteorological data from the Indian Meteorological Department (IMD) Data Supply Portal, https://www.imdpune.gov.in/cmpg/Griddata/Rainfall_25_NetCDF.html which provides gridded daily rainfall data in NetCDF format for India at 0.25° resolution and is ideal for ecological and climate analysis. The code for downloading and extracting the meteorological data in .csv (comma separated values) format is given in Annexure 1.

ArcGIS 10.3 served as the primary platform for spatial analysis, and map composition. Key tasks included georeferencing, image classification, raster calculations, and overlay analysis to derive ecological indicators and visualizing.

QGIS 3.22.6, an open-source GIS application, was used for complementary spatial tasks such as vector editing, and plugin-based analysis. Its flexibility and compatibility with diverse data formats supported efficient integration of field data, satellite imagery, and ancillary layers.

Google Earth Engine (GEE) was employed for Land Use and Land Cover (LULC) classification and time-series analysis of satellite imagery. Its cloud-based geospatial processing capabilities enabled efficient handling of large datasets, including Landsat and Sentinel imagery, without the need for local storage or high-end computing infrastructure. GEE's built-in algorithms and JavaScript API facilitated supervised classification using training samples, spectral indices (e.g., NDVI), and decision tree classifiers. The platform also supported cloud masking, image compositing, and temporal filtering, which were critical for generating accurate LULC maps across multiple years and seasons.

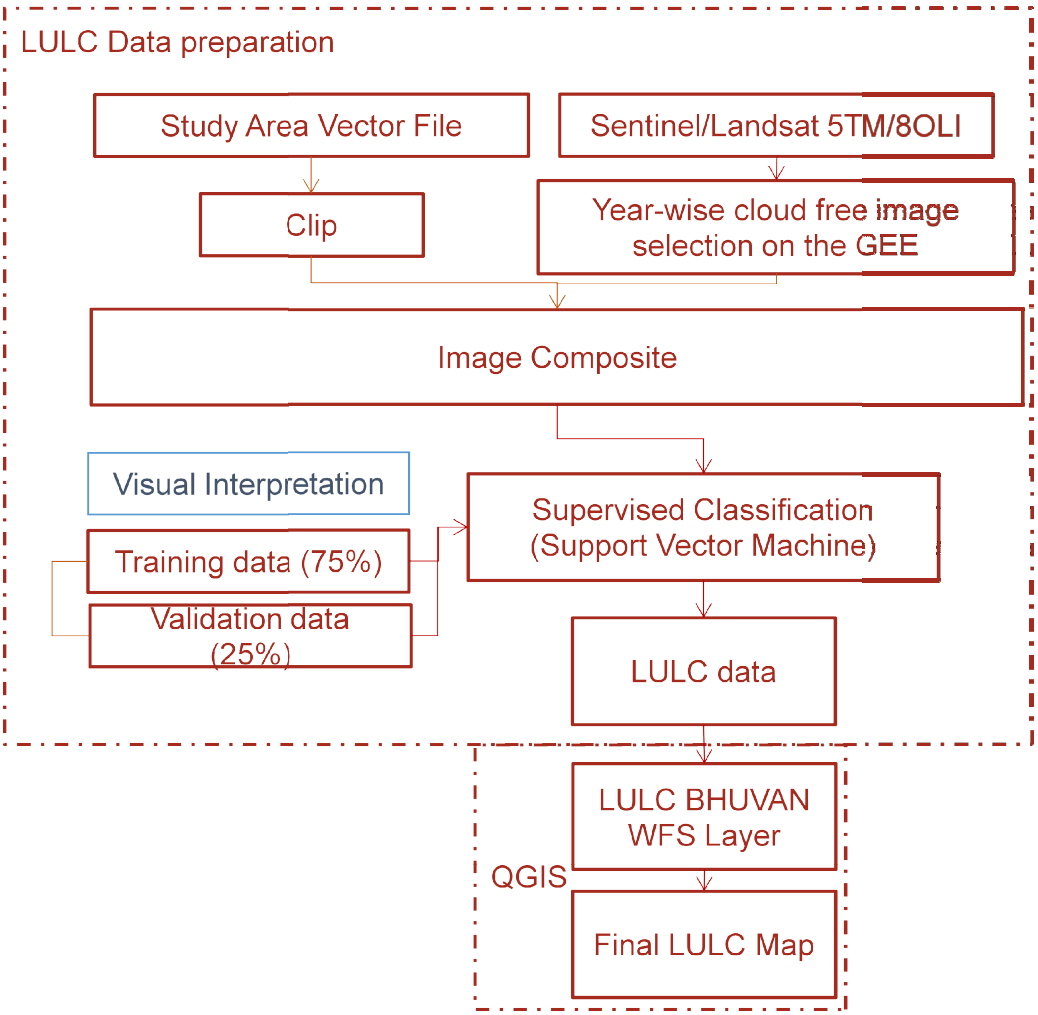

Figure 3 Methodology flowchart for deriving LULC data preparation

1.8. Review of Literature

Franklin *et al.* (2016) investigated the interplay between global environmental change and terrestrial plant community dynamics. The research emphasizes on how vegetation is one of the most vital components of the Earth's systems, shaping how ecosystems function and supporting both nature and people. It regulates the movement of water, carbon, and energy between the land and the atmosphere, making it a central player in global biogeochemical cycles. Beyond providing ecosystem services, plant communities are central to the cycling of carbon, oxygen, water, and nitrogen, all of which interact with oceans, the atmosphere, and climate systems. Moreover, vegetation shapes habitats for animal species, influencing

patterns of biodiversity. The dynamic relationship between climate, vegetation, and fauna has even been linked to long-term evolutionary processes, including the development of early human societies.

Parida *et al.*, (2020) analyzed the greening and browning trends of vegetation in India and their responses to climatic and non-climatic drivers. From a climatic standpoint, India's ecosystems are predominantly influenced by the monsoon, which contributes over 75% of the country's annual rainfall during June to September. Consequently, even minor alterations in monsoon behavior can have far-reaching effects on agriculture, forestry, and water resources. Vegetation growth and distribution across the subcontinent remain closely tied to this rainfall-driven system, which is itself strongly regulated by the distinct orographic features of the Himalayas, Karakoram, and Hindukush ranges.

Arun Kumar et al. (2021) introduced the Integrated Drought Monitoring Index (IDMI), a methodological framework for assessing agricultural drought through time-series datasets obtained from space-based Earth observation satellites. Their study highlights the growing recognition of satellite-based vegetation monitoring, attributed to its affordability, synoptic coverage, frequent revisit capabilities, and proven reliability. Furthermore, remote sensing technologies provide comprehensive spatial data across vast regions, with resolutions ranging from a few centimetres to several kilometres—making them indispensable for large-scale environmental monitoring and decision-making.

Motohka *et al.*, (2010) studied the applicability of green-red vegetation index for remote sensing of vegetation phenology. In this they evaluated the use of the Normalized Difference Vegetation Index and Green-Red Vegetation Index (GRVI) as a phenological indicator based on multiyear stand-level observations of spectral reflectance and phenology at several representative ecosystems in Japan. The GRVI and NDVI values were studied for the years 2004 to 2008 and their maximum and minimum values were analysed to understand how they can be phonological indicator in deciduous broadleaf forest (Takayama site: TKY), deciduous coniferous

forest (Fuji-hokuroku site: FHK), grassland (Terrestrial Environment Research Center in the University of Tsukuba: TGF), and paddy field (Mase site: MSE).

Krishnan & Ct, 2016 used indices from satellite data namely, Normalized Vegetation Index (NDVI), Vegetation Condition Index (VCI), Rainfall records, Moisture Stress Index (MSI) and Yellowness Vegetation Index (YVI) is to assess the drought in Chittur Taluk, Palakkad District, Kerala. The study recorded that the temporal variations of NDVI anomaly, VCI, LST and MSI are closely linked with Rainfall and a strong linear relationship exists between them. The study found that generally, the intensity and affected area of drought had mainly decreased, but the trends varied for different drought intensities, regions and time periods. NDVI, precipitation index, MSI index and LST shared a strong correlation.

Palmate *et al.*, (2017) evaluated the effect of climate change (described in terms of temperature and rainfall) on forest cover and vegetation (described in terms of Normalized Difference Vegetation Index) in the Betwa river basin, a tributary of River Yamuna in Central India. In pre-monsoon season, temperature and forest cover analysis showed regression coefficient value of 0.6876 and, temperature and vegetation analysis showed regression coefficient value of 0.5751. Further, in post-monsoon season analysis rainfall and forest cover showed regression coefficient value of 0.8417 and, temperature and vegetation analysis showed regression coefficient value of 0.6854. The study revealed that, in pre-monsoon season, temperature was significantly related with forest cover and vegetation. In post-monsoon season, rainfall exhibited positive response to forest cover and, temperature exhibited negative response to vegetation.

Xu *et al.,* (2019) applied RSEI-CVA approach to Fujian province, China to quantify and detect the ecological changes of the province in a period from 2002 to 2017 using Moderate Resolution Imaging Spectroradiometer (MODIS) data. In this study, integration of four indices Wet, NDVI, IBI, LST was used to generate RSEI. The result showed that the RSEI-CVA method could effectively quantify and detect spatiotemporal changes in ecological conditions of the province, which revealed an ecological improvement in the province during the study period.

Niu and Li (2020) demonstrated the utility of multi-temporal Landsat imagery in assessing ecological dynamics by extracting four key indicators viz. humidity, vegetation, heat, and dryness, to construct the Remote Sensing Ecological Index (RSEI) through principal component analysis (PCA). Their study, focused on Anqing City, revealed a decline in ecological quality between 1999 and 2009, followed by a gradual recovery through 2019, highlighting the sensitivity of vegetation and ecological conditions to long-term climatic and anthropogenic influences. This approach underscores the relevance of multi-index remote sensing techniques for monitoring ecological change over time.

Li, 2022 did a comprehensive and objective evaluation of ecological environment quality using Landsat remote sensing images of 1991, 2000, 2004, 2010, 2013, 2018, and 2019 to evaluate the changes of ecological environment quality in the Headwaters of Dongjiangyuan River by using remote sensing ecological index RSEI. The results showed that, from 1991 to 2019, thee environmental quality of the Dongjiangyuan River showed a good trend of development. Humidity index, greenness index, and dryness index all fluctuated in a small range; the greenness and dryness showed an overall increase. The average temperature in the Headwaters of the Dongjiangyuan River presented a rising trend.

Maity S., *et al.*(2022) studied the four ecological indicators that were prepared in the year 1990, 2000, 2010 and 2020 of Kolkata urban agglomeration (KUA) to evaluate the ecological environmental condition. These were Greenness, Wetness, Heat and Dryness indicated by NDVI (Normalized Difference Vegetation Index), WET, LST (Land Surface Temperature) and NDSI (Normalized Difference Soil Index) respectively. The principal component analysis (PCA) and spatial autocorrelation analysis could relate all indicators with each other's and RSEI (Remote Sensing Ecological Index) to find that Greenness has greater impact on the eco-environment than the other three indicators, having positive effect along with Wetness unlike Heat and Dryness which had negative impact.

Maity S., (2022) replicated the above study for Delhi Urban Agglomeration and added five other indices to the above given set of indicator's based indices. The

additional indices were NDBI (Normalized Difference Built-up Index), DBI (Dry Built-up Index), DBSI (Dry Bare Soil Index), Enhanced Built-up and Bareness Index (EBBI) and NDBaI (Normalized Difference Bareness Index).The results showed that greenness (NDVI) and wetness (WET) have negative effects while dryness (WET), heat (LST), and the other five indices have positive effects on the eco-environmental quality. The normalized difference soil index (NDSI), normalized difference built-up index (NDBI), dry bare-soil index (DBSI), and enhanced built-up and bareness index (EBBI) have a greater impact on the eco-environment than the others.

Hao H., Lian Z., Zhao J., *et al.* (2022) produced a study based on Landsat-8 image data and deried the remote sensing ecological index (RSEI) to evaluate the dynamic changes and spatial and temporal differences of the ecological environment in the study area of Xunwu County, Ganzhou City, Jiangxi Province at the junction of Gan, Guangdong, and Fujian Provinces under the longterm multi means comprehensive management. Greenness, Wetness, Heat and Dryness indicated by NDVI (Normalized Difference Vegetation Impact), WET, LST (Land Surface Temperature) and NDBSI (Normalized Difference Bare Soil Index) were used to derive RSEI in this study.

Jiang *et al.*, (2021) assessed vegetation growth and drought conditions using satellite based vegetation health indices in Jing-Jin-Ji region of China. In this study, they used various Vegetation Health Indices and algorithms such as NDVI, BT, Smoothed NDVI (SMN), Smoothed BT (SMT), Vegetation Condition Index (VCI), Temperature Index (TCI) and Vegetation Health Index (VHI). Results indicated that monthly SMN had increased throughout the year especially during growing season at April and ends at about October. The correlation analysis between SMN and SMT, SMN and precipitation indicated that the vegetation growth was affected by joint effects of temperature and precipitation. The VCI during growing season was positive trends dominated and vice versa for TCI. The relationships between VHIs and drought made it possible to identify and quantify drought intensity, duration and affected area using different ranges of VHIs.

Zeng et al., (2022) studied an improved global vegetation health index dataset in detecting vegetation drought in which they used Improved Vegetation Health Index

(VHI) dataset from 1981 to 2021 integrating climate, vegetation and soil moisture. The VHI was composed of Thermal Condition Index and Vegetation condition Index. Based on the principle that a low normalized differences vegetation index (NDVI) and high land surface temperature (LST) suggest poor vegetation health and the contributions of VCI and TCI to VHI are assumed to be equal, since there are no data on the relative contributions of other conditions to vegetation health35, the study was carried out. The study found that global drought detection efficiency of the improved high resolution VHI dataset reached values as high as 85%, which is 14% higher than the original VHI dataset. The study also found that improved VHI dataset was also more sensitive to mild droughts and more accurate regarding the extent of droughts.

1.9. Significance of the Study

Understanding the relationship between climatological variation and vegetation cover is crucial for regions like Nagaland, which lies within the Indo-Burma biodiversity hotspot and is highly vulnerable to both climatic shifts and anthropogenic pressures. Vegetation serves as a key regulator of ecological processes, including carbon sequestration, water regulation, and soil stabilization, while also providing essential habitat for diverse species. Any alteration in vegetation dynamics has direct consequences for ecosystem stability, biodiversity conservation, and human livelihoods in the region.

This study is significant for several reasons. Firstly, it contributes to filling the knowledge gap on how climate variability interacts with land-use change to influence vegetation cover in Nagaland, a region where integrated, geospatially based analyses remain limited. By employing advanced remote sensing and geospatial techniques, the research provides spatially explicit and temporally consistent evidence of vegetation trends, which can be used to detect patterns of degradation or recovery.

Secondly, the findings will generate actionable insights for policymakers, conservationists, and local communities. With the increasing frequency of climate-induced hazards such as floods, landslides, and forest fires, evidence-based

understanding of vegetation dynamics is essential for developing adaptation and mitigation strategies. The outcomes of this study can inform sustainable land-use planning, resource management, and conservation policies tailored to the ecological and socio-cultural context of Nagaland.

Finally, this research holds broader scientific value by contributing to ongoing discussions on ecosystem resilience in the face of climate change. The methodological framework, integrating climatological data with vegetation indices derived from remote sensing which can be applied to other ecologically sensitive regions, thereby enhancing comparative studies and supporting global efforts toward biodiversity conservation and sustainable development.

1.10. Organization of the Thesis

The assessment of climate change impacts is an evolving research area, with relatively limited empirical and conceptual studies conducted at global, national, and regional scales. This thesis is compiled to address this gap by presenting a geospatially supported analysis of how climatological variations influence vegetation cover in the state of Nagaland. This thesis is composed into the three main chapters based on the aim and objectives undertaken for the study.

The first 2 chapters give the background of why, where and how the study is undertaken explaining the background of the study, the geographical framework of the study area, and the data, methodology used in the study. The main chapters are given in Chapter 4, 5 and 6 detailing the various works done as per the objectives of the study.

Chapter 3 explores climate variability and its influence on vegetation cover, focusing specifically on rainfall and temperature as key climatic parameters. It presents trend analyses of these variables across the study area using ground-truth data, and compares them with corresponding satellite imagery to assess their impact on Nagaland's vegetation dynamics. This comparative approach serves as a critical baseline, establishing the analytical framework that supports the subsequent objective-driven chapters. By anchoring the study in empirical observations, Chapter

4 provides the foundational reference for interpreting ecological changes throughout the region.

Chapter 4 builds on the climatic foundation by utilizing remote sensing data to derive geospatial indices that assess ecological condition over the study area. Here, temporal trends in these indices are investigated to evaluate the ecological condition of the study area. Further analysis is also carried out with a particular focus on land use and land cover dynamics. Through a two-decade impact assessment, the chapter analyzes shifts in ecological patterns and attributes these changes to climatological variability understood as a consequence of sustained anthropogenic influence. By tracing these changes over time, it offers deeper insight into the evolving health of the ecosystem and sets the stage for informed environmental planning. This integrative approach deepens the understanding of landscape transformation and complements the ground-truth analysis presented in Chapter 4, reinforcing the study's broader narrative on ecosystem health.

Chapter 5 evaluates the changes with respect to the health of the vegetation cover of the study area. Building on the climatological and ecological analyses of the previous chapters, it employs vegetation health metrics, such as NDVI and other spectral indices, to assess spatial and temporal variations in greenness and biomass. The chapter synthesizes satellite-derived data with field observations to identify patterns of degradation, recovery, and stability across different land use categories. By tracing these dynamics, it offers varied understanding of ecosystem resilience and vulnerability.

Chapter 6 brings together the core findings of the study, offering a concise synthesis aligned with the three primary research objectives. It distills insights from the vegetation condition analysis, climatological correlations, and geospatial index integration, highlighting how rainfall variability, temperature stress, and land-use dynamics have shaped vegetation health across the study area. The chapter also acknowledges key limitations encountered during the research—such as data resolution constraints, limited ground validation, and sensor variability—and reflects on how these factors may have influenced the outcomes. Finally, it presents targeted suggestions for future research, emphasizing the potential of high-resolution satellite

data, multi-seasonal ecological monitoring, and socio-environmental modeling to deepen understanding and support adaptive conservation planning.

CHAPTER 2

Chapter 2: Geographical Framework of the Study Area – Nagaland

2.1. Location and Geographical Extent

The state is located in the north-eastern part of India covering an area of 16,579 sq. km. area and occurring between 93°20' E to 95°15' E longitude and 25°6' N to 27°4' N latitude. It shares borders with the state of Assam to the west, Arunachal Pradesh and part of Assam to the north, Manipur to the south and international borders with Myanmar to the east. The altitude of the state ranges from 100m in the low-laying plains bordering Assam to over 3,800 meters at the highest peak in Mount Saramati, bordering with Myanmar. It located at the confluence of the Indo-Burma Biodiversity hotspot bordering the rich Indo-Chinese zoogeographic sub-region with favorable geo-climatic condition permitting an ideal condition for the luxuriant growth of vegetation from tropical rain forest to alpine and from evergreen to sub tropical.

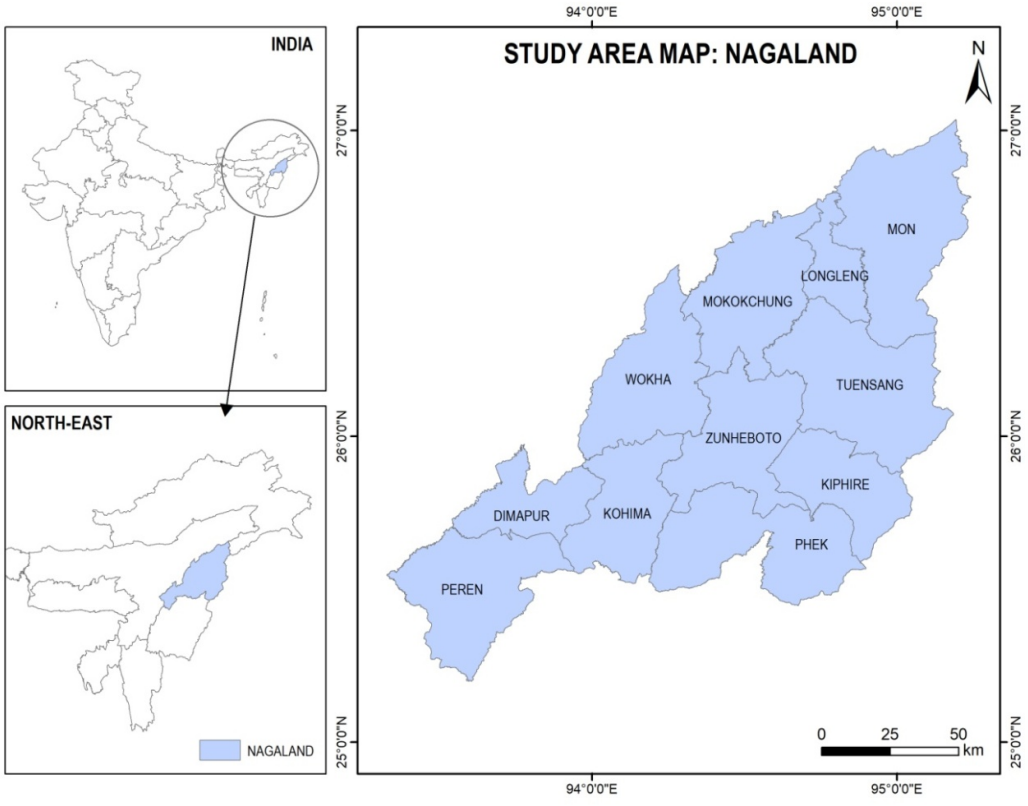

Figure 4 Study Area Location Map

2.2. Topography, Physiography and Drainage

Nagaland's topography is predominantly mountainous, with approximately 94% of its land area comprising hilly and rugged terrain. The remaining 6% consists of relatively flat plains, primarily located along the western boundary adjoining the Assam plains. It is located at the hilly mountainous terrain where the Arakan Patkai extension of Myanmar meets the Eastern Himalayan ranges. The Barail range enters the state from the southwestern corner and continues in a northeasterly direction, reaching close to Kohima. In the vicinity of Kohima, this range converges with other mountain systems that extend into Manipur, where the primary ridge shifts toward a more northerly orientation. This central range rises significantly higher than the Barail, featuring prominent peaks such as Mount Saramati (3826.15 m) in the easternmost part of the state. Between Mao and Kohima, notable elevations such as Japfü peak are found. Moving northward from Kohima, the terrain gradually descends in altitude, with the Japukong range in Mokokchung district averaging around 750 meters in elevation. The state features a rolling landscape characterized by low-lying hills densely covered with vegetation, contributing to its ecological richness and complexity (Martemjen & Lanusashi Longkumer, 2019).

Nagaland is traversed by a network of both perennial and seasonal rivers and streams that intricately dissect its terrain. The Barail and Japfu ranges, along with their extensions into Mokokchung and Tuensang districts, form a significant watershed that delineates the Brahmaputra and Chindwin river basins. Toward the southwestern part of the state, the Meghna drainage system also exerts its influence. The overall drainage configuration is predominantly dendritic, shaped by geological structures such as trend lines and lineaments. In the plains, rivers exhibit a meandering course, while in the eastern mountainous regions, the drainage tends to follow a structurally guided trellis pattern (Imchen & Rawat, 2015).

Among the principal rivers contributing to these three drainage systems are the Doyang, Dikhu, Dhansiri, Tisu, Tsurong, Nanung, Tsurang, Menung, Dzu, Langlong, Zunki, Likimro, Lanye, Dzuza, and Manglu. These rivers typically display dendritic patterns and fall within stream orders seven to nine. Notably, the Dhansiri, Doyang,

and Dikhu rivers flow westward into the Brahmaputra basin, whereas the Tizu River stands out as the only eastward-flowing river in Nagaland, eventually joining the Chindwin River across the border in Myanmar (Rawat, 2014).

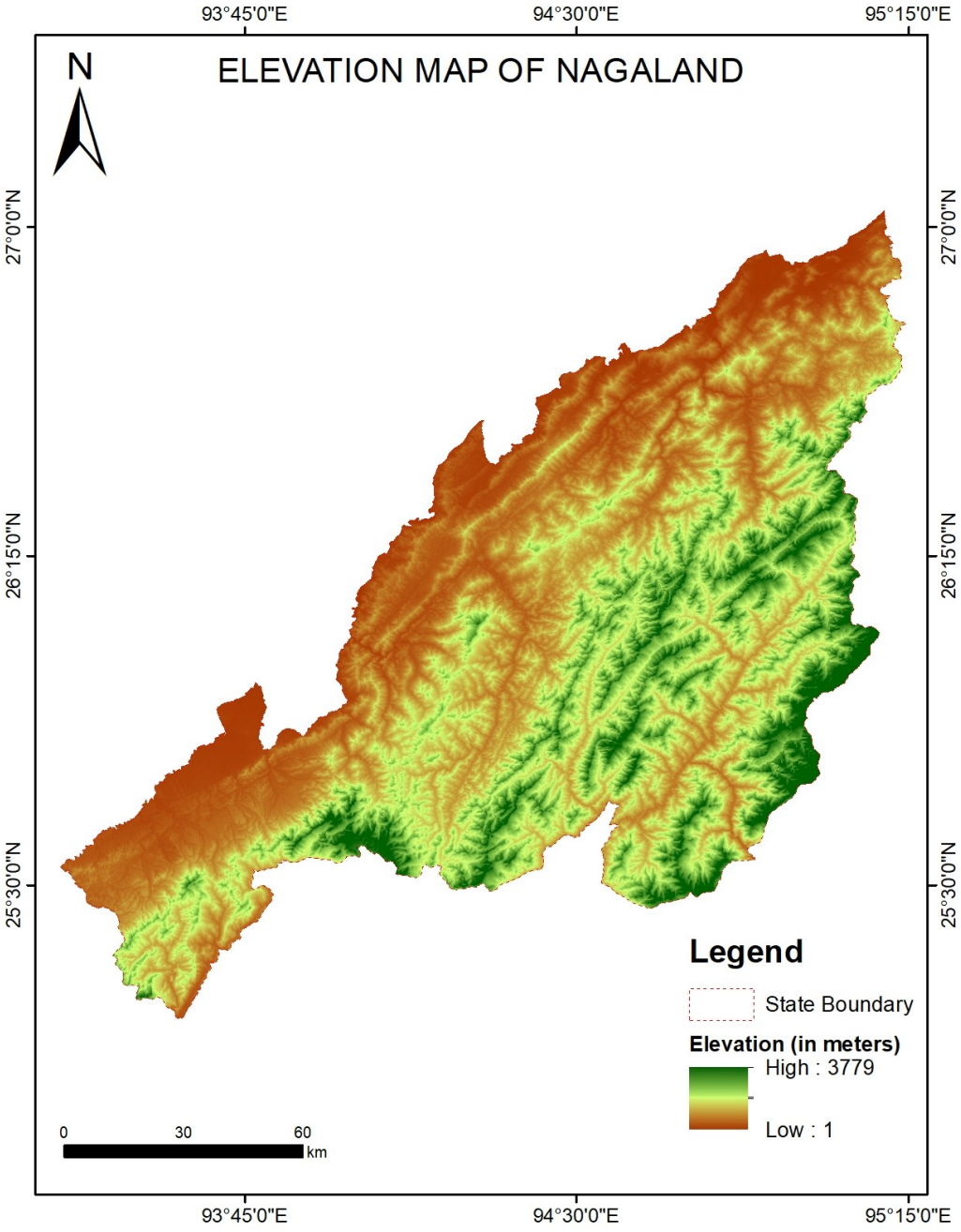

Figure 5 Elevation Map of the Study Area prepared using ALOS PALSAR DEM

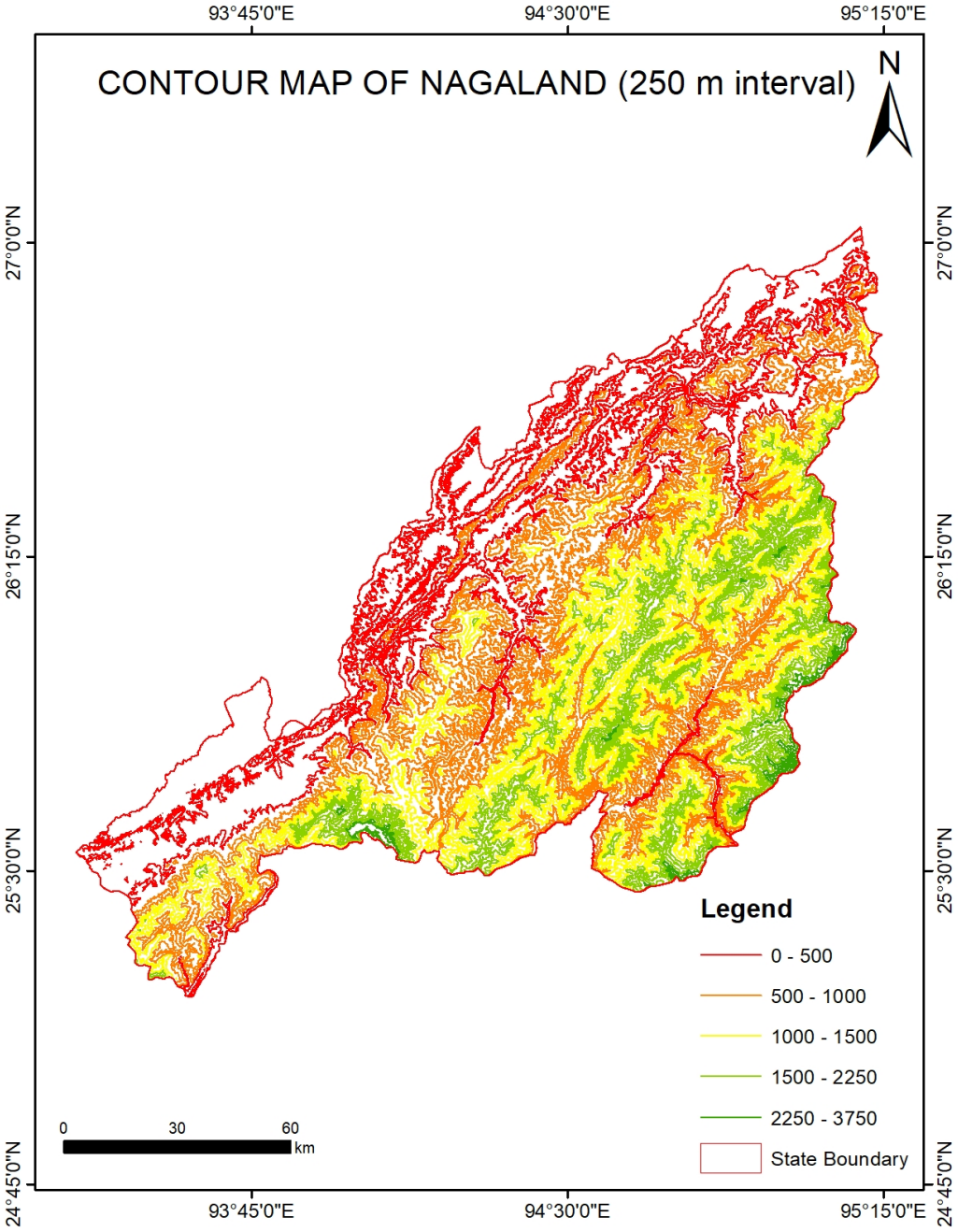

Figure 6 Contour Map of the Study Area prepared using ALOS PALSAR DEM

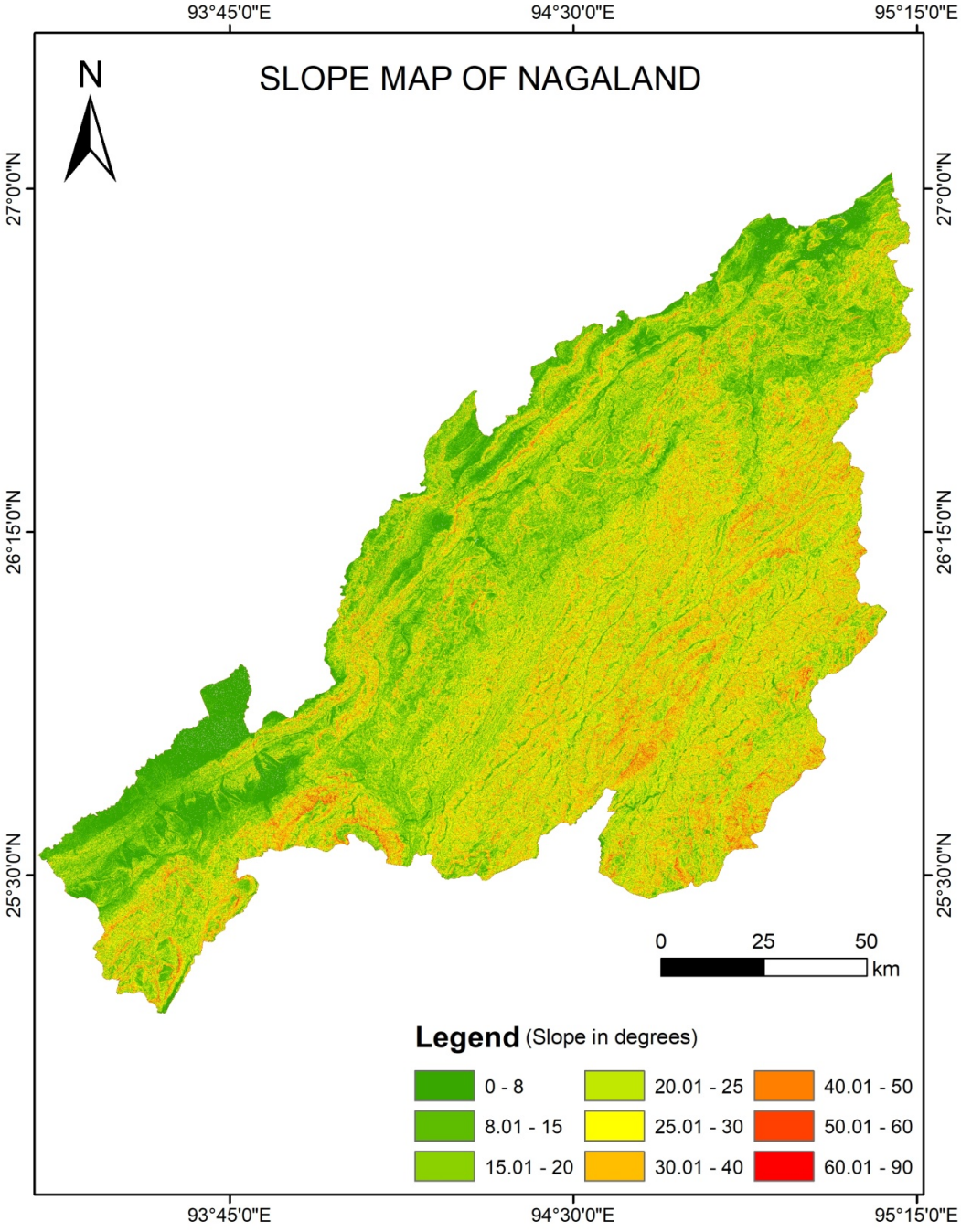

Figure 7 Slope Map of the Study Area prepared using ALOS PALSAR DEM

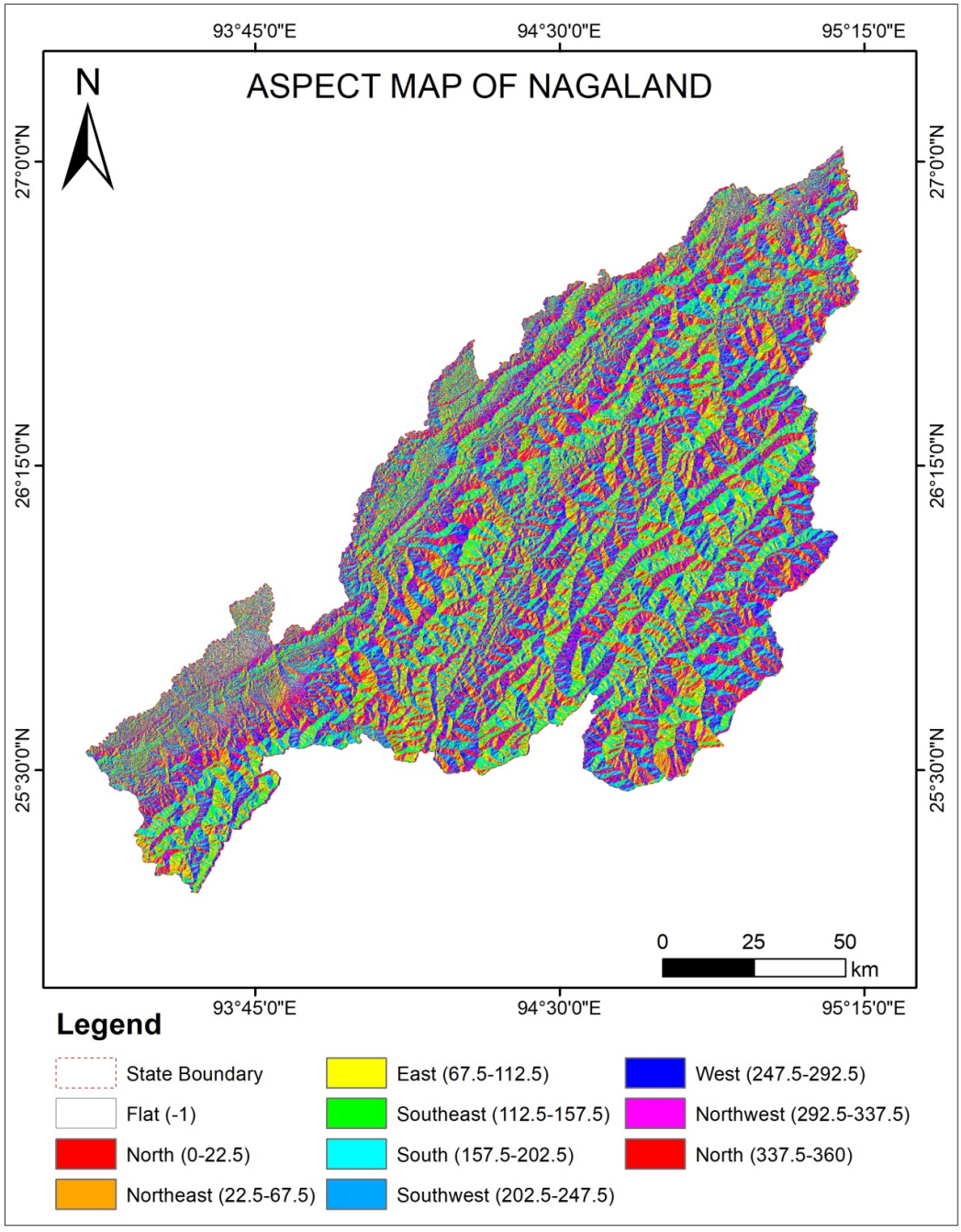

Figure 8 Aspect Map of the Study Area prepared using ALOS PALSAR DEM

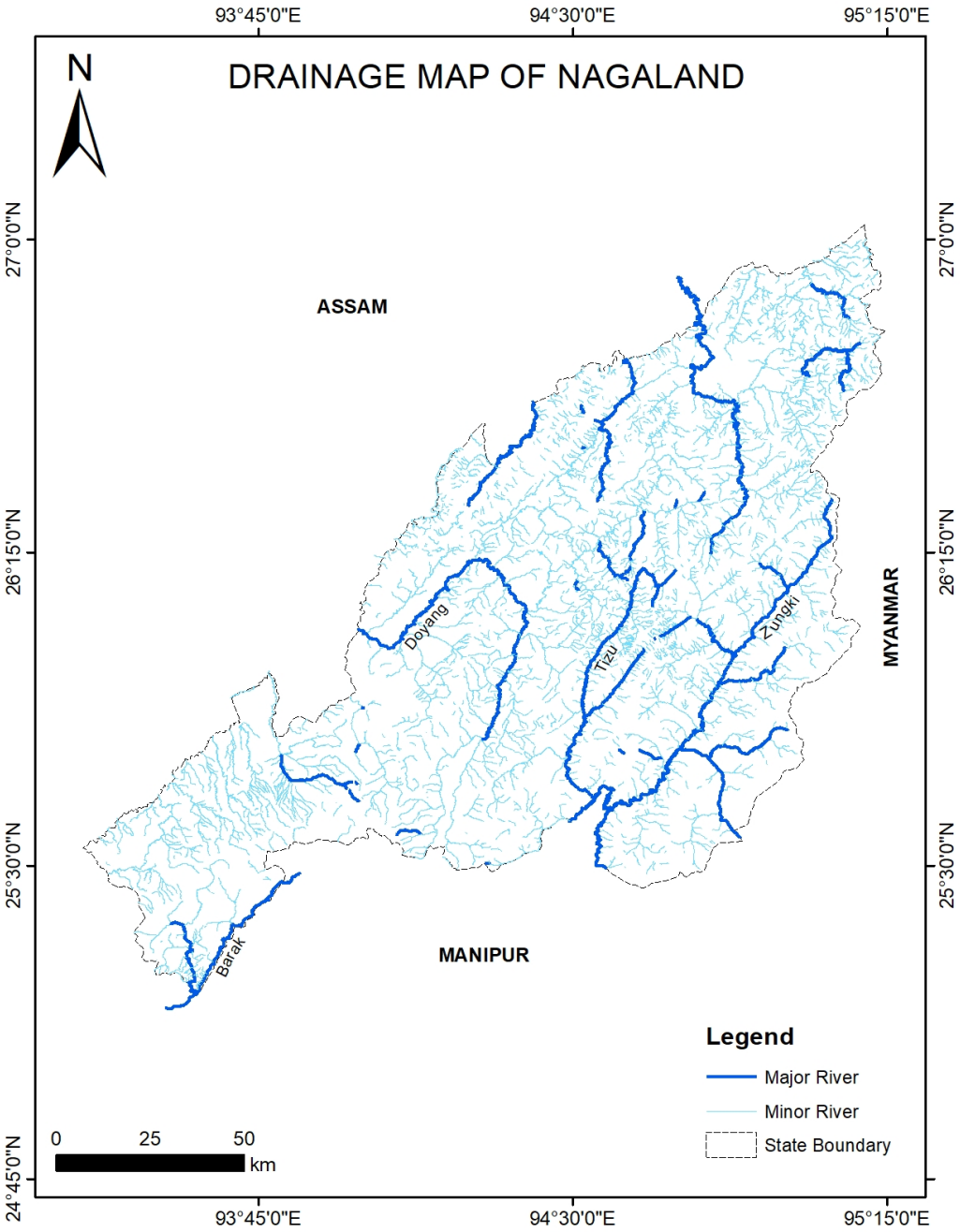

Figure 9 Drainage Map of the Study Area prepared using ALOS PALSAR DEM

2.3 Climatic Characteristics

Nagaland experiences a predominantly monsoonal climate characterized by high humidity and distinct seasonal variation. The state receives substantial annual rainfall, averaging between 1,800 mm and 2,500 mm, primarily concentrated during

the monsoon months from May to September. The period from May to August witnesses particularly intense precipitation, while September and October continue to record significant rainfall levels, often exceeding 2,000 mm.

Temperature patterns in Nagaland reflect its varied topography. During the summer season, temperatures typically range from 16°C to 31°C. In winter, temperatures seldom fall below 4°C in most areas, although frost is frequently observed at higher elevations, where snowfall is also common. The maximum average temperature during winter is approximately 24°C. The state's climatic regime is broadly divided into three well-defined seasons: summer, monsoon, and winter. Additionally, strong northwesterly winds are prevalent during February and March, influencing local weather conditions and contributing to seasonal transitions.

2.4. Geology, Vegetation and Forest Cover

Geologically, they represent the northern extension of the Indo-Burma Ranges (IBR), serving as a transitional corridor between the Arunachal Himalayas in the north and the Andaman-Nicobar Islands in the south. The Patkai, Barail, and associated ranges, trending predominantly north–south, exhibit varied structural styles that contribute to the region's youthful geomorphology. Approximately 95% of Nagaland's surface geology comprises Cenozoic sedimentary formations, while the remaining area is underlain by igneous and crystalline rocks of Mesozoic to Cenozoic age. These lithological units generally follow a NNE–SSW orientation, with moderate to steep dips toward the northwest and southeast (Imchen & Rawat, 2015).

Morphotectonically, the Naga Hills are subdivided into three longitudinal belts from west to east: the Schuppen Belt, the Inner Fold Belt, and the Ophiolite Belt.

- **Schuppen Belt**: This narrow, linear zone of imbricate thrust slices runs parallel to the Assam valley alluvium for approximately 350 km along the western flank of the Naga-Patkai ranges. It is postulated to contain eight or more overthrusts, facilitating northwestward displacement of the Naga Hills relative to the Foreland spur. The belt is bounded by the Haflong-Disang thrust to the east and the en-echelon Naga thrust to the west. Sedimentary

sequences within this belt range from the Eocene-Oligocene to the Plio-Pleistocene, with a notable absence of Disang rocks.

- **Inner Fold Belt**: Occupying the central portion of the Naga Hills, this belt extends northeastward to the Pangsu Pass in Arunachal Pradesh. It is characterized by extensive exposures of Disang rocks, interspersed with Barail formations and transitional sequences. Palaeogene strata are folded into multiple anticlines and synclines, bounded by the Haflong-Disang thrust on the west and the Ophiolite-Disang thrust on the east. Two major synclinoria dominate this belt—the Kohima synclinorium in the south and the Patkai synclinorium in the north—with Mokokchung marking their convergence. The Kohima synclinorium notably contains younger Surma rocks at its core.
- **Ophiolite Belt**: This belt trends NE–SW along Nagaland's eastern frontier, extending for approximately 200 km adjacent to the Myanmar border. It comprises dismembered tectonic fragments of serpentinites, cumulates, and volcanic rocks. Associated pelagic sediments include bedded cherts and limestones, often interlayered with volcanic material. Radiolarian-bearing cherts and fossil assemblages from limestone interbands suggest an Upper Cretaceous to Lower Eocene age for these ophiolitic units. These rocks are unconformably overlain by volcaniclastic deposits and marine to paralic sedimentary sequences, collectively referred to as the Phokphur Formation.

Nagaland, though modest in geographic extent, exhibits a striking diversity of forest ecosystems, shaped by its distinctive bio-geographic location and complex physiographic terrain. Based on the classification by Champion and Seth (1968), the forests of Nagaland are grouped into seven major Type Groups, comprising ten distinct Forest Types. Tropical wet evergreen and semi-evergreen forests dominate the lower elevations, while mid-altitude zones are characterized by tropical wet hill forests and subtropical pine formations. At higher altitudes, moist mixed deciduous forests prevail, contributing to the ecological heterogeneity of the region.

Of the state's total geographical area of 16,579 sq. km., approximately 12,222 sq. km., equivalent to 73.72%, is under forest cover. However, according to the India State of Forest Report (ISFR) 2023, Nagaland experienced a net decline of 125.22 square kilometers in forest cover compared to the 2021 assessment, underscoring the need for strengthened conservation and monitoring efforts. Furthermore, in the year 2000, forest cover accounted for 80.49% of the state's area, suggesting a significant downward trend, with a decrease of about a 6.82% corresponding to roughly 1,130.7 sq. km. of forest loss, over the past two decades.

Table 5 Forest Cover of Nagaland in 2000, ISFR 2021

Class	**Area (sq. km.)**	**% of Calculated Area by SoI**
Very Dense Forest	5,393	32.53
Open Forest	7,952	47.96
Total	13,345	80.49

Table 6 Forest Cover of Nagaland in 2021-2023, ISFR 2023

Class	**Area (sq. km.)**	**% of Calculated Area by SoI**
Very Dense Forest	1,256.38	7.58
Moderately Dense Forest	4,461.81	26.91
Open Forest	6,504.28	39.23
Total	**12,222.47**	**73.72**
Scrub	667.27	4.03

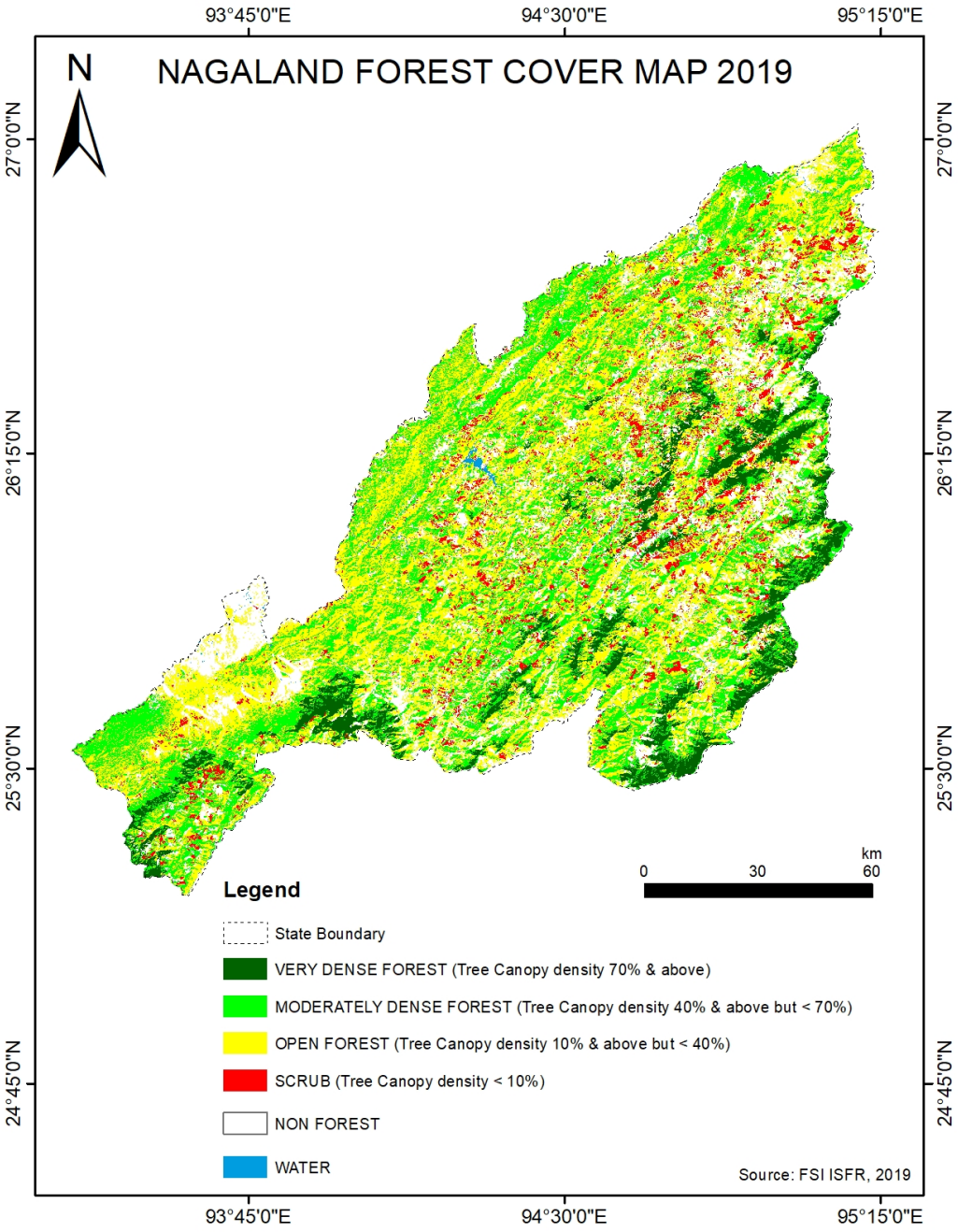

Figure 10 Forest Cover Map of the Study Area (FSI, 2019)

The area under different Forest Types in Nagaland (as per the Champion & Seth Forest Classification, 1968) based on the Forest Cover Map (FCM), ISFR-2023, is presented in the following table.

Table 7 Forest Types of Nagaland, ISFR 2023

Area Statistics of the Forest Types Found in Nagaland			
Sl. No.	**Forest Type Area**	**Area in sq. km.**	**% of the total mapped area[1]**
1	1B/C1 Assam Valley tropical wet evergreen forest (Dipterocarpus)	71.66	0.55
2	1/2S1 Pioneer Euphorbiaceous scrub	667.27	5.17
3	2B/C1/2S2 Eastern alluvial secondary semi-evergreen forest	2,436.73	18.88
4	2/2S1 Secondary moist bamboo brakes	491.42	3.81
5	3C/C3b East Himalayan moist mixed deciduous forest	4,899.37	37.95
6	8B/C2 Khasi subtropical wet hill forest	2,008.62	15.56
7	9/C2 Assam subtropical pine forest	700.8	5.43
8	11B/C2 Naga hill wet temperate forest	1,446.81	11.21
9	12/DS1 Montane bamboo brakes	15.44	0.12
	Sub Total	12,738.12	98.68
10	TOF/ Plantation	151.62	1.17
	Total (Forest Cover & Scrub)	**12,889.74**	**99.86**
	Grassland forest type (outside forest cover)		
11	9/C2/DS1 Assam subtropical pine savannah	18.39	0.14
	Grand Total	12,908.13	100

2.5. Population Distribution of Nagaland

As per the 2011 Census, Nagaland had a total population of 1,978,502, comprising 1,024,649 males and 953,853 females. This yields a sex ratio of 931 females per 1000 males, which, while below the national average of 943, reflects gradual improvements in gender balance across several districts. The state's population accounts for approximately 0.16% of India's total, placing it among the least populous states nationally. Nagaland remains predominantly rural, with 71.14% of its

[1] Forest Types have been assigned to the natural forest formations under forest cover and scrub categories shown in the forest cover mapping (ISFR, 2023).Grassland forest type outside forest cover has also been mapped. The total mapped area, therefore, is sum of forest cover, scrub and grassland forest types (found in non-forest). TOF- Trees outside forests.

population residing in villages as of 2011. Urban areas accounted for 28.86%, though this share has been steadily increasing. Despite this trend, rural settlements continue to dominate the demographic landscape, especially in districts like Mon, Tuensang, and Phek, where infrastructure and accessibility remain limited. Nagaland's population density stands at 119 persons per square kilometer, significantly lower than the national average of 382. This sparse distribution reflects the state's mountainous terrain, fragmented settlement patterns, and low urban sprawl.

Table 8 District-wise Population Distribution of Nagaland, (Census 2011)

	State/District	Total Population	Sex Ratio (females per 1000 males)	Density (per sq. km.)	Literacy rate (%)
*	Nagaland	19,78,502	931	119	79.55
1	Kohima	2,67,988	928	213	85.23
2	Mokokchung	1,94,622	925	120	91.62
3	Tuensang	1,96,596	929	90	73.08
4	Mon	2,50,260	899	140	56.99
5	Phek	1,63,418	951	81	78.05
6	Wokha	1,66,343	968	102	87.69
7	Zunheboto	1,40,757	976	112	85.26
8	Dimapur	3,78,811	919	410	84.79
9	Kiphire	74,004	956	66	69.54
10	Longleng	50,484	905	89	72.17
11	Peren	95,219	915	55	77.95

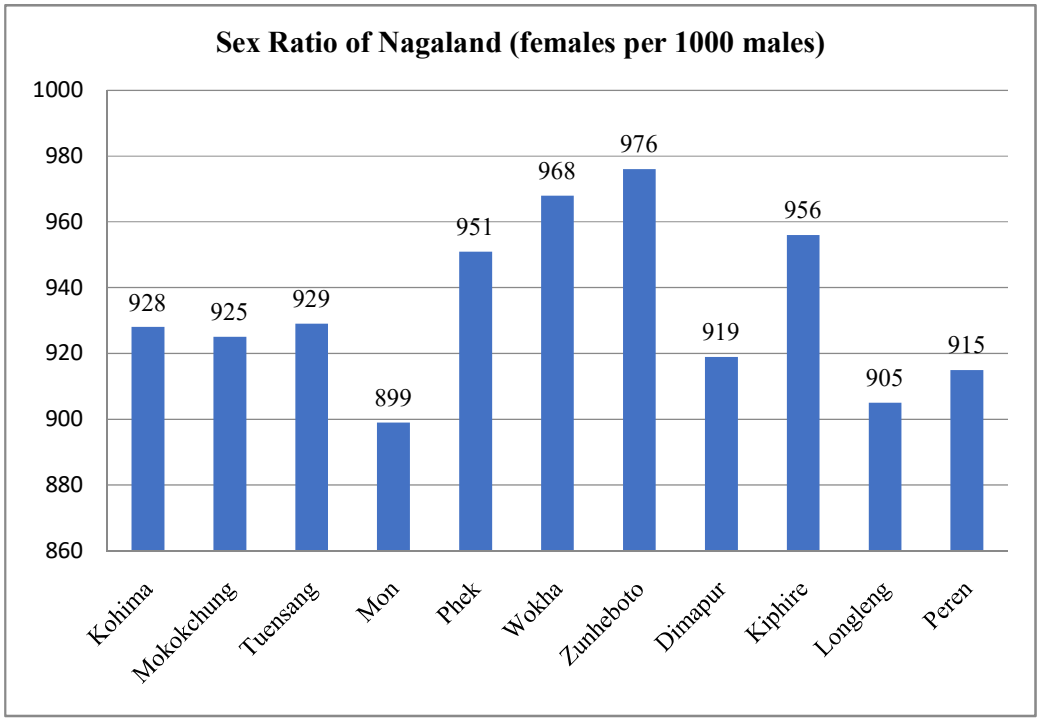

Figure 11 *District-wise sex-ratio distribution of Nagaland (females per 1000 males) (Census, 2011)*

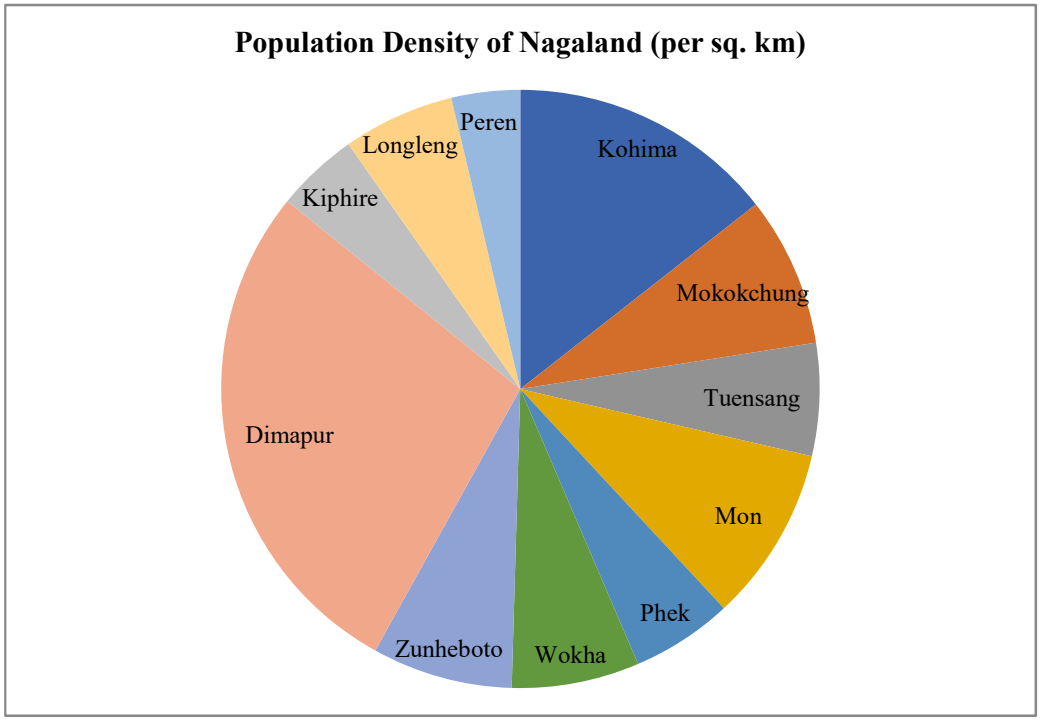

Figure 12 *District-wise Population density distribution of Nagaland (per sq. km.).(Census, 2011)*

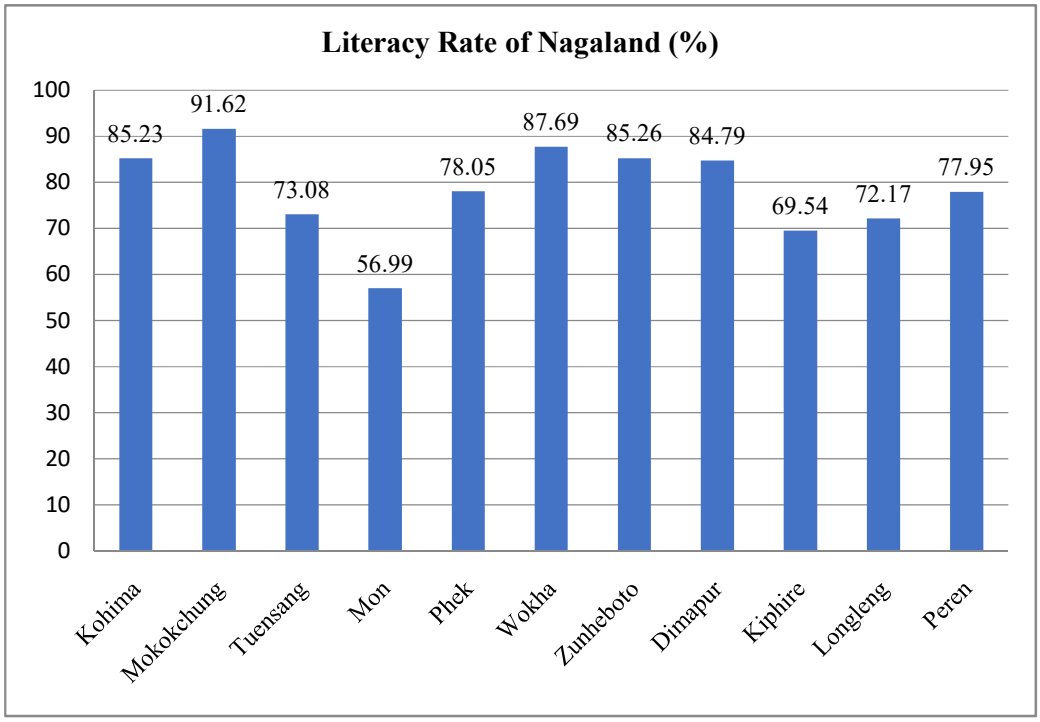

Figure 13 District-wise Literacy rate distribution of Nagaland (in %) (Census, 2011)

2.6. Socio-Ecological Context

Nagaland's ecological richness is evident in its diverse forest types, presence of endemic species, and sensitive watershed systems. This ecological complexity is closely interwoven with the state's social fabric, which is deeply rooted in Indigenous Traditional Knowledge (ITK) and customary institutions. As a predominantly tribal state, Nagaland comprises seventeen administrative districts inhabited by seventeen major tribes and several sub-tribes. The Indigenous communities, collectively referred to as the "Nagas," are primarily of Mongoloid origin and maintain strong cultural ties to their ancestral landscapes. Although each Naga tribe possesses its own distinct social and cultural identity, there are shared characteristics that unify them across the region. Traditionally, every village functioned as an autonomous entity, effectively a sovereign village-state, with clearly demarcated land, defined boundaries, a recognized citizenry, and its own governance system rooted in customary law. Strategically, Naga villages were often established atop hill summits, a practice that served both defensive purposes and reflected the communities' deep connection to their surrounding landscapes.

Agriculture remains the backbone of Nagaland's economy, employing over 70% of the population. Among rural communities, shifting cultivation, locally known as jhum, has historically been the dominant agricultural practice. This system is not only a livelihood strategy but also a reflection of the region's socio-cultural diversity and ecological adaptation (Talukdar & Thakuria, 2015). The Naga community are also largely dependent on the forest and rely on the forest and its resources for their subsistence and livelihood.

Over time, certain tribal groups have transitioned to more settled forms of agriculture, including terrace (wet-rice) cultivation and other Indigenous systems such as alder-based agro-forestry and zabo farming. These practices, developed in sloping hill terrains, offer ecologically sustainable alternatives to shifting cultivation. Studies have shown that these Indigenous farming systems enhance soil stability, improve water retention, and contribute to increased agricultural productivity, while remaining environmentally sound and culturally embedded (Murry & Das, 2021). Moreover, forestry and wildlife resources contribute substantially in meeting the needs of subsistence economy of Nagas, which make the dependency of the people on the ecological resources very high.

2.6 Justification for Selection of the Study Area

Nagaland is predominantly covered by vegetation cover from the various land-use land cover classes with over 73% of the state's geographical area under forested lands. The region's unique physiographic and climatic characteristics, coupled with its rich biodiversity and socio-environmental dynamics, make it an ideal case for such an investigation. As discussed through the earlier review of various literatures, following are the brief summarized justification for the selection of Nagaland as the study area.

2.6.1. **Ecological Sensitivity and Biodiversity Richness**

Nagaland harbors a mosaic of forest types, from tropical evergreen to montane subtropical forests, supporting high levels of endemism and ecological diversity. These ecosystems are particularly sensitive to climatic fluctuations, making them

valuable indicators of vegetation response to changing temperature and precipitation regimes. Nagaland's landscapes are deeply intertwined with the socio-economic fabric and ecological resilience of its communities. The use of forest-rich areas and wildlife resources, along with the extraction of various forest products, has long been an accepted and culturally embedded practice across the region (Changkija, 2019). Biomass, particularly wood, agricultural residues, and forest-derived materials, continues to serve as a primary source of energy and livelihood for a majority of the population (Amer, 2019). This dependence underscores the critical role of forests not only in ecological stability but also in sustaining rural economies.

2.6.2. **Topographic and Climatic Variability**

The state's rugged terrain, ranging from low-lying valleys to elevations above 3,000 meters, creates microclimatic zones that influence vegetation patterns. This heterogeneity allows for comparative analysis across elevation gradients, enhancing the understanding of climate-vegetation interactions in complex mountainous systems.

2.6.3. **Climatic Vulnerability and Emerging Trends**

Nagaland has witnessed increasing variability in rainfall patterns, rising temperatures, and shifting seasonal cycles. These trends are consistent with broader climate change impacts in the Eastern Himalayas. These changes have direct implications for vegetation health, phenology, and land cover transitions, warranting focused climatological analysis. In light of rapid population growth and shifting climatic patterns, meeting resource demands without compromising ecological integrity has become a central concern for agriculturists, environmentalists, and development planners. There is an urgent need to promote sustainable agricultural strategies that ensure livelihood security while adapting to climate variability and change (Sarma, P. K., 2019). However, as climate change intensifies—posing one of the greatest ecological and environmental challenges—the ability of communities to access and rely on these indispensable resources is increasingly constrained (Amer, 2019).

2.6.4. **Anthropogenic Pressures and Land-Use Change**

Traditional land-use practices such as jhum (shifting cultivation), expanding peri-urban development, and resource extraction exert pressure on forest cover. Studying vegetation dynamics in this context provides insights into how climatological parameters interact with human-induced changes, especially in fragile socio-ecological systems. Over generations, Naga communities have cultivated a rich repository of traditional ecological knowledge, enabling them to sustain livelihoods through innovative local practices and conservation-oriented land use. This indigenous knowledge system has played a pivotal role in fostering sustainable resource utilization and ecological stewardship (Yaden and Pongener, 2019). Yet, with mounting pressures on natural resources—driven by demographic expansion, land-use change, and market integration—the ecological condition of the region demands systematic assessment. Quantifying the rate and extent of these changes is essential for informed decision-making and long-term sustainability planning.

2.6.5. **Data Scarcity and Research Gaps**

Despite its ecological importance, Nagaland remains underrepresented in global, national and regional-scale climatological and vegetation studies. Selecting this region addresses a critical research gap and contributes to more inclusive environmental monitoring frameworks for Northeast India.

2.6.6. **Policy Relevance and Conservation Planning**

Understanding climate-driven vegetation changes in Nagaland can inform adaptive land-use planning, biodiversity conservation, and climate resilience strategies. The findings can support regional efforts and contribute to evidence-based policy interventions.

CHAPTER 3

Chapter 3: Climate Variability and Its Impact on Vegetation Cover

3.1. Overview of Climate-Vegetation Linkages

Climatic variation has become a pressing global issue, with significant implications for sustainable development, human health, and environmental conservation (IPCC, 2013). The past two decades have witnessed significant changes in climate parameters, including rising temperatures, altered precipitation patterns, and increased frequency of extreme weather events (Mann *et al.*, 2017).

One of the most significant consequences of climatic variation is its impact on ecosystems and biodiversity. Rising temperatures and changing precipitation patterns are altering the distribution and abundance of flora and fauna, potentially threatening the survival of many species (Hansen *et al.*, 2016). Moreover, climatic variation is also affecting the frequency and severity of natural disasters, such as floods, droughts, and heatwaves, which can have devastating impacts on human populations and infrastructure (UNISDR, 2015).

In addition to its environmental impacts, climatic variation also has significant social and economic implications. Changes in climate parameters are affecting agricultural productivity, water availability, and human health, potentially threatening the livelihoods of millions of people (WHO, 2018). Moreover, the impacts of climatic variation are often disproportionately felt by vulnerable populations, including the poor, women, and children, who may lack the resources and capacity to adapt to changing climate conditions (IPCC, 2014). In India, approximately 60% of agricultural land relies on rainfall, making it highly susceptible to the impacts of climate change. Furthermore, with 80% of Indian farmers being small and marginal, they face significant challenges in adapting to climate-related phenomena, including extreme events like droughts, floods, and cyclones (Sarma P.K. (2019).

Vegetation is a vital component of the terrestrial biosphere, playing a central role in regulating climate through the exchange of energy, carbon, and water with the atmosphere. Over recent decades, alterations in land use and increasing climate variability have disrupted these interactions, affecting the Earth's energy balance. Among climatic variables, temperature and precipitation are the primary drivers of

vegetation growth and distribution. However, other environmental factors, such as soil moisture, solar radiation, atmospheric CO_2 concentration, and nutrient availability, also significantly influence plant dynamics (Parida *et al.*, 2020).

In India, the southwest monsoon (June–September) delivers over 75% of the country's annual rainfall, making vegetation growth highly sensitive to monsoon variability. Variations in rainfall not only impact agricultural productivity but also forest ecosystems and freshwater resources. Furthermore, the spatial distribution of precipitation is modulated by the complex orographic features of the Indian subcontinent, including the Himalayas, Karakoram, and Hindukush mountain ranges (Parida *et al.*, 2020).

Rising global temperatures are already exerting considerable stress on vegetation across India. Changes in temperature influence plant phenology, altering the timing of critical biological events such as flowering, fruiting, and leaf senescence. Increased heat can cause physiological stress, lowering plant productivity and disrupting ecological interactions, such as those between plants and pollinators. Concurrently, changes in rainfall patterns—especially delayed monsoons, seasonal droughts, and extreme precipitation—further exacerbate these impacts. Prolonged dry spells reduce water availability and hinder nutrient uptake, while intense rainfall leads to soil erosion and degradation of plant habitats (Verma & Sahu, 2021).

Globally, climate change—particularly temperature increases, altered precipitation regimes, and land use changes—has led to notable transformations in vegetation structure and distribution. However, the degree of impact varies locally, depending on factors such as topography, soil type, elevation, and slope orientation. Even minor elevational gradients can influence vegetation due to their effects on microclimate and evapotranspiration. In the Indian context, a strong correlation between rainfall variability and vegetation dynamics has been well documented, highlighting the high sensitivity of ecosystems to monsoon fluctuations (Banerjee *et al.*, 2023).

Vegetation also plays a crucial ecological role by controlling soil erosion, enhancing carbon sequestration, and moderating climate. Through interception of rainfall and

regulation of surface runoff, vegetation helps maintain soil integrity and fertility. However, land degradation due to deforestation, overgrazing, and unsustainable land use can exacerbate erosion, alter surface albedo, and disturb local and regional climate systems (Vishvendra Raj Singh *et al.*, 2024).

Temperature variations influence vegetation both directly and indirectly. Elevated temperatures can increase evapotranspiration, leading to soil moisture depletion and impaired nutrient absorption. These changes may disturb species interactions, including those involving fauna, and may shift plant community compositions. Similarly, altered rainfall regimes can disrupt nutrient cycling in the soil, affecting plant health and ecosystem resilience (Gupta & Gupta, 2024).

3.2. Regional studies on Climate-Vegetation Linkages

In Northeast India, and particularly Nagaland, vegetation systems are highly sensitive to climatic fluctuations. The region's dependence on the southwest monsoon, which accounts for over 75% of annual rainfall, makes it particularly vulnerable to shifts in monsoon onset and intensity. Studies have reported increasing irregularities in rainfall, including delayed monsoons and growing incidence of drought and extreme precipitation events, all of which negatively affect vegetation health and productivity (Jamir *et al.*, 2023; Maharana et al., 2021).

A study using 10-day SPOT-Vegetation NDVI time-series data (1998–2013) in Northeast India identified a negative correlation between NDVI and precipitation during the monsoon season. This counterintuitive result suggests that excessive rainfall may suppress vegetation greenness due to cloud cover, waterlogging, and reduced solar radiation, thereby limiting photosynthesis (Changkakati, 2019). These findings challenge conventional assumptions and emphasize the need for region-specific analyses of vegetation-climate interactions.

Temperature variability has also been shown to affect vegetation in the region. Higher temperatures contribute to increased evapotranspiration and plant stress, while also disturbing phenological processes and species interactions (Banerjee *et al.*, 2023). Additionally, even slight changes in elevation and slope orientation

significantly affect vegetation patterns by altering microclimatic conditions, such as moisture availability and solar exposure (Liu *et al.*, 2022; Sharma *et al.*, 2014).

The Northeast region, characterized by a subtropical climate and an average annual rainfall of about 2450 mm, is experiencing increasing climatic stress. The southwest monsoon typically begins in mid-May and continues through October. However, recent patterns indicate more erratic rainfall, delayed monsoon onset, and increasing frequency of seasonal droughts, all of which are impacting rice cultivation and broader agricultural productivity in the region (Jamir *et al.*, 2023).

A study conducted in the Brahmaputra Basin revealed that farmers associate climate change with an increase in floods, landslides, droughts, and outbreaks of crop and livestock diseases. Projections suggest that climate change may reduce India's agricultural productivity by 4.5% to 9% annually between 2020 and 2039, which could lead to a corresponding annual GDP reduction of 0.7% to 1.35%. Perceptions from local communities also indicate growing climate-related challenges. (Baraj *et al.*, 2024).

Rainfed agriculture in Northeast India, including in Nagaland, is particularly vulnerable to both climatic and anthropogenic pressures. Between 2001 and 2020, the region experienced a forest cover decline of 5–14%, with Nagaland alone losing approximately 17% of its forests—the highest rate of decline during this period. This widespread deforestation, driven by shifting cultivation and land use change, further exacerbates the region's vulnerability to climate change by degrading ecosystem services and weakening the landscape's resilience (Lotha *et al.*, 2024)

Vulnerability assessment in the region remains challenging due to data limitations and the complexity of climate-vegetation interactions. IMD's 2018 analysis revealed declining rainfall trends across Nagaland, Manipur, Arunachal Pradesh, Mizoram, and Tripura. Increasing aridity, coupled with temperature rise and humidity decline, has caused unpredictable shifts in the monsoon system (Lotha *et al.*, 2024). These changes, alongside continued deforestation, threaten the ecological stability of the region. Forests in Nagaland and the wider Northeast not only support biodiversity but

also play a critical role in climate mitigation through carbon sequestration. Enhancing forest carbon stocks and curbing deforestation are therefore essential components of any climate-resilient strategy in the region. Although Nagaland is situated within the ecologically significant Hindu Kush Himalaya (HKH) mountain system and encompasses the globally recognized Naga-Manipuri-Chin Hills Moist Forests eco-region, there remains a notable absence of region-specific data on the impacts of climate change on its forest ecosystems. This knowledge gap is concerning, given projections of rising temperatures, erratic and extreme rainfall events, and monsoon-season droughts. Such climatic shifts are expected to alter vegetation dynamics, placing additional stress on water resources, biodiversity, and the livelihoods of rural communities (Meru & Pandey, 2024).

Understanding the gap in the existing research database, the current study investigates the impact of climatic change on vegetation dynamics in Nagaland over the past two decades using advanced remote sensing and Geographic Information System (GIS) technologies. The study involves analyzing historical climatic data, including temperature and precipitation collected from 17 weather stations scattered across the state. Geospatial data mainly in the form of Land Use-Land Cover data is integrated to provide a better perspective of the region's environmental dynamics. Geographic Information System (GIS) tools are used to map and visualize these climatic trends and their spatial distribution. Analysis is conducted to identify significant trends, patterns, and anomalies in the climatic data. Geospatial analysis, which combines geographic information systems (GIS), remote sensing, and spatial analysis, offers a powerful tool for understanding the complex relationships between climate, environment, and human populations (Nabizada *et al.*, 2022). By analyzing spatial data and trends over the past 20 years, this research aims to provide insights into the impacts of climatic variation on Nagaland's environment and ecosystems.

3.3. Climatic Characteristics of Nagaland

The analysis of rainfall and temperature data from the Department of Soil and Water Conservation, Nagaland was processed as indicated in the earlier chapter which upon further analysis revealed significant trends and patterns.

3.3.1 Rainfall Pattern Analysis

The monthly rainfall averages showed a peak during the monsoon season (June-September), with the highest average rainfall recorded in Wokha station in the year 2007 (2878.1 mm). The dry season (October-May) exhibited relatively low rainfall averages, with the lowest average rainfall recorded in Sechu Station in the year 2012 (228.8 mm).

The annual rainfall averages indicated an increasing trend over the study period (2001-2021), with an average annual rainfall of 1551.329 mm with an exception of Zunheboto station which showed a decreasing rainfall pattern ranging from over 2000mm in 2002 to 1276mm in 2021. The Coefficient of Variation (CV) for annual rainfall for entire state was 22.69%, indicating high variability while the highest CV was shown in Zunheboto station with 37.54% indicating high variability and lowest CV was shown in Mangkolemba with 15.09%, indicating moderate variability.

3.3.2 Temperature Pattern Analysis

The analysis of temperature data revealed a warming trend over the study period. The monthly average temperature showed a peak during the summer season (April-June), with the highest average temperature recorded in Mon station in the year 2009 (39.99°C). The winter season (December-February) exhibited relatively low average temperatures, with the lowest average temperature recorded in Zunheboto station in the year 2005 (13.03°C).

The CV for annual temperature for Nagaland was 6.31% while the highest CV was shown in Mon station with 19.55% and lowest CV was shown in Mangkolemba with 2.19%.

3.4. Station-wise temperature-rainfall pattern analysis.

3.4.1. Key Observations from Bhandari Climatological Data

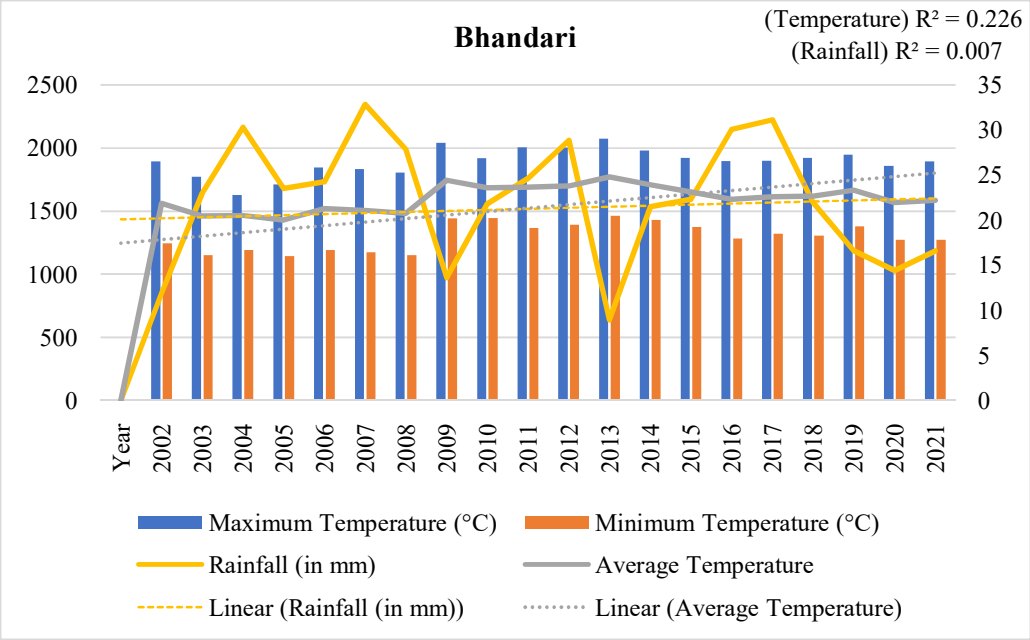

Figure 14 Time series of rainfall (mm) and Temperature (°C) data for Bhandari station, Nagaland.

Temperature Trends

- Visual Pattern: Maximum and Minimum Temperatures fluctuate annually but generally show a gradual increase over time.
- Statistical Insight: The Average Temperature also shows a slight upward trend, supported by the linear trend line with an R^2 value of 0.226. This indicates a moderate correlation, suggesting that average temperatures have increased over the two-decade period, though not dramatically.

Rainfall Trends

- Visual Pattern: Rainfall values vary significantly year to year, with no clear upward or downward pattern.
- Statistical Insight: The linear trend line for rainfall has an R^2 value of just 0.007, indicating almost no correlation or trend, rainfall has remained highly variable and unpredictable.

3.4.2. Key Observations from Dimapur Climatological Data

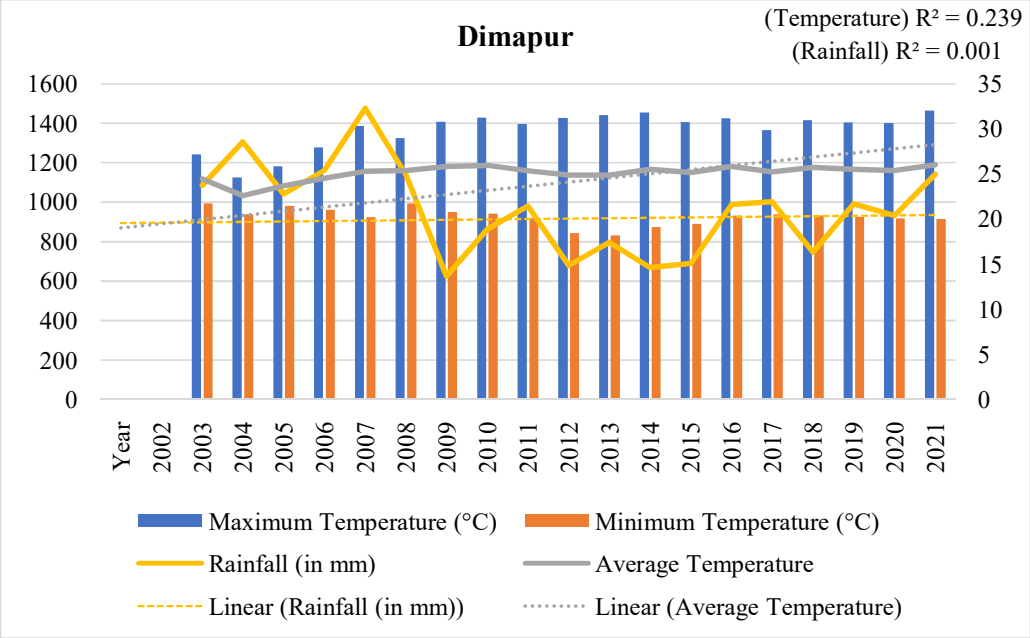

Figure 15 Time series of rainfall (mm) and Temperature (°C) data for Dimapur station, Nagaland.

Temperature Trends

- Visual Pattern: Minimum, maximum and average temperature all show a gradual increase over time.
- Statistical Insight: The R^2 value of 0.239 for the average temperature trend suggests a moderate positive correlation, indicating a warming trend across the study period.

Rainfall Trends

- Visual Pattern: Rainfall values show high interannual variability, with no consistent upward or downward trend.
- Statistical Insight: The R^2 value of 0.001 for the rainfall trend line indicates virtually no correlation, suggesting that rainfall patterns have remained erratic and unpredictable over the two-decade period.

3.4.3. Key Observations from Jalukie Climatological Data

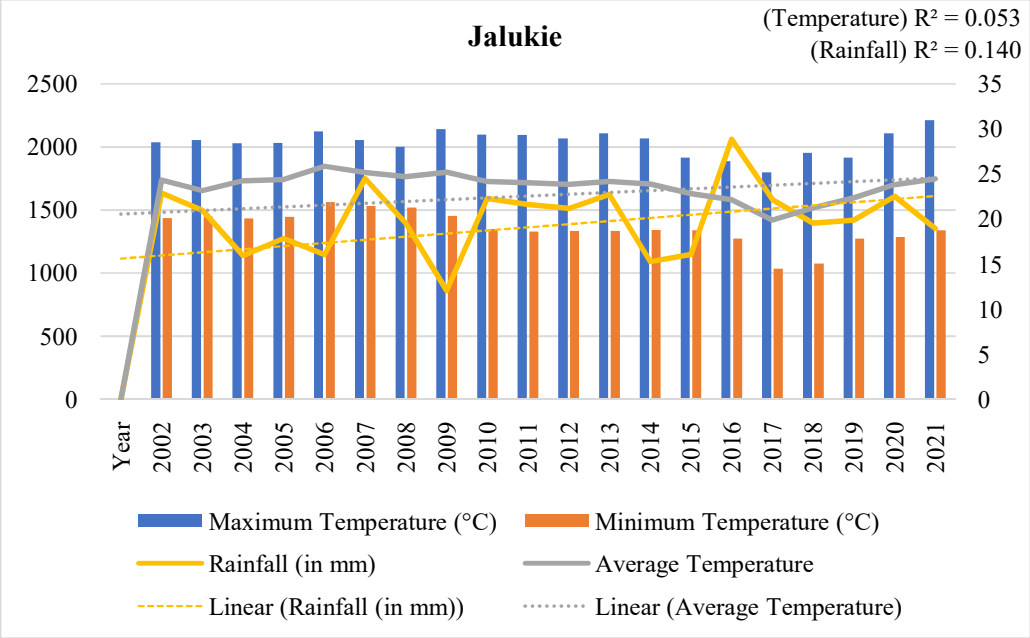

Figure 16 Time series of rainfall (mm) and Temperature (°C) data for Jalukie station, Nagaland.

Temperature Trends

- Visual Pattern: Maximum, minimum, and average temperature show minor fluctuations, with no strong upward or downward trend.
- Statistical Insight: The R^2 value of 0.053 for the average temperature trend line indicates a very weak correlation, suggesting minimal change in temperature over the study period.

Rainfall Trends

- Visual Pattern: Rainfall shows notable year-to-year variability, with some years experiencing sharp peaks and others marked by significant declines.
- Statistical Insight: The R^2 value of 0.140 for the rainfall trend line suggests a weak correlation, indicating a slight downward trend in rainfall over the two-decade period.

3.4.4. Key Observations from Kiphire Climatological Data

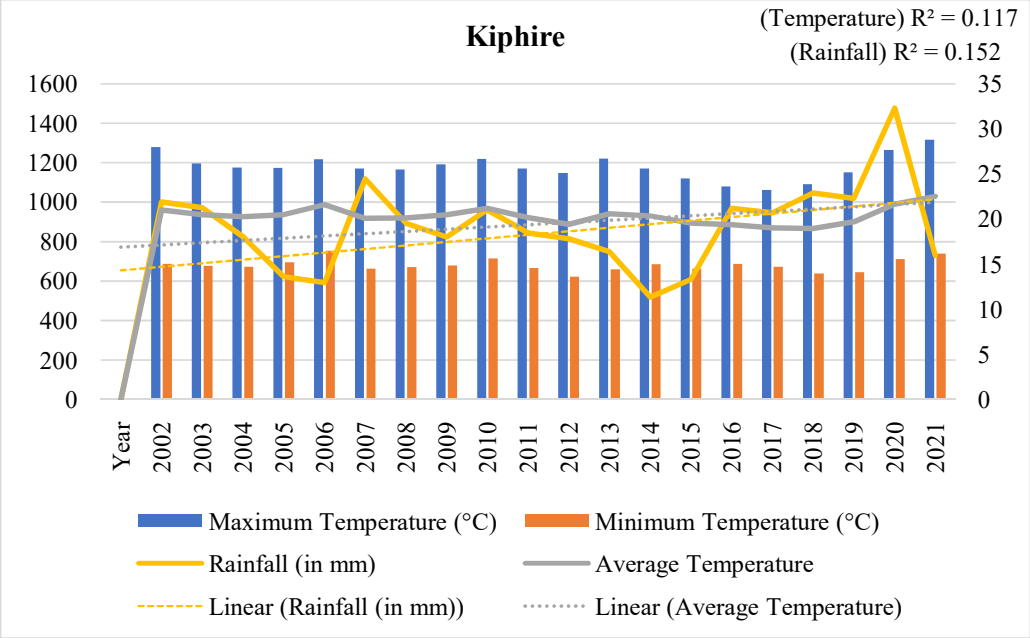

Figure 17 Time series of rainfall (mm) and Temperature (°C) data for Kiphire station, Nagaland.

Temperature Trends

- Visual Pattern: Maximum, minimum and average temperature show minor fluctuations, with a slight upward trajectory.
- Statistical Insight: The R^2 value of 0.117 for the average temperature trend indicates a weak positive correlation, suggesting a modest warming trend.

Rainfall Trends

- Visual Pattern: Rainfall shows noticeable interannual variability, with alternating periods of high and low precipitation.
- Statistical Insight: The R^2 value of 0.152 for the rainfall trend line suggests a weak downward trend, indicating a gradual decline in rainfall over the two-decade period.

3.4.5. Key Observations from Kohima Climatological Data

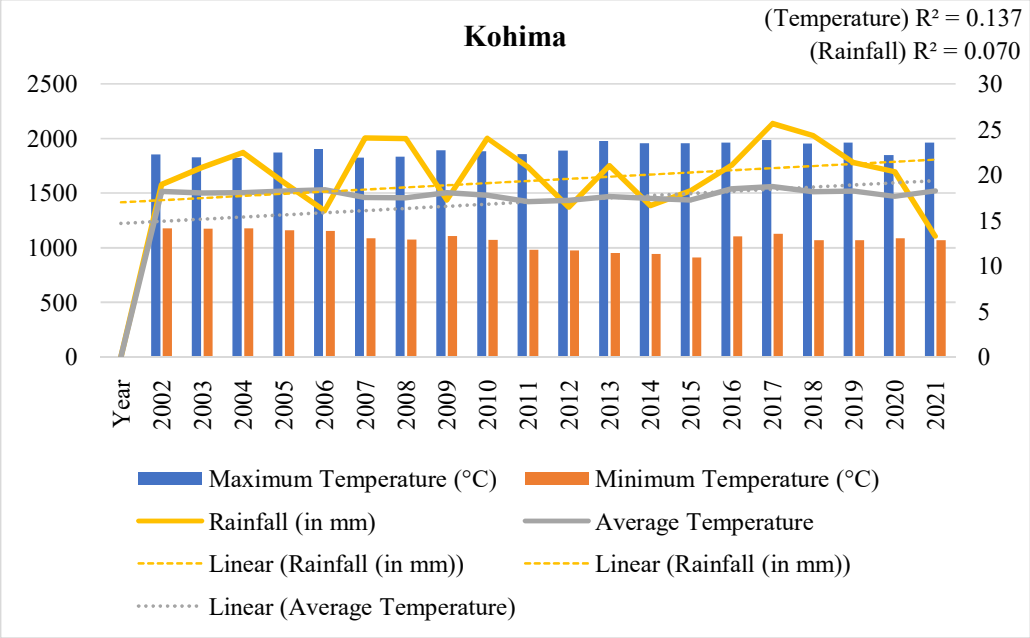

Figure 18 Time series of rainfall (mm) and Temperature (°C) data for Kohima station, Nagaland.

Temperature Trends

- Visual Pattern: Maximum temperature, minimum temperature, and average temperature show minor fluctuations with a gentle upward trajectory in the average temperature. The dotted trendline indicates a slight warming pattern over time.
- Statistical Insight: The R^2 value of 0.137 for the average temperature trendline suggests a weak positive correlation, indicating a modest warming trend across the two-decade period.

Rainfall Trends

- Visual Pattern: Rainfall displays high interannual variability, with alternating periods of elevated and reduced precipitation. The dotted trendline shows a slight upward slope, though visually overshadowed by fluctuations.
- Statistical Insight: The R^2 value of 0.070 for the rainfall trendline reflects a very weak positive correlation, suggesting no strong directional change in rainfall, but rather stochastic variability.

3.4.6. Key Observations from Longleng Climatological Data

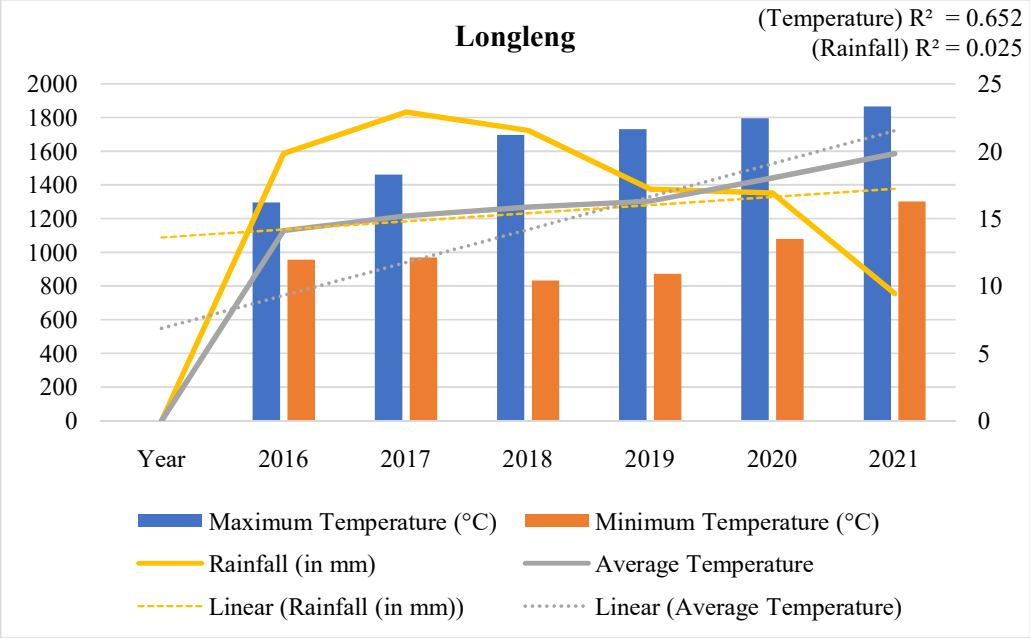

Figure 19 Time series of rainfall (mm) and Temperature (°C) data for Longleng station, Nagaland.

Temperature Trends

- Visual Pattern:Maximum temperature, minimum temperature and average temperature show a clear upward trajectory, with relatively consistent year-to-year increases. The dashed trendline for average temperature reinforces this visual pattern of warming.
- Statistical Insight: The R^2 value of 0.652 for the average temperature trendline indicates a strong positive correlation, suggesting a significant warming trend over the six-year period.

Rainfall Trends

- Visual Pattern: Rainfall exhibits high interannual variability, with no consistent directional pattern. Peaks and troughs alternate irregularly, and the dashed trendline appears nearly flat.
- Statistical Insight: The R^2 value of 0.025 for the rainfall trendline reflects a very weak correlation, indicating no meaningful trend in rainfall over the observed period.

3.4.7. Key Observations from Mangkolemba Climatological Data

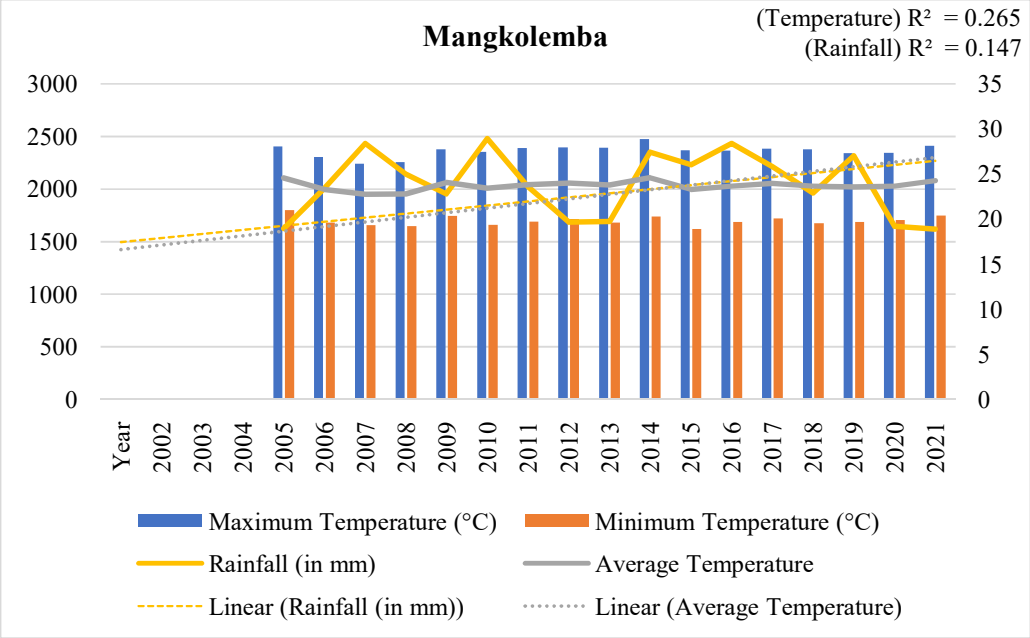

Figure 20 Time series of rainfall (mm) and Temperature (°C) data for Mangkolemba station, Nagaland.

Temperature Trends

- Visual Pattern: Maximum and minimum temperatures show moderate fluctuations across the years, while the average temperature line exhibits a gentle upward trajectory. The linear trendline for average temperature suggests a gradual warming pattern.
- Statistical Insight: The R^2 value of 0.265 for the average temperature trendline indicates a moderate positive correlation, suggesting a discernible warming trend over the two-decade period.

Rainfall Trends

- Visual Pattern: Rainfall data shows notable interannual variability, with alternating periods of high and low precipitation. The linear trendline for rainfall appears slightly declining, though masked by fluctuations.
- Statistical Insight: The R^2 value of 0.147 for the rainfall trendline reflects a weak negative correlation, suggesting a gradual decline in rainfall over the observed period.

3.4.8. Key Observations from Meluri Climatological Data

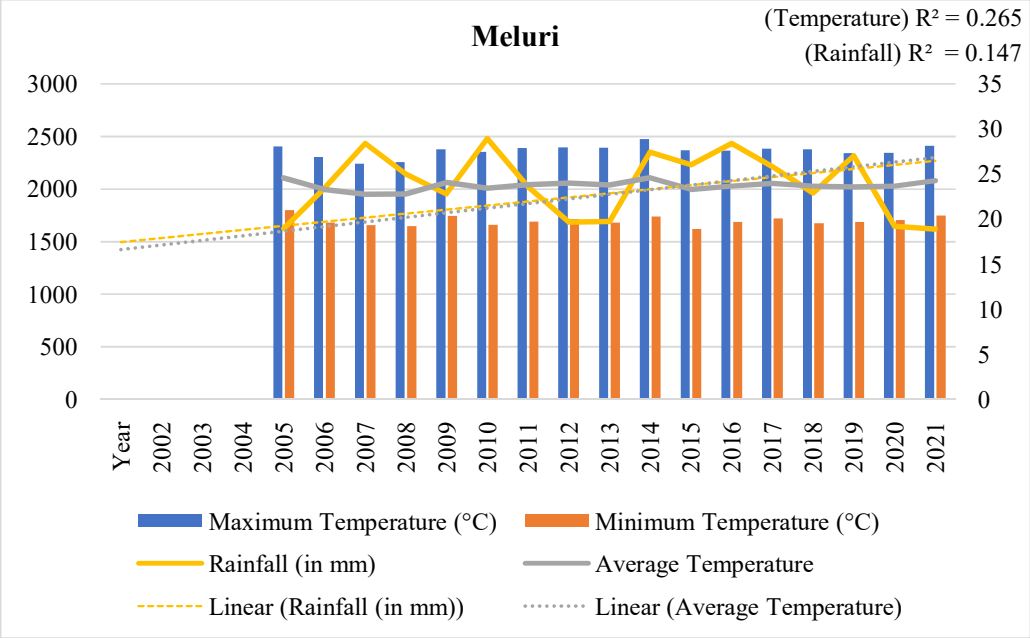

Figure 21 Time series of rainfall (mm) and Temperature (°C) data for Meluri station, Nagaland.

Temperature Trends

- Visual Pattern: Maximum and minimum temperatures show moderate fluctuations across the years, while the average temperature line reveals a gradual upward trajectory. The linear trendline for average temperature supports a warming pattern over the observed period.
- Statistical Insight: The R^2 value of 0.265 for the average temperature trendline indicates a moderate positive correlation, suggesting a discernible warming trend across the two-decade span.

Rainfall Trends

- Visual Pattern: Rainfall data exhibits notable interannual variability, with alternating periods of high and low precipitation. The linear trendline for rainfall appears slightly declining, though the variability masks any strong directional pattern.
- Statistical Insight: The R^2 value of 0.147 for the rainfall trendline reflects a weak negative correlation, indicating a gradual decline in rainfall over the study period.

3.4.9. Key Observations from Mokokchung Climatological Data

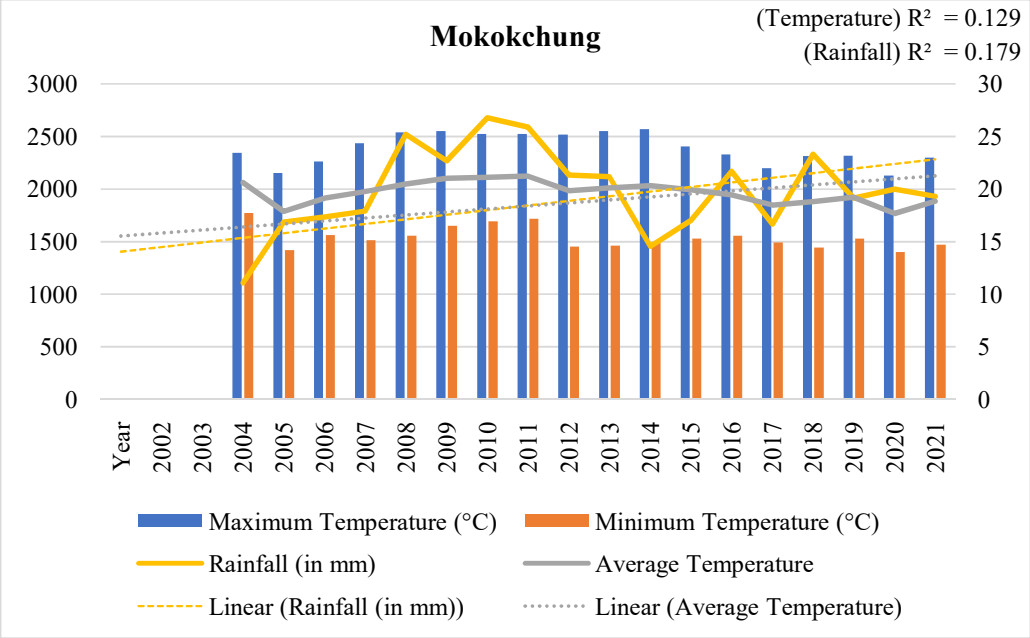

Figure 22 Time series of rainfall (mm) and Temperature (°C) data for Mokokchung station, Nagaland.

Temperature Trends

- Visual Pattern: Maximum and minimum temperatures show minor fluctuations across the years, while the average temperature line reveals a slight upward trajectory. The linear trendline for average temperature suggests a gradual warming pattern.
- Statistical Insight: The R^2 value of 0.129 for the average temperature trendline indicates a moderate positive correlation, suggesting a slight warming trend over the two-decade period.

Rainfall Trends

- Visual Pattern: Rainfall data shows noticeable interannual variability, with alternating periods of high and low precipitation. The linear trendline for rainfall appears slightly declining, though the variability masks any strong directional pattern.
- Statistical Insight: The R^2 value of 0.179 for the rainfall trendline reflects a weak negative correlation, suggesting a slight decline in rainfall over the observed period.

3.4.10. Key Observations from Mon Climatological Data

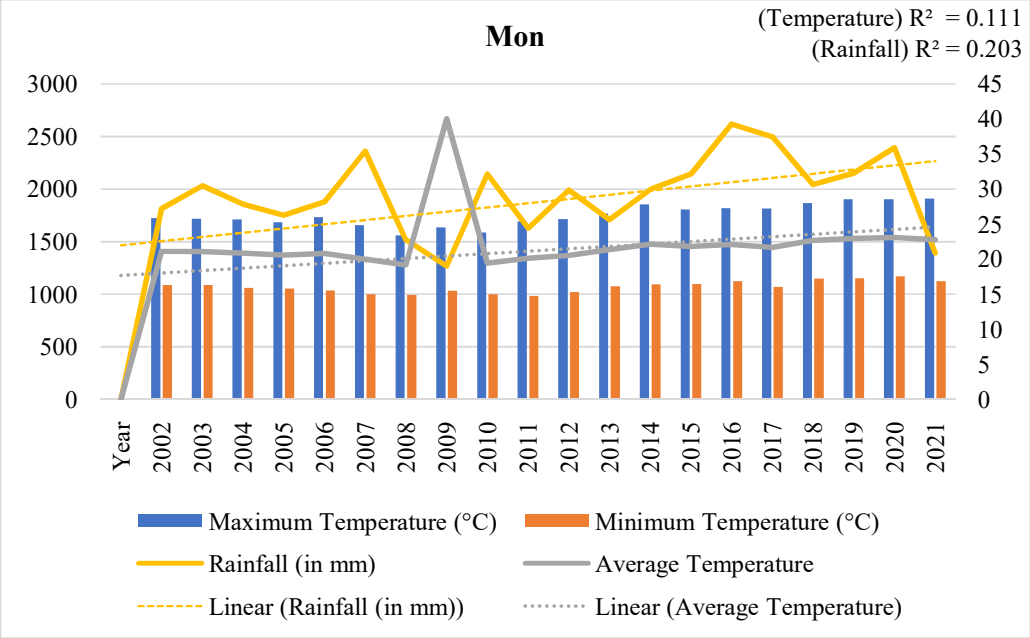

Figure 23 Time series of rainfall (mm) and Temperature (°C) data for Mon station, Nagaland.

Temperature Trends

- Visual Pattern: Maximum and minimum temperatures show minor fluctuations across the years, while the average temperature line reveals a slight upward trajectory. The linear trendline for average temperature suggests a gradual warming pattern.
- Statistical Insight: The R^2 value of 0.111 for the average temperature trendline indicates a weak positive correlation, suggesting a slight warming trend over the two-decade period.

Rainfall Trends

- Visual Pattern: Rainfall data exhibits noticeable interannual variability, with alternating periods of high and low precipitation. The linear trendline for rainfall appears slightly declining, though variability dominates the pattern.
- Statistical Insight: The R^2 value of 0.203 for the rainfall trendline reflects a weak negative correlation, suggesting a slight decline in rainfall over the observed period.

3.4.11. Key Observations from Phek Climatological Data

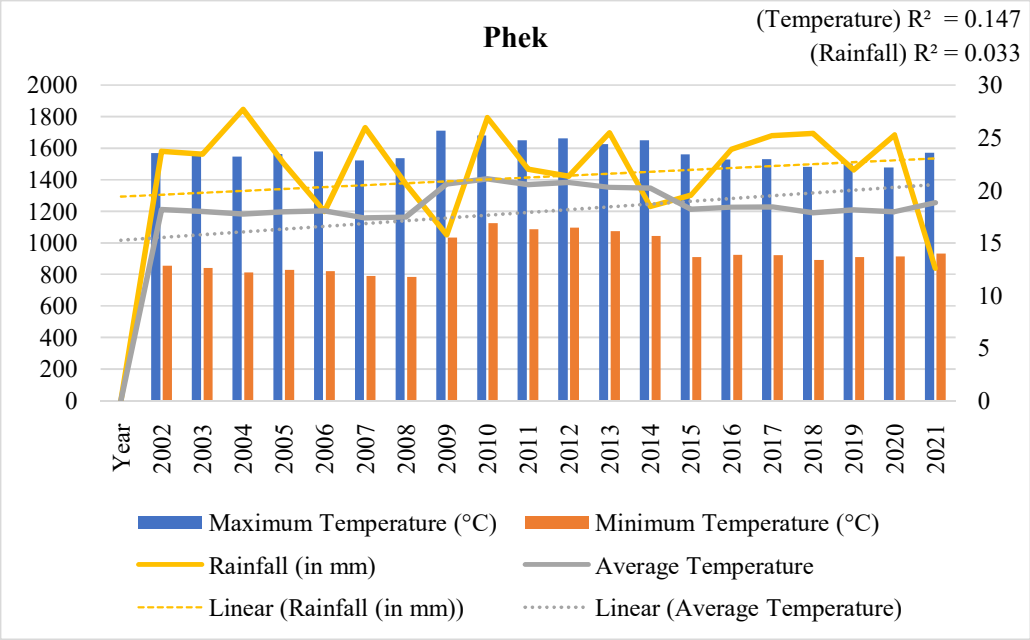

Figure 24 Time series of rainfall (mm) and Temperature (°C) data for Phek station, Nagaland.

Temperature Trends

- Visual Pattern: Maximum and minimum temperatures show minor fluctuations across the years, while the average temperature line reveals a slight upward trajectory. The linear trendline for average temperature suggests a gradual warming pattern.
- Statistical Insight: The R^2 value of 0.147 for the average temperature trendline indicates a weak positive correlation, suggesting a slight warming trend over the two-decade period.

Rainfall Trends

- Visual Pattern: Rainfall data exhibits noticeable interannual variability, with alternating periods of high and low precipitation. The linear trendline for rainfall appears slightly declining, though variability dominates the pattern.
- Statistical Insight: The R^2 value of 0.033 for the rainfall trendline reflects a very weak negative correlation, suggesting a slight decline in rainfall over the observed period.

3.4.12. Key Observations from Sechu Climatological Data

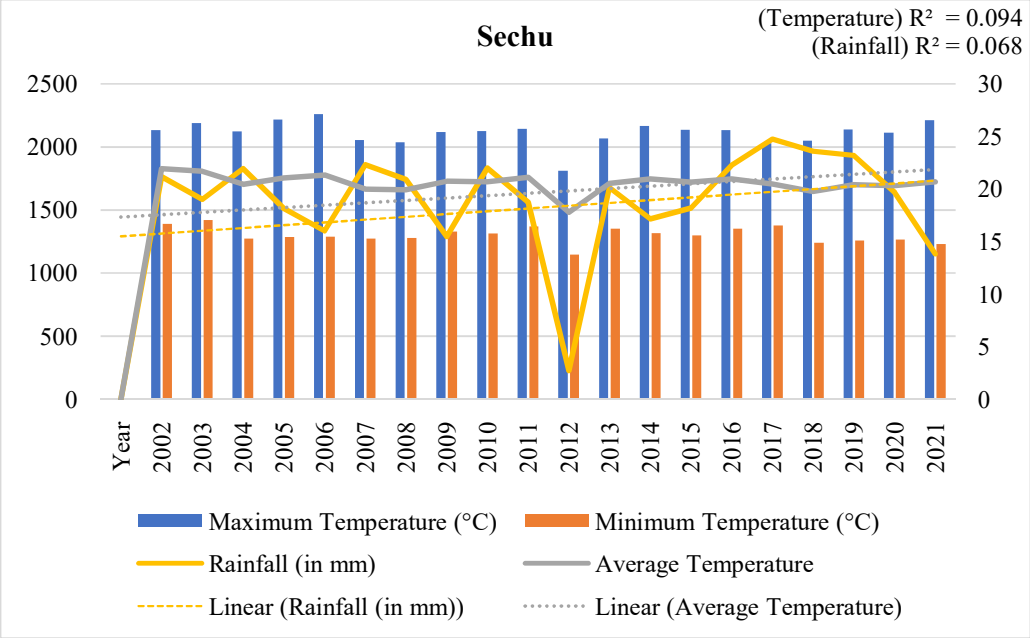

Figure 25 Time series of rainfall (mm) and Temperature (°C) data for Sechu station, Nagaland.

Temperature Trends

- Visual Pattern: Maximum and minimum temperatures exhibit minor fluctuations over the years, with average temperature showing a minimal upward trend, nearly constant. The linear trendline for average temperature suggests a very slight warming pattern.
- Statistical Insight: The R^2 value of 0.094 for the average temperature trendline indicates a very weak positive correlation, suggesting a negligible warming trend over the two-decade period.

Rainfall Trends

- Visual Pattern: Rainfall demonstrates noticeable interannual variability, characterized by alternating periods of high and low precipitation. The linear trendline for rainfall appears slightly declining, though the variability dominates the pattern.
- Statistical Insight: The R^2 value of 0.068 for the rainfall trendline reflects a very weak negative correlation, hinting at a negligible decline in rainfall across the observed span.

3.4.13. Key Observations from Shamator Climatological Data

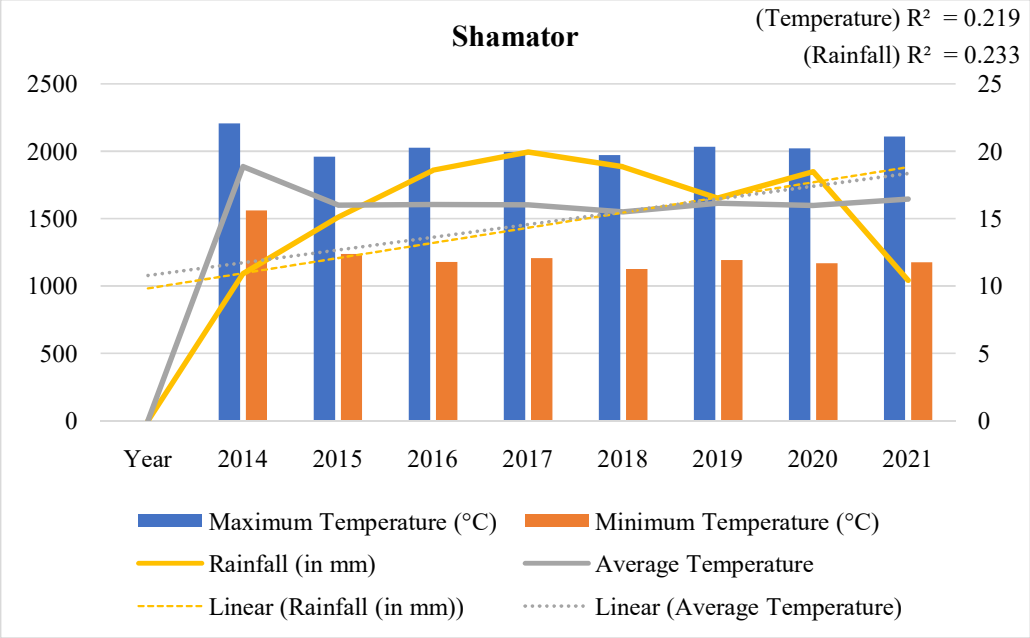

Figure 26 Time series of rainfall (mm) and Temperature (°C) data for Shamator station, Nagaland.

Temperature Trends

- Visual Pattern: Maximum and minimum temperatures show moderate fluctuations across the years, while the average temperature line reveals a gradual upward trajectory. The linear trendline for average temperature suggests a steady warming pattern.
- Statistical Insight: The R^2 value of 0.219 for the average temperature trendline indicates a moderate positive correlation, suggesting a gradual increase in temperature over the observed period.

Rainfall Trends

- Visual Pattern: Rainfall data exhibits alternating periods of abundance and reduction, with no consistent directional pattern. The linear trendline for rainfall shows a slight downward slope, though variability remains dominant.
- Statistical Insight: The R^2 value of 0.233 for the rainfall trendline reflects a moderate negative correlation, suggesting a marginal decline in precipitation over the eight-year span.

3.4.14. Key Observations from Tuensang Climatological Data

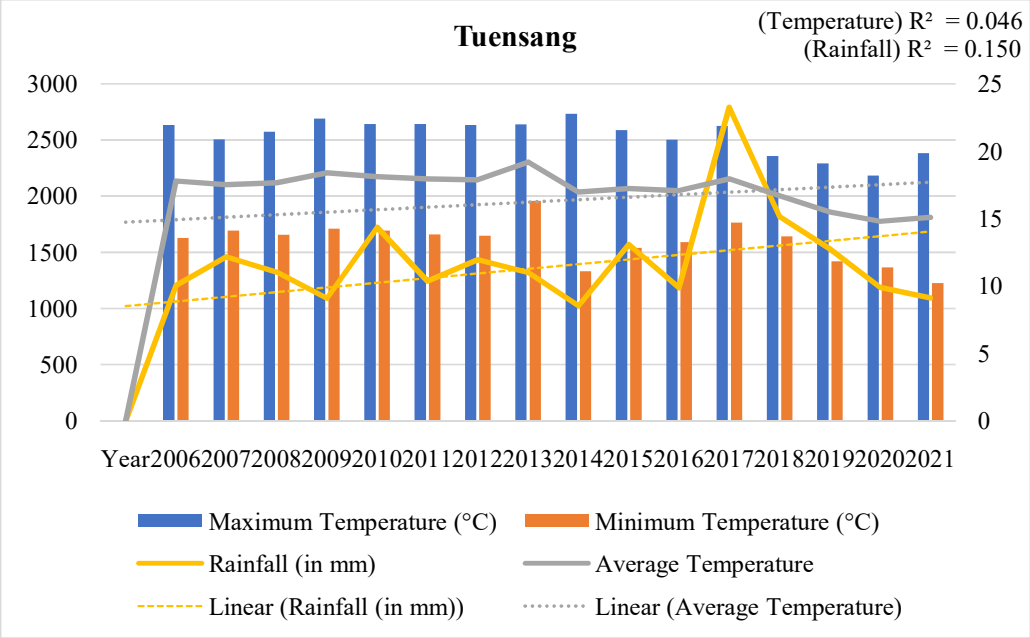

Figure 27 Time series of rainfall (mm) and Temperature (°C) data for Tuensang station, Nagaland.

Temperature Trends

- Visual Pattern: Maximum and minimum temperatures show moderate fluctuations across the years, while the average temperature line reveals a flat trajectory. The linear trendline for average temperature suggests temperature stagnancy.
- Statistical Insight: The R^2 value of 0.046 for the average temperature trendline indicates a very weak positive correlation, suggesting negligible warming over the observed period.

Rainfall Trends

- Visual Pattern: Rainfall data exhibits high variability, with alternating periods of abundant and reduced precipitation. The linear trendline for rainfall shows a slight downward trajectory, though variability remains dominant.
- Statistical Insight: The R^2 value of 0.150 for the rainfall trendline reflects a weak negative correlation, suggesting a gradual decline in precipitation over the observed period.

3.4.15. Key Observations from Tseminyu Climatological Data

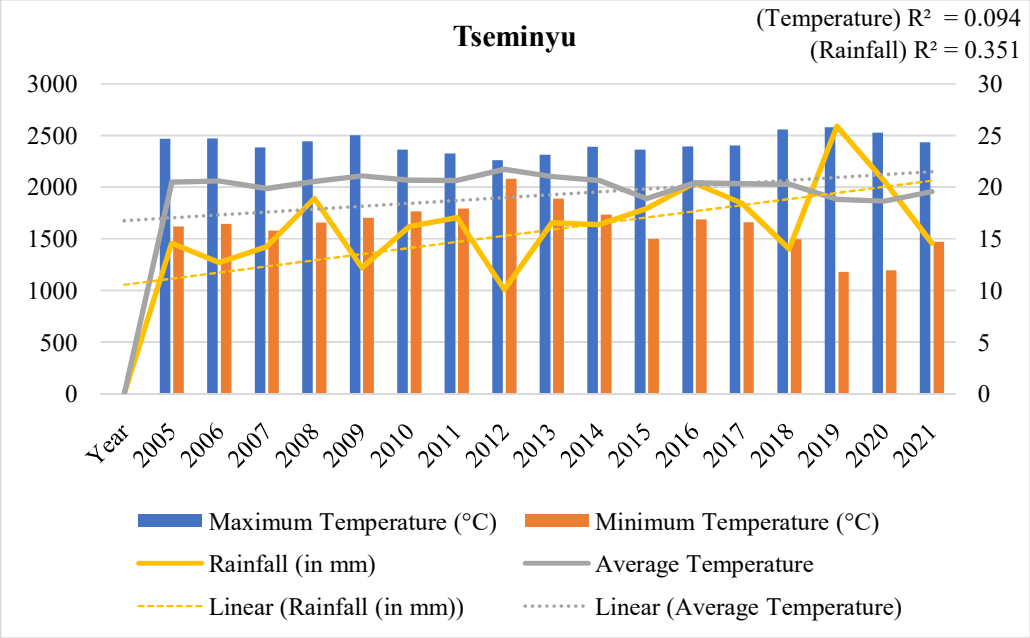

Figure 28 Time series of rainfall (mm) and Temperature (°C) data for Tseminyu station, Nagaland.

Temperature Trends

- Visual Pattern: Maximum and minimum temperatures show moderate fluctuations across the years, while the average temperature line reveals minor variation with a largely flat trajectory. The linear trendline for average temperature suggests temperature stagnation.
- Statistical Insight: The R^2 value of 0.094 for the average temperature trendline indicates a very weak positive correlation, suggesting negligible warming over the observed period.

Rainfall Trends

- Visual Pattern: Rainfall data exhibits high interannual variability, with alternating periods of elevated and reduced precipitation. The linear trendline for rainfall shows a slight downward slope, more pronounced than in other districts.
- Statistical Insight: The R^2 value of 0.351 for the rainfall trendline reflects a moderate negative correlation, suggesting a gradual decline in precipitation over the 16-year span.

3.4.16. Key Observations from Wokha Climatological Data

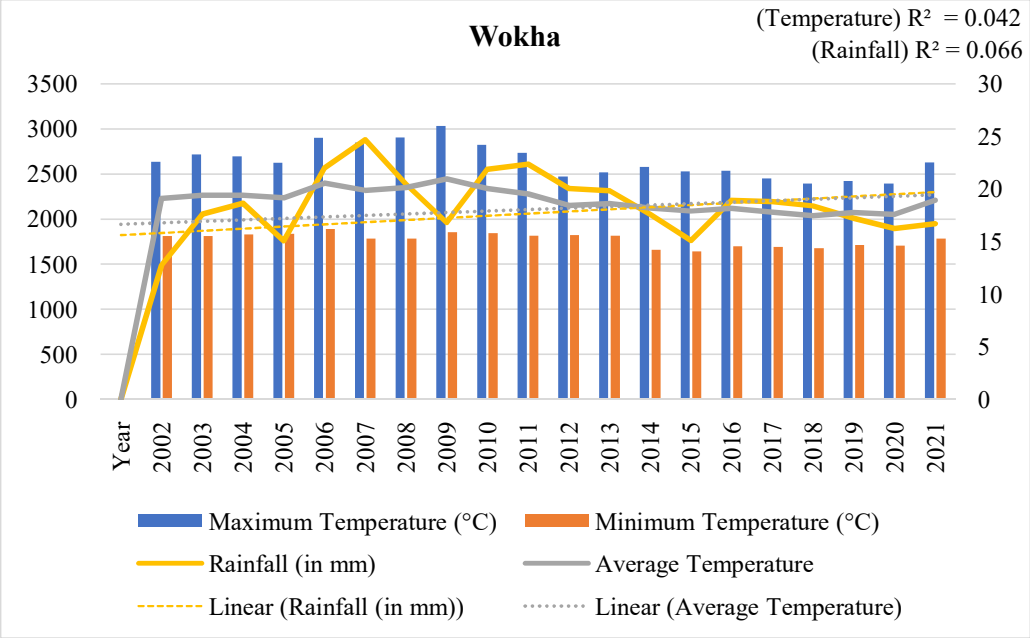

Figure 29 Time series of rainfall (mm) and Temperature (°C) data for Wokha station, Nagaland.

Temperature Trends

- Visual Pattern: Maximum and minimum temperatures show moderate fluctuations across the years, while the average temperature line remains largely flat, with no pronounced upward or downward trajectory. The linear trendline for average temperature suggests minimal change.
- Statistical Insight: The R^2 value of 0.042 for the average temperature trendline indicates a very weak positive correlation, suggesting negligible warming over the two-decade period.

Rainfall Trends

- Visual Pattern: Rainfall data exhibits high interannual variability, with alternating periods of elevated and reduced precipitation. The linear trendline for rainfall shows a slight downward slope, though variability dominates the pattern.
- Statistical Insight: The R^2 value of 0.066 for the rainfall trendline reflects a very weak negative correlation, suggesting a marginal decline in precipitation over the observed period.

3.4.17. Key Observations from Zunheboto Climatological Data

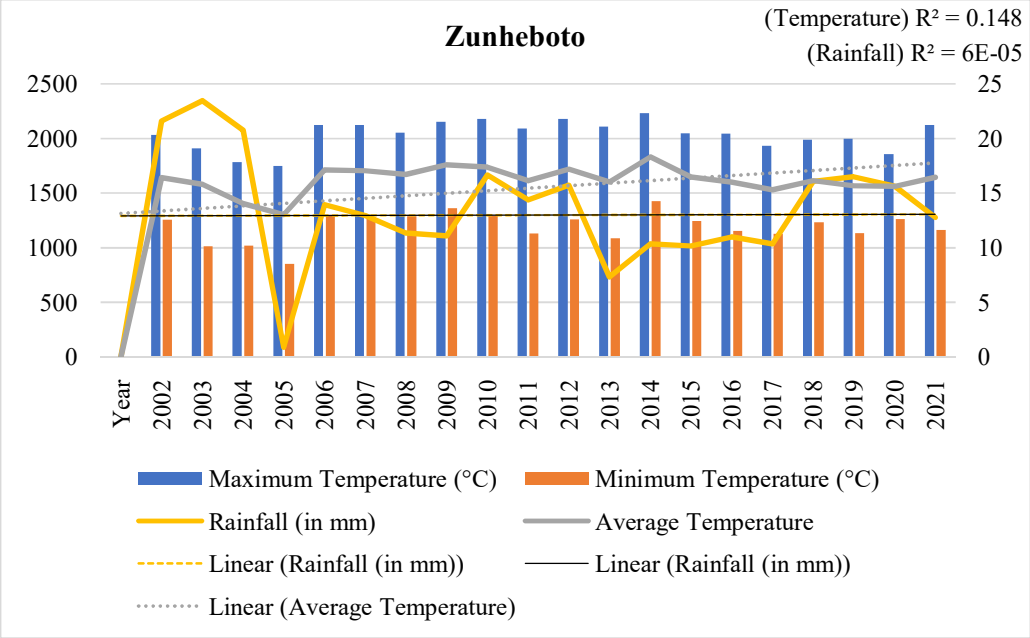

Figure 30 Time series of rainfall (mm) and Temperature (°C) data for Zunheboto station, Nagaland.

Temperature Trends

- Visual Pattern: Maximum and minimum temperatures show moderate fluctuations across the years, while the average temperature line reveals a slight upward trajectory. The linear trendline for average temperature suggests a gradual warming pattern.
- Statistical Insight: The R^2 value of 0.148 for the average temperature trendline indicates a weak positive correlation, suggesting a slight warming trend over the two-decade period.

Rainfall Trends

- Visual Pattern: Rainfall demonstrates high variability, with alternating periods of abundant and reduced precipitation. The linear trendline for rainfall appears nearly flat, with no discernible directional change.
- Statistical Insight: The R^2 value of 0.00006 for the rainfall trendline reflects a negligible correlation, indicating no meaningful trend in rainfall over the observed period.

3.5. Temperature-Rainfall Correlation Analysis

Table 9 R^2 (Coefficient of determination) for Rainfall and Temperature over the study period.

District	Temperature R^2	Rainfall R^2
Kohima	0.137	0.07
Longleng	0.652	0.025
Mangkolemba	0.265	0.147
Meluri	0.265	0.147
Mokokchung	0.129	0.179
Mon	0.111	0.203
Phek	0.147	0.033
Sechu	0.094	0.068
Shamator	0.219	0.233
Tuensang	0.046	0.15
Tseminyu	0.094	0.351
Wokha	0.042	0.066
Zunheboto	0.148	0.00006

Most districts show a slight to moderate warming trend in average temperature, with R^2 values ranging from ~0.04 to ~0.65. Districts like Longleng and Shamator, where the AWS has been installed only in the last decade show stronger warming signals, while places like Wokha and Tuensang exhibit near-stagnant temperature trends. This indicates that the warming trend is seen more in the past decade than over the last 20 years. Rainfall patterns are highly variable, with R^2 values mostly below 0.25 with most districts for e.g. Tseminyu, Shamator, showing a moderate decline.

The correlation analysis between rainfall and temperature revealed a significant negative correlation ($r = -0.042$, $p < 0.01$) between annual rainfall and temperature. This suggests that increased temperature is associated with decreased rainfall.

3.6. Temperature-Rainfall Spatial Analysis

The spatial analysis of rainfall and temperature data revealed significant variations across different districts of Nagaland. The Mangkolemba and Wokha stations received the highest average rainfall with over 2000mm, while the Kiphire and Dimapur received the lowest average rainfall of less than 1000mm. Similarly, Dimapur station experienced the highest average temperatures of 25.11°C while

Shamator station and Zunheboto station experienced the lowest average temperatures at 16.38°C and 16.22°C respectively.

3.7. LULC Trend Analysis

The LULC analysis for the years over 2000-2021 showed that except forest cover, grassland and water body, all other classes show an increasing trend. From 2005-2006 to 2020-2021, built-up increased by 0.57%, agricultural land increased by 3.08% and barren land increased by 4.64% while forest cover decreased drastically by 7.74%. The results indicate that the loss of forest cover is due to increase in built-up areas, agriculture and barren land.

Table 10 Time series Land Use Land Cover data as derived from the satellite imagery in %.

LULC	2005-2006 (%)	2011-2012 (%)	2015-2016 (%)	2020-2021 (%)
Built-up	2.19	2.12	2.21	2.76
Agricultural Land	11	10.69	9.03	14.08
Forest	73.69	71.45	68.8	65.95
Grassland	0.04	0.11	0.11	0.08
Barren Land	11.94	14.39	18.68	16.58
WaterBody	1.14	1.24	1.17	0.55
Total	100	100	100	100

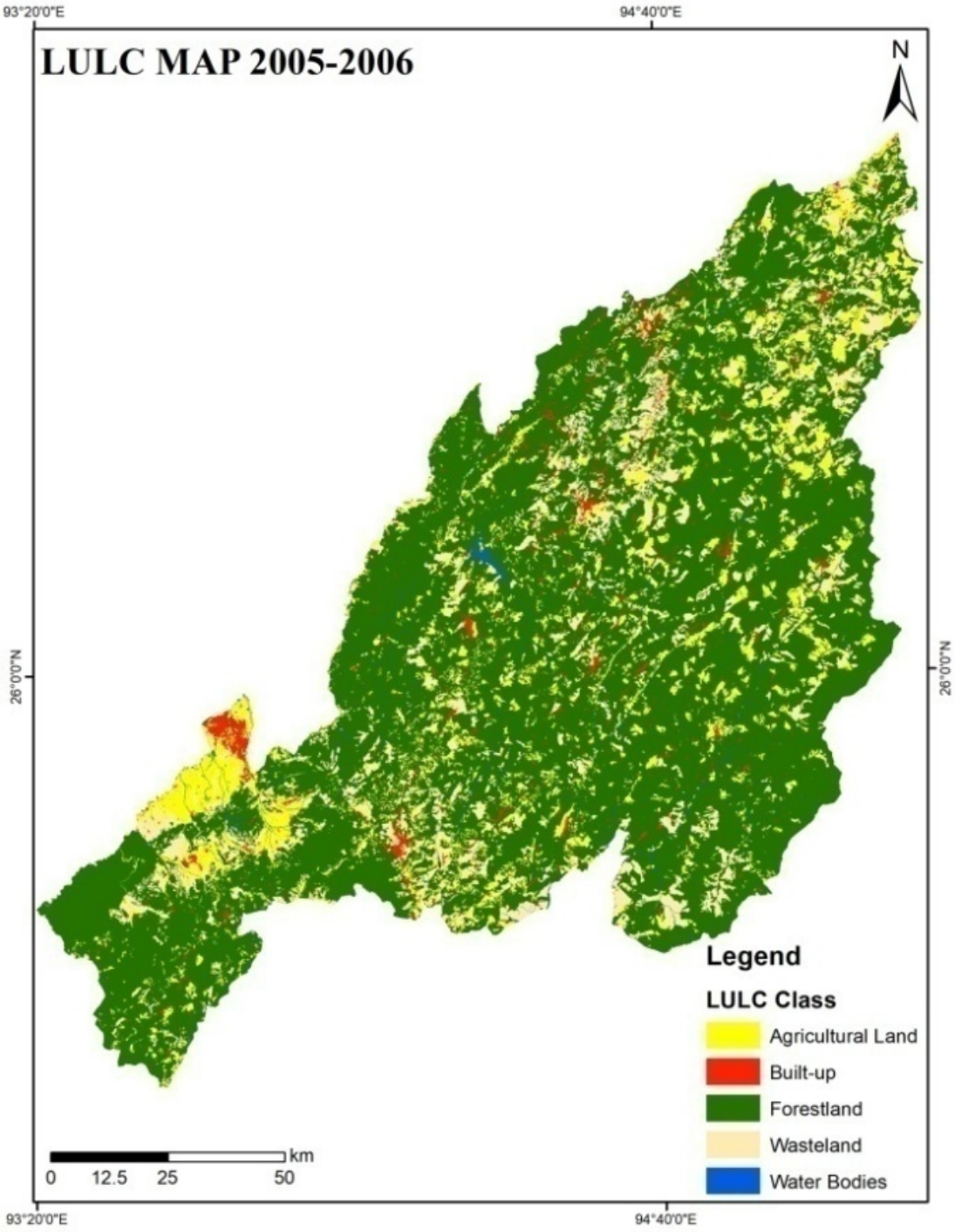

Figure 31 LULC Nagaland for the years 2005-2006

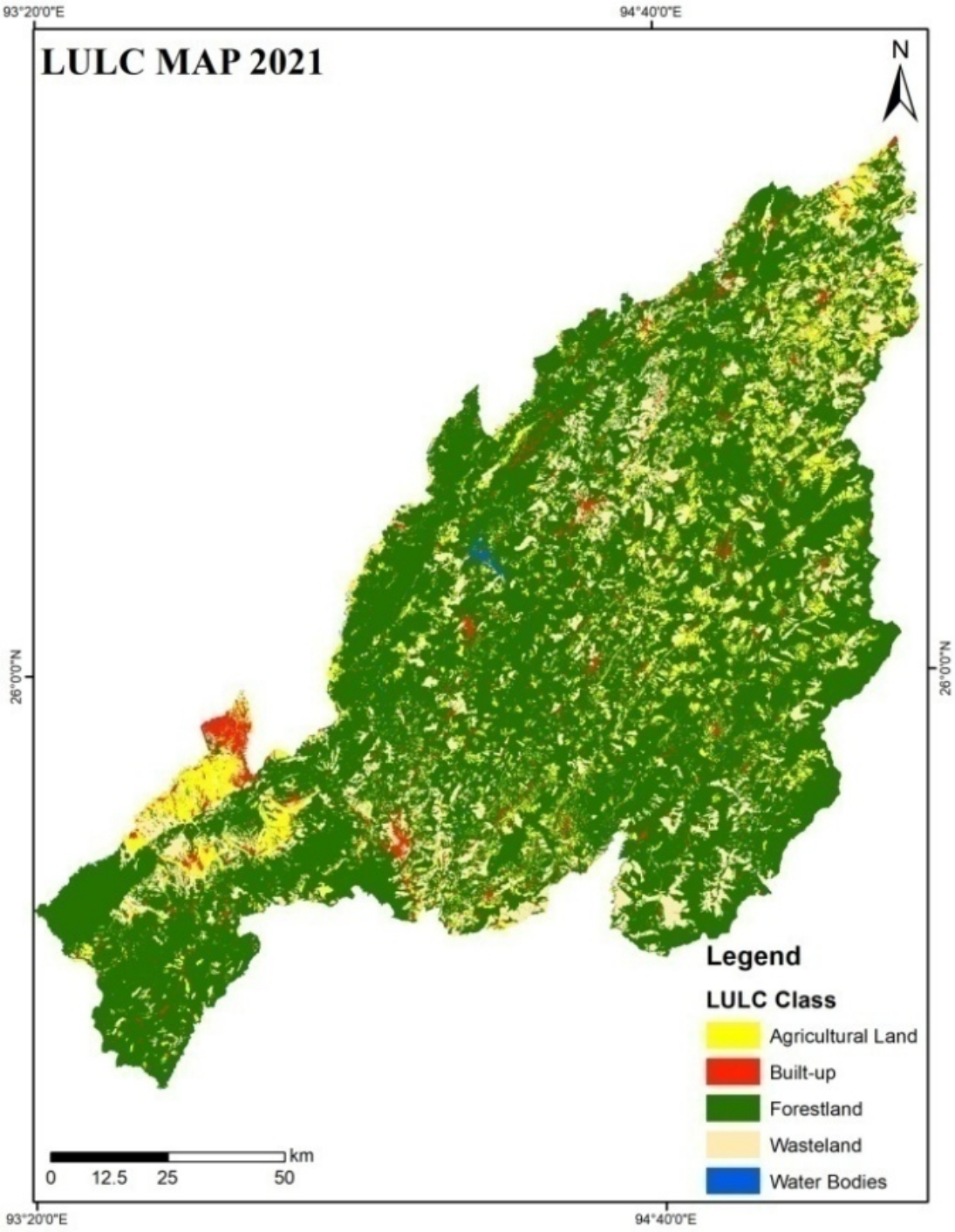

Figure 32 LULC Nagaland for the year 2021.

3.8. NDVI Trend Analysis

Table 11 Time series NDVI values as derived from the satellite imagery.

Year	NDVI Max	NDVI Min
2000	0.882353	-0.5528
2006	0.707317	-0.18367
2011	0.756522	-0.28571
2013	0.599242	-0.19912
2018	0.561767	-0.13275
2023	0.524726	-0.0694

The LULC derivation revealed that the NDVI values have been decreasing with time but with slight decrease in the year 2011. The coefficient of correlation (r) between precipitation and NDVI (r=0.19) shows a weak negative correlation. As precipitation increases, NDVI tends to decrease: There is a slight inverse relationship between the two variables. However, the relationship is weak, close to zero, indicating that the relationship is not strong. The relationship between precipitation and NDVI is not strong, indicating that other factors might have a more significant influence on vegetation health. Whereas, the correlation coefficient (r) of -0.81 between temperature and NDVI indicates a strong Negative Correlation indicating a strong inverse relationship between the two variables. The correlation coefficient is close to -1, indicating that the relationship is statistically significant and robust. A strong negative correlation (r = -0.81) suggests that Temperature has a profound impact on vegetation health with High temperatures strongly associating with decreased vegetation health, as measured by NDVI. The strong correlation between temperature and NDVI suggests that temperature might be a key factor influencing vegetation dynamics.

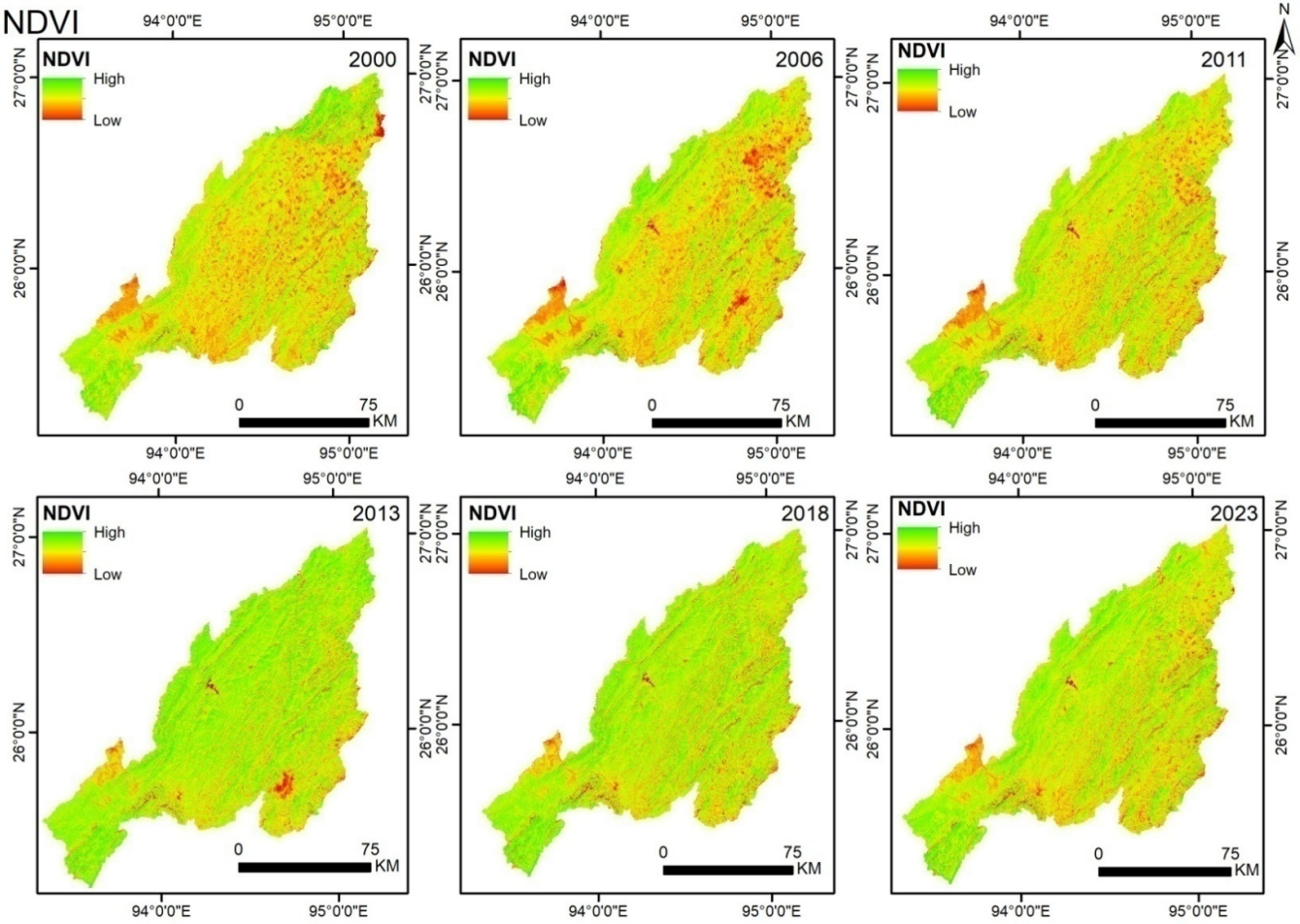

Figure 33 NDVI trend for Nagaland for the year 2000-2023.

CHAPTER 4

Chapter 4: Vegetation Analysis Using Recent Trends in Geospatial Indices by Integration of Remotely Sensed Data

4.1. Importance of Geospatial Indices for Vegetation Monitoring

Researchers have formulated vegetation indices (VIs) to enable both qualitative and quantitative assessment of vegetative cover through spectral reflectance measurements. The spectral signature of vegetated surfaces often reflects a complex mixture of vegetation type, soil properties, and atmospheric conditions, which must be carefully considered in index development and application (Abderrazak *et al.*, 1996).

Satellite-based remote sensing provides a cost-effective means of analyzing land cover over large geographic regions (Lu, 2006; Lunetta *et al.*, 2006). One of its key advantages lies in the ability to acquire and process time-series imagery, often freely available, which supports long-term ecological monitoring (Hame *et al.*, 1997). Landsat data, in particular, have been widely adopted due to their extensive historical archive, spanning over decades, and their utility in detecting land cover change with high precision. For example, Wilson and Sader (2002) successfully utilized multi-date Landsat imagery to identify forest transformations, demonstrating the effectiveness of VIs in capturing dynamic landscape patterns. The integration of such datasets into monitoring workflows is further facilitated by their accessibility and temporal depth (Nagendra *et al.*, 2013; Kefalas *et al.*, 2018).

In practice, vegetation indices are calculated using data collected from various remote sensing platforms, including satellites, drones, aerial systems, and ground-based sensors. These indices provide valuable insights into vegetation health, growth stages, and overall condition, making them indispensable tools in ecological monitoring (Vidican *et al.*, 2023). Remote sensing has emerged as a cornerstone in ecological research and resource management, offering robust capabilities for monitoring vegetation ecosystem status and detecting change dynamics across diverse landscapes. Indicators derived from satellite and aerial imagery are widely employed to assess vegetation health, contributing significantly to biodiversity surveillance and environmental assessment frameworks (Li *et al.*, 2023).

Among these indicators, vegetation indices (VIs) have gained prominence due to their simplicity, interpretability, and operational reliability. VIs are designed to capture spectral reflectance properties of vegetation, particularly in the visible and near-infrared regions of the electromagnetic spectrum (Shokirov *et al.*, 2025). Over the past several decades, extensive research has produced a wide array of indices tailored to different ecological contexts. While this diversity enhances their applicability across disciplines, it can also present challenges for users navigating the complex landscape of index selection (Yan *et al.*, 2025).

Despite their utility, many vegetation indices are designed to monitor specific biochemical traits and may fall short in detecting stress responses caused by multiple interacting factors such as heat, salinity, and drought. Indices that focus primarily on single-leaf parameters often fail to capture the complex physiological responses of vegetation under compound stress conditions (Kumar *et al.*, 2025). This limitation underscores the need for more integrative approaches that account for multi-scalar and multi-factorial vegetation dynamics.

Remote sensing-based approaches for assessing vegetation condition have been widely adopted and refined across diverse regional contexts worldwide (Li *et al.*, 2023). These advancements in remote sensing technology have significantly expanded the availability of land surface data, enabling more effective ecosystem monitoring and providing robust indicators of ecological conditions across multiple spatial scales. By capturing reflected radiation from the Earth's surface, remote sensing imagery facilitates the detection of various ecosystem components, including soil, vegetation, and open water, thereby offering valuable insights into ecological status across different landscapes (Shan *et al.*, 2019)

Among the indices developed for ecological monitoring, the Remote Sensing Ecological Index (RSEI) has emerged as a robust tool for integrated ecological assessment. Developed as a composite index, RSEI combines four environmental indicators—greenness (vegetation), wetness (moisture), heat (surface temperature), and dryness (built-up/barren land)—into a single metric using principal component

analysis (Xu *et al.*, 2019). This approach reduces subjectivity, provides spatially explicit insights, and allows tracking of ecological changes across time.

RSEI has been increasingly applied worldwide to evaluate ecosystem health and spatio-temporal ecological change (Zhu *et al.*, 2019; Jiang *et al.*, 2021). Recent studies in India have demonstrated its utility in assessing ecological quality in urban and peri-urban contexts (Halder & Bose, 2024) as well as in fragile landscapes such as the Akkulam-Veli Lake basin in Kerala (Philip *et al.*, 2024) However, applications in Northeast India remain limited, despite the region's ecological and cultural importance. Addressing this gap, the present study applies a geospatial approach using RSEI to evaluate the ecological condition of the lower part of Nagaland.

4.2. Remote Sensing Ecological Index

The Remote Sensing Ecological Index (RSEI) is a comprehensive metric developed to evaluate ecosystem health using satellite-derived remote sensing data. By integrating four key environmental indicators into a single index, it provides an overall assessment of ecological conditions across both spatial and temporal scales. The four indicators involved in RSEI are greenness (representing vegetation), moisture (representing Surface moisture), heat (representing temperature), and dryness (representing built-up/barren dry areas), which are often involved in assessing ecological status as the four indicators are closely linked to ecological health and are easily observable (Xu *et al.*, 2019). RSEI is formulated through the integration of four key environmental parameters with vegetation represented by Normalized Difference Vegetation Index (NDVI), Surface moisture represented by WET, temperature represented by LST and built-up area represented by Normalized difference soil index (NDSI) and is mathematically expressed as

$$RSEI = f\,(NDVI,\ Wet,\ LST,\ NDSI)$$

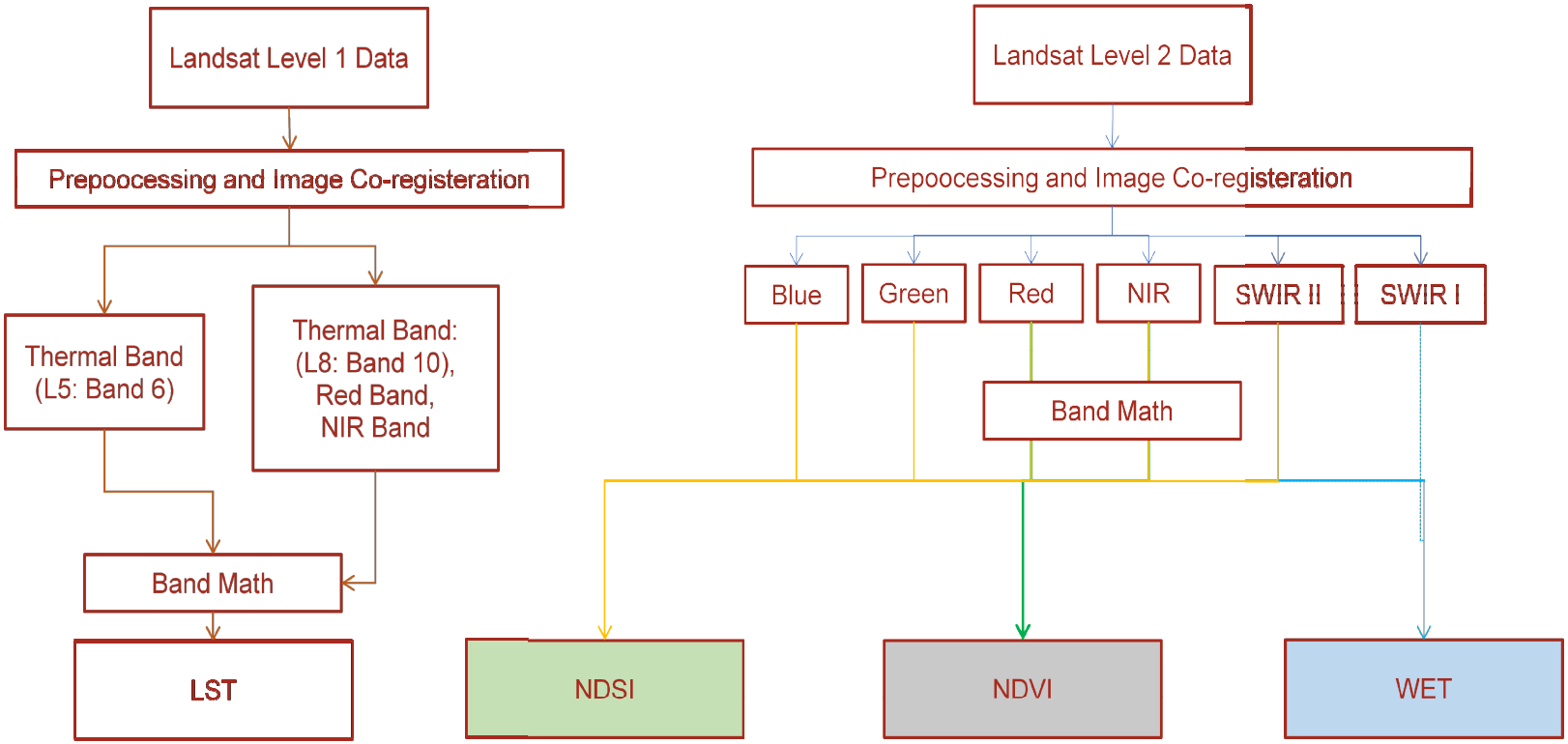

Figure 34 Methodology Flowchart for deriving RSEI

4.2.1. NDVI Estimation

The study area was clipped from the pre-processed satellite imagery to derive Normalized Difference Vegetation Index (NDVI) which signifies greenness of the area. The NDVI is calculated for the pre-processed imagery by using the following equation proposed by Rouse *et al.* (1973)

$$NDVI = \frac{\rho NIR - \rho Red}{\rho NIR + \rho Red}$$

In the above equation, ρRed refers to the visible reflectance of red light, while ρNIR represents the reflectance in the near-infrared spectrum. The wavelength range for the NIR band is 750–1300 nm, for the Red band it is 600–700 nm, and for the Green band it is 550 nm. The Normalized Difference Vegetation Index (NDVI) is based on the observation of vegetation, calculated as the difference between the NIR and Red bands. A higher NDVI value indicates a greater density of chlorophyll (Gandhi *et al.*, 2015). The range of NDVI values is between -1 and 1, with the vegetation having NDVI between 0.2-1.0, while the values lesser than 0.2 indicate areas without vegetation cover, usually barren, or with rock, snow, water, or ice (Rousta *et al.*, 2022).

4.2.2. WET Estimation

Wetness reflects the moisture of surface water, soil and vegetation (Shan *et al.*, 2019), the Tasseled Cap transformation has been frequently utilized in ecological monitoring, and wetness is measured with land surface moisture (LSM) in this study, as expressed in the following Eqs.

$$Wet_{TM} = 0.1446\rho Blue + 0.1761\rho Green + 0.3322\rho NIR + 0.3396\rho SWIR1 - 0.6210\rho SWIR2$$

$$Wet_{OLI} = 0.1511\rho Red + 0.1972\rho Blue + 0.3283\rho Green + 0.3407\rho NIR + 0.7117\rho SWIR1 + 0.4559\rho SWIR2$$

4.2.3. LST Estimation

The temperature Indicator in this paper is expressed in the form of Land Surface Temperature. The surface temperature is the temperature of the ground that absorbs

solar heat radiation, which affects the growth and development of vegetation and has a strong intervention effect on the water cycle. At the same time, it is also one of the factors affecting the evaporation and transpiration of natural water and indirectly affects the change of ecological environment. Higher LST values indicate higher surface temperature (Kumari *et al.*, 2018).

LST Estimation for Landsat 5 TM

$$L\lambda = \frac{LMAX\lambda - LMIN\lambda}{QCALMAX - QCALMIN}(QCAL - QCALMIN) + LMIN\lambda$$

Where,

L = Spectral radiance

QCAL = Quantized calibrated pixel value in DN

LMAX Spectral radiance scaled to QCALMAX

LMIN Spectral radiance scaled to QCALMIN

$$T = \frac{K2}{ln(\frac{K1}{L\lambda} + 1)} - 273.15$$

Where,

T = Effective at-satellite temperature in Kelvin

K2 = Calibration constant 1260.56

K1 = Calibration constant 607.76

LST Estimation for Landsat 8 OLI

$$TOA\ (L) = M_L * Q_{cal} + A$$

Where,

M_L = RADIANCE_MULT_BAND_x

Q_{cal} = corresponds to band 10.

A_L = RADIANCE_ADD_BAND_x

$$TOA = 0.0003342 * \text{“Band 10”} + 0.1$$

$$BT = (K_2 / (\ln (K_1 / TOA) + 1)) - 273.15$$

Where,

K_1 = K1_CONSTANT_BAND_x

K_2 = K2_CONSTANT_BAND_x

$$BT = (1321.0789 / Ln ((774.8853 / TOA) + 1)) – 273.15$$

$$NDVI = (\rho NIR – \rho Red) / (\rho NIR + \rho Red)$$

$$P_v = Square ((NDVI – NDVI_{min}) / (NDVI_{max} – NDVI_{min}))$$

$$\varepsilon = 0.004 * P_v + 0.986$$

$$LST = (BT / (1 + (0.00115 * BT / 1.4388) * Ln(\varepsilon)))$$

Where, BT stands for Brightness Temperature, Pv stands for Proportion of vegetation, ε and stands for emissivity.

4.2.4. NDSI Estimation

The soil drying represents the degree of surface exposure and dryness. The continuous desiccation of soil has a serious impact on the ecological environment quality in this region. It is also one of the important factors of ecosystem imbalance. In this paper, the average value of the building index (IBI) and bare soil index (SI) was used to construct the dryness index (NDSI). The higher the NDSI value is, the higher the degree of drying is (Li, 2022).

$$NDSI = (SI + IBI)/2$$

Where,

$$SI = \{(\rho SWIR1 + \rho Red) - (\rho Blue + \rho NIR)\}/ \{(\rho SWIR1 + \rho Red) + (\rho Blue + \rho NIR)\}$$; and

$$IBI = [\{(2 \times \rho SWIR1)/(\rho SWIR1 + \rho Red) - \rho NIR/ (\rho NIR + \rho Red) + \rho Green/(\rho Green + \rho SWIR1)\}]/ [\{(2 \times \rho SWIR1)/(\rho SWIR1 + \rho NIR) - \rho NIR/ (\rho NIR + \rho Red) + \rho Green/(\rho Green + \rho SWIR1)\}]$$

4.2.5. Integration of the Indicators

$RSEI_0$ is calculated by integrating four indicators (f) through Principal Component Analysis (PCA) instead of weighted sum approach. PCA is a multivariate statistical technique that reduces data dimensionality while addressing issues of multi-collinearity among variables. The data range and units of the four indices are different. Therefore, they were normalized in between 0 to 1 before running the PCA. The PCA method is a multi-dimensional data compression technology that can

remove the impact of co-linearity among the four variables (Seddon *et al.*, 2016), and better combine the four variables into one single index. More importantly, the weight of each factor is automatically and objectively allocated according to their contribution to the principal components. This can prevent the variation or error in the weight definition caused by individual characteristics (Xu, 2013).

$$Normalization = (X\text{-}Xmin)/(Xmax\text{-}Xmin)$$

Where, X is the band 'x',

Xmin is the Minimum value of 'x', and

Xmax is the Maximum value of 'x'

Subsequently, the variance of the principal components is used as the weight function, always PC1, to evaluate the standardized evaluation indicators (Xu, 2013a; Shan *et al.*, 2019).

Accordingly, initial RSEI, $RSEI_0$, is represented by PC1:

$$RSEI_0 = PC1\ [f\ (NDVI, Wet, NDSI, LST)]$$

$$RSEI = 1 - RSEI_0 = 1 - PC1\ [f\ (NDVI, Wet, NDSI, LST)]$$

4.3. Trends shown through Remote Sensing Ecological Index (RSEI), 2000–2023

The bands of satellite images are integrated to produce normalized indexes as indicated by Wet, NDVI, NDSI and LST, which were used to get the result of PCA. Table 1 showed that the contribution rates of the four main indicators of the first principal component (PC1) reached nearly 68.30%, 61.84%, 69.98%, 85.81%, 84.34%, and 79.50% during the years of 2000, 2006, 2011, 2013, 2018 and 2023, respectively.

The first principal component (PC1), which explains between 61.8% and 85.8% of total variance across years, is dominated by negative NDVI and positive NDSI loadings. This indicates a strong contrast between healthy vegetation and snow or exposed soil surfaces. Higher PC1 scores therefore correlate with ecologically degraded areas — regions with reduced vegetation cover and higher surface reflectance or exposure. Over time, the increasing contribution of PC1 suggests a trend of declining ecological health, marked by vegetation loss and expansion of bare or stressed land surfaces in the study area.

Table 12 Table showing the Results of principal component analysis (PCA).

Year	Indicators	PC1	PC2	PC3	PC4
2000	NDVI	-0.72	0.60	0.22	-0.26
	Wet	-0.16	-0.45	-0.28	-0.83
	NDSI	0.65	0.41	0.41	-0.48
	LST	0.18	0.51	-0.84	-0.03
	Eigenvalue	0.01	0.00	0.00	0.00
	% Eigenvalue	68.30	25.05	6.25	0.41
2006	NDVI	-0.76	0.52	0.31	0.25
	Wet	-0.17	-0.40	-0.39	0.81
	NDSI	0.61	0.36	0.47	0.53
	LST	0.16	0.66	-0.73	0.01
	Eigenvalue	0.01	0.00	0.00	0.00
	% Eigenvalue	61.84	30.63	7.24	0.29
2011	NDVI	-0.89	0.35	0.21	0.19
	Wet	-0.05	-0.44	-0.25	0.86
	NDSI	0.44	0.61	0.45	0.47
	LST	0.03	0.56	-0.83	0.04
	Eigenvalue	0.01	0.00	0.00	0.00
	% Eigenvalue	69.98	24.68	5.19	0.15
2013	NDVI	-0.61	-0.63	-0.41	0.27
	Wet	-0.09	0.35	0.20	0.91
	NDSI	0.79	-0.46	-0.26	0.32
	LST	-0.03	-0.52	0.85	0.02
	Eigenvalue	0.01	0.00	0.00	0.00
	% Eigenvalue	85.81	11.07	3.04	0.09
2018	NDVI	-0.80	-0.51	-0.26	0.17
	Wet	-0.05	0.33	0.13	0.93
	NDSI	0.59	-0.68	-0.29	0.32
	LST	-0.04	-0.41	0.91	0.02
	Eigenvalue	0.02	0.00	0.00	0.00
	% Eigenvalue	84.34	12.51	3.10	0.05
2023	NDVI	-0.73	-0.63	-0.23	0.16
	Wet	-0.08	0.30	0.10	0.95
	NDSI	0.68	-0.63	-0.26	0.28
	LST	0.02	-0.36	0.93	0.01
	Eigenvalue	0.01	0.00	0.00	0.00
	% Eigenvalue	79.50	17.69	2.75	0.06

The ecological condition of the study area, as reflected by PC1, shows a consistent decline in environmental quality from 2000 to 2023. PC1, driven by strong negative

NDVI and positive NDSI loadings, reveals a dominant trend of vegetation degradation and surface exposure. The years 2011, 2013, and 2018 exhibited the most intense ecological stress, with PC1 accounting for over 80% of total variance, indicating widespread environmental transformation. These results suggest that without active ecological restoration and land management, the region is likely to face long-term environmental instability and loss of ecosystem services.

4.4. Classification of RSEI

In order to further analyze the representativeness of RSEI, the RSEI values were segmented into five equal-grade intervals of 0.2. These included: 'Very Poor' (0.00–0.20), 'Poor' (0.21–0.40), 'Medium' (0.41–0.60), 'Good' (0.61–0.80), and 'Very Good' (0.81–1.00), enabling clearer differentiation of ecosystem health across spatial units.

Table 13 Table showing the temporal variation of values for RSEI Classes.

RSEI Class	2000	2006	2011	2013	2018	2023
Very Poor	0	0	0.003	0.001	0.271	0.025
Poor	0.004	0.521	8.744	1.671	10.714	7.149
Medium	27.482	25.887	54.371	22.563	40.556	45.7
Good	72.503	69.53	36.021	71.493	47.34	46.329
Very Good	0.01	4.061	0.862	4.272	1.12	0.797

Over the span of two decades, the ecological quality of the study area has undergone notable fluctuations, reflecting a dynamic landscape affected by both degradation and recovery phases.

In the year 2000, the ecological condition was predominantly favorable, with over 72% of the area classified under the "Good" category and nearly 28% under "Medium." There were virtually no areas in the "Poor" or "Very Poor" classes, indicating a largely healthy ecological environment at the start of the study period.

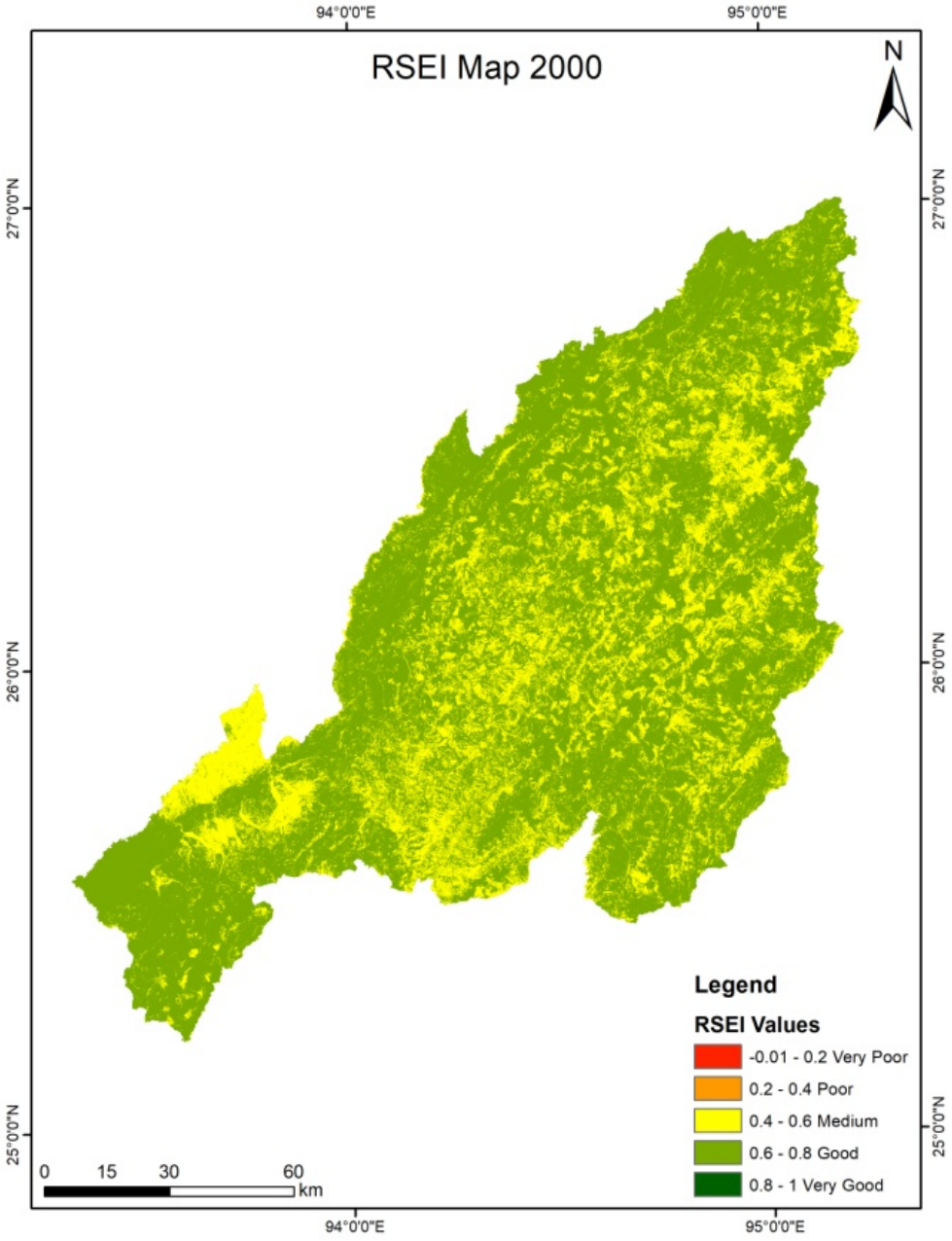

Figure 35 Map showing the Spatio-temporal distribution of RSEI index for the year 2000.

However, a gradual shift began to emerge in the following years. By 2006 and more evidently by 2011, the share of "Good" ecological areas had significantly declined, while the "Medium" and "Poor" classes expanded.

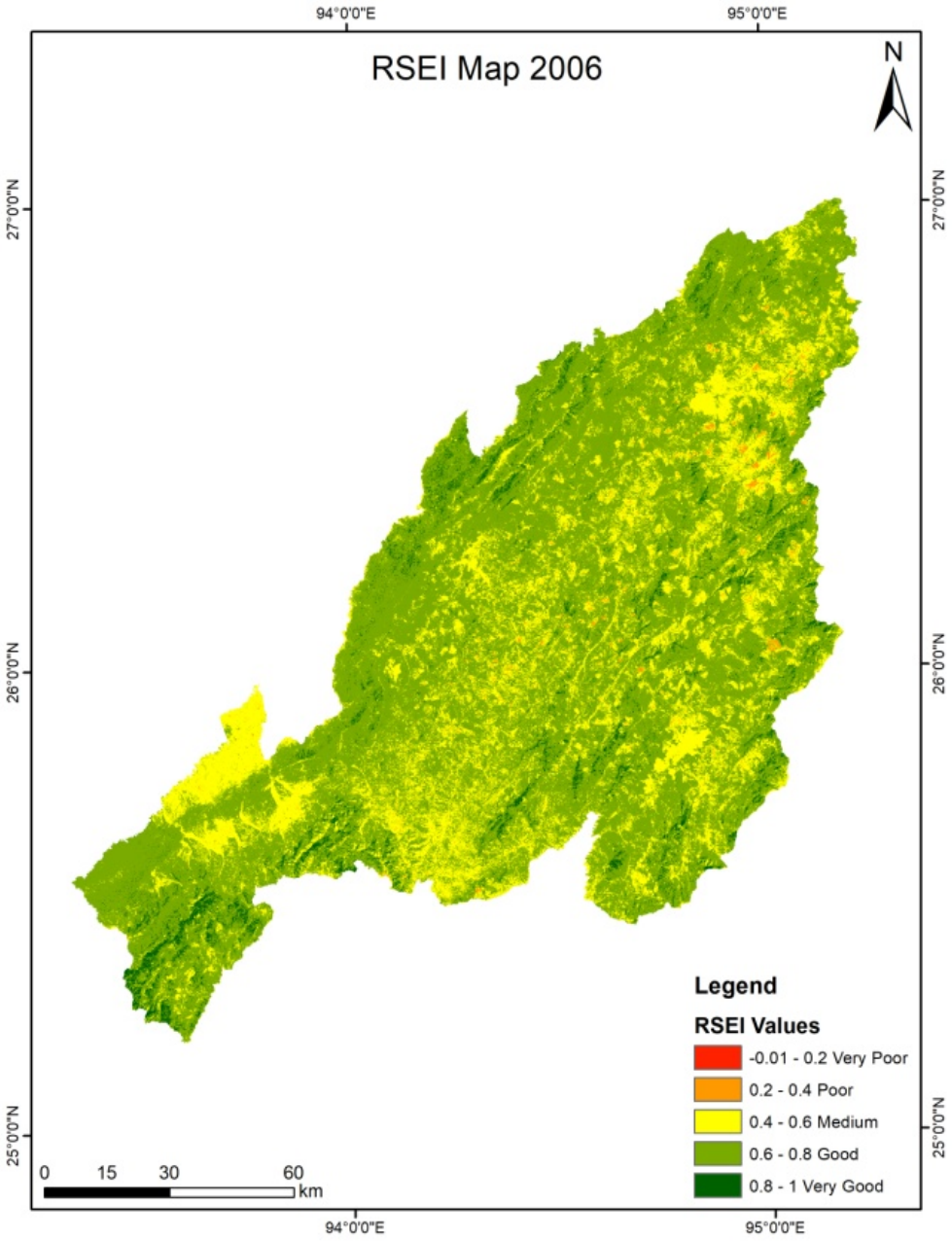

Figure 36 Map showing the Spatio-temporal distribution of RSEI index for the year 2006.

The year 2011 marked a low point, with a steep rise in the "Poor" category (8.74%) and the highest share of "Medium" class observed during the period (54.37%). This trend signaled increasing ecological stress or degradation, possibly due to anthropogenic pressures or climatic variability.

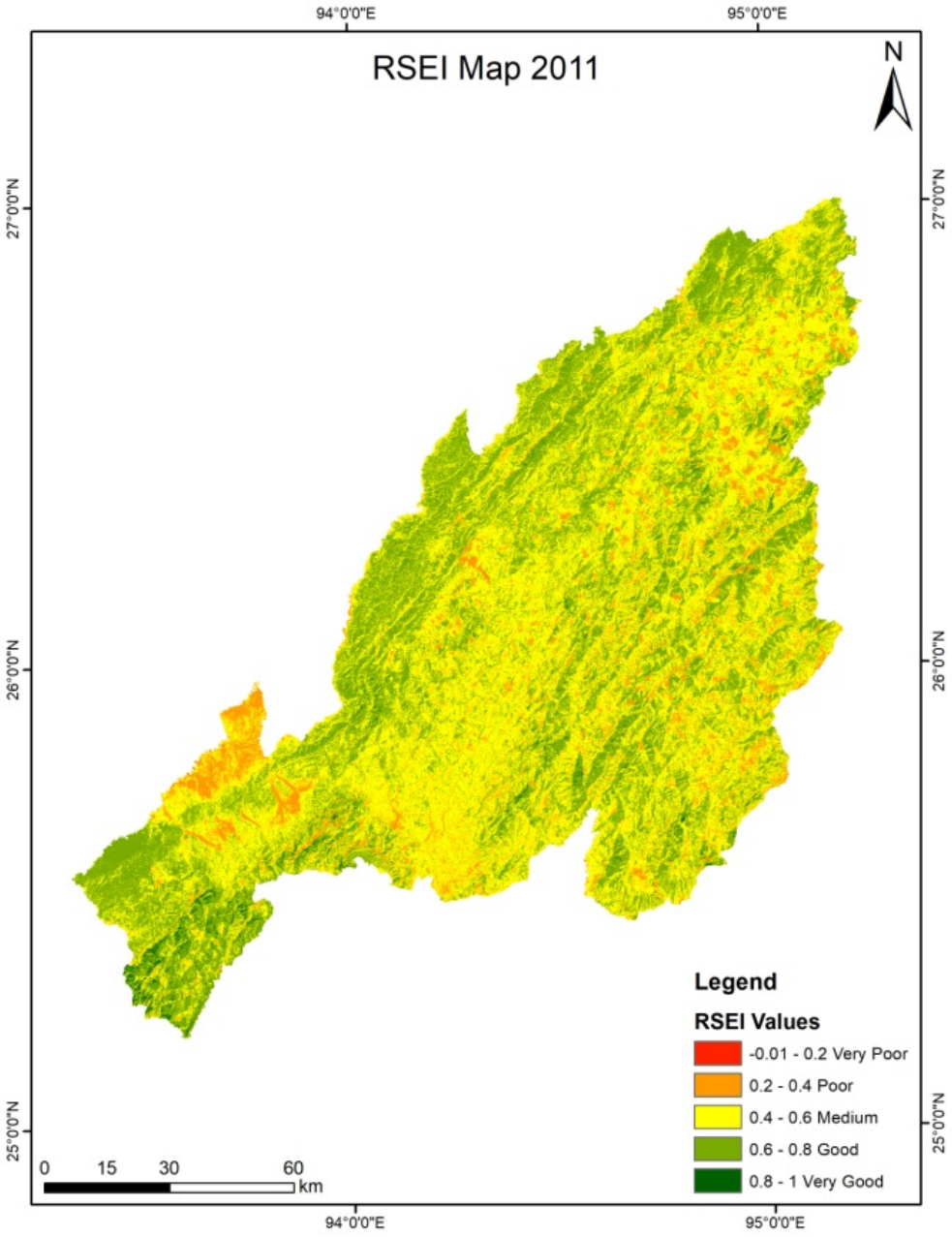

Figure 37 Map showing the Spatio-temporal distribution of RSEI index for the year 2011.

A phase of ecological recovery was notably observed in 2013. The "Good" category rebounded to over 71%, while the "Poor" and "Very Poor" classes saw a considerable drop. This improvement, however, was short-lived.

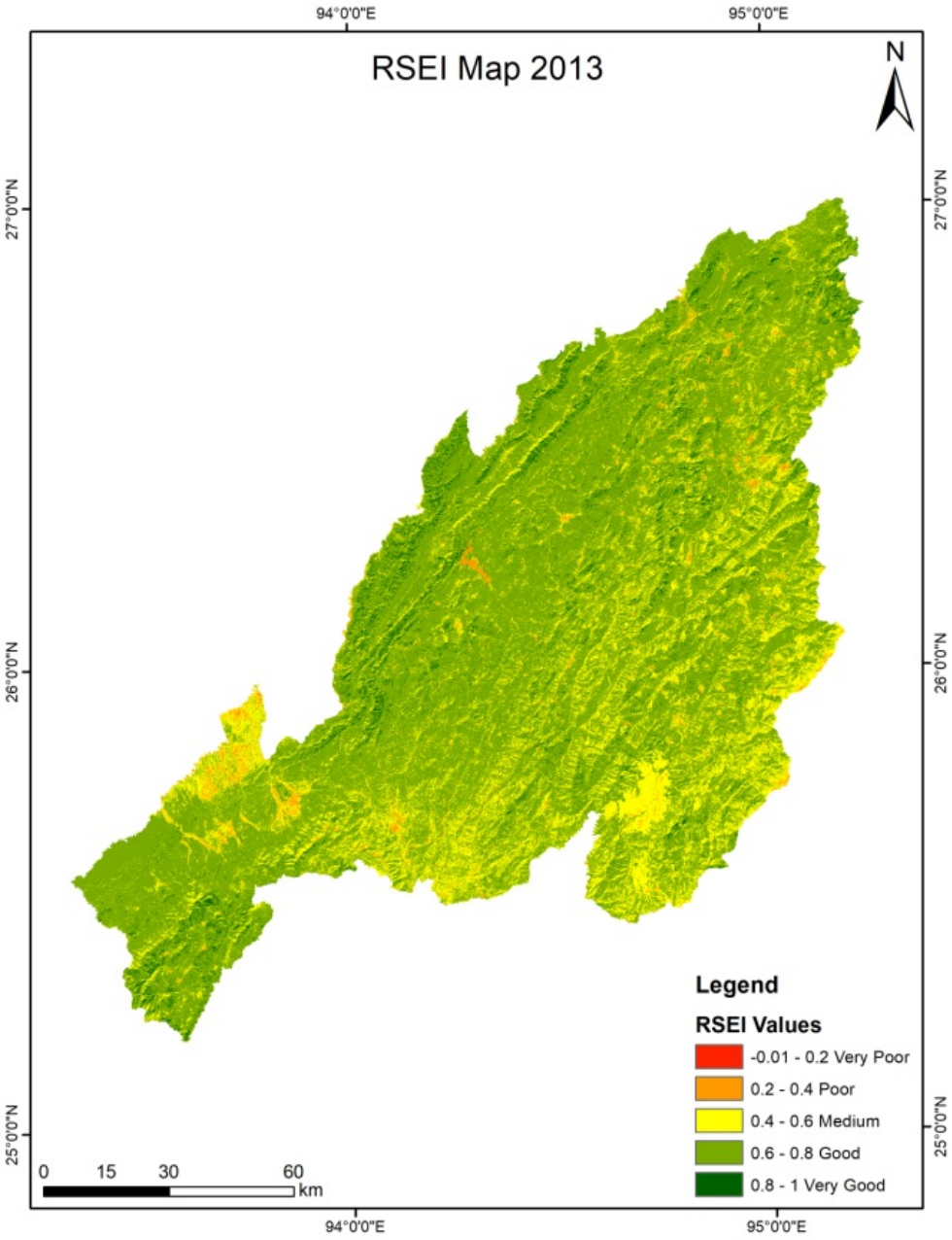

Figure 38 Map showing the Spatio-temporal distribution of RSEI index for the year 2013.

By 2018, the ecological condition had once again declined — the "Poor" and "Very Poor" classes reached their peak values (10.71% and 0.27%, respectively), while the share of "Good" areas decreased sharply.

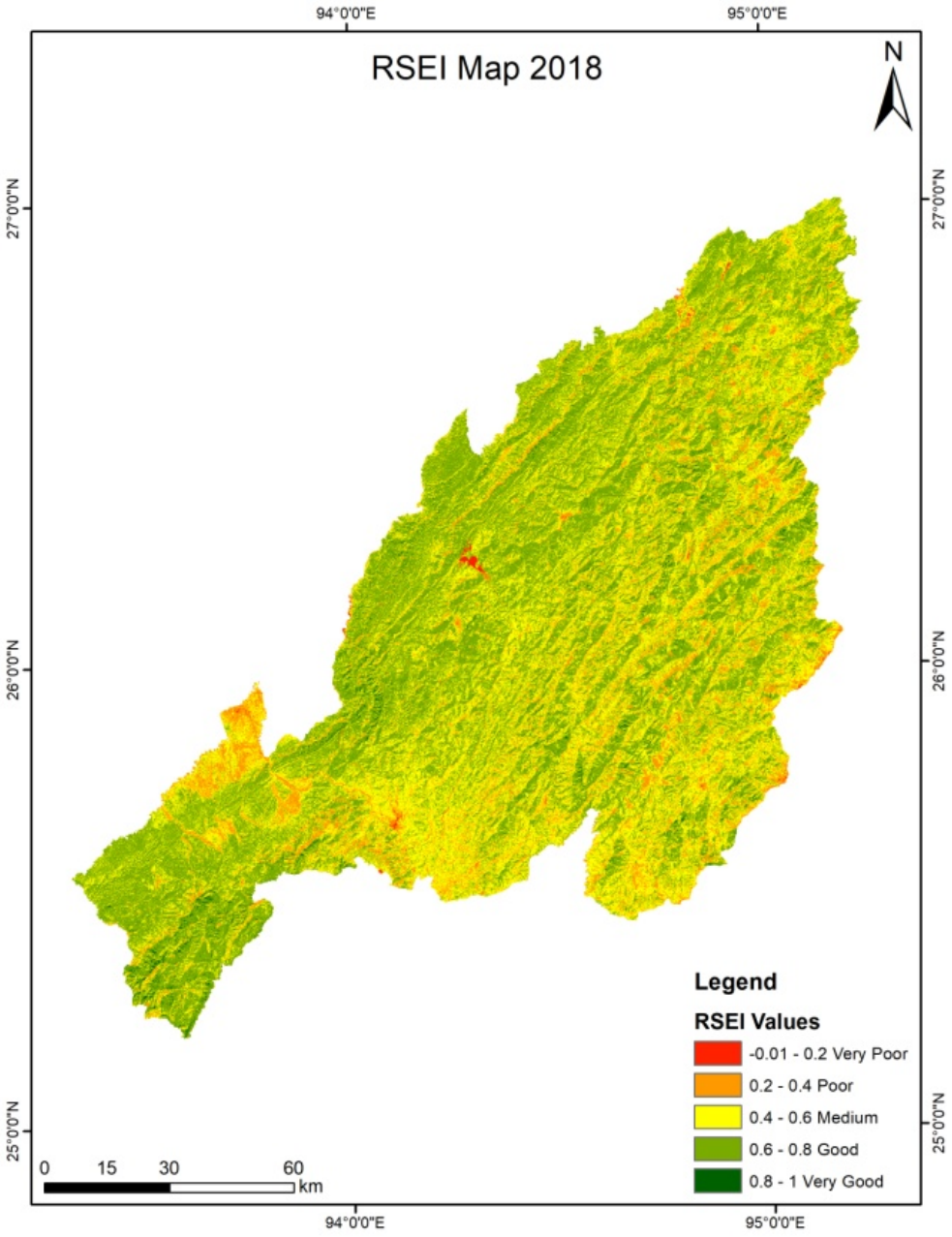

Figure 39 Map showing the Spatio-temporal distribution of RSEI index for the year 2018.

In 2023, the ecological scenario stabilized to some extent, with "Good" and "Medium" classes almost equally dominant. Yet, the persistence of degraded classes ("Poor" at 7.15% and "Very Poor" at 0.025%) highlights ongoing ecological challenges. The "Very Good" class remained consistently minimal throughout the

period, never exceeding 4.3%, suggesting that only a small portion of the landscape reached optimal ecological conditions at any point in time.

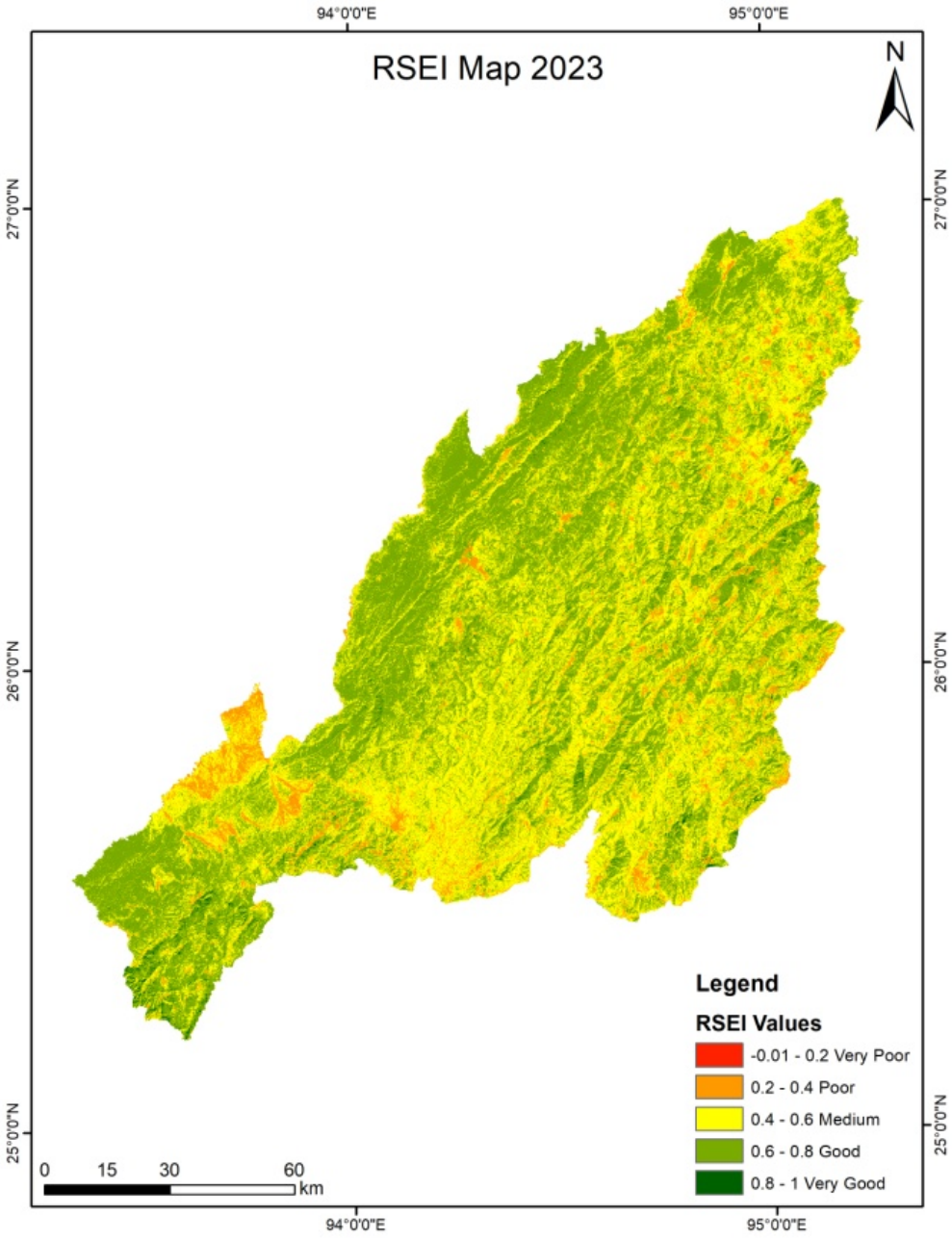

Figure 40 Map showing the Spatio-temporal distribution of RSEI index for the year 2023.

Overall, the trend reveals a cyclical pattern of ecological degradation and partial recovery, with a general shift away from high-quality ecological conditions and an increase in medium to poor-quality landscapes. This underscores the need for

continuous monitoring and targeted conservation efforts to reverse the trend and enhance ecological resilience in the region.

The classified RSEI outputs were evaluated in relation to Land-Use and Land-Cover (LULC) patterns across multiple time periods to assess the ecological implications of different land-use types. Interestingly, it was noted that areas consistently identified as fallow Jhum fields were associated with lower RSEI scores, indicating persistently poor ecological conditions. Additionally, zones adjacent to water bodies exhibited heightened ecological sensitivity, with their conditions consistently falling within the 'Very Poor' to 'Poor' categories over the years. Between 2013 and 2018, a noticeable transition from 'Good' to 'Medium' ecological quality was observed in several regions, primarily driven by an expansion of built-up areas and the emergence of barren zones resulting from road excavation and intensified Jhum cultivation. Furthermore, the Dzükou grasslands, previously categorized as 'Good' to 'Very Good' in ecological health, registered a dramatic shift to the 'Very Poor' class. This anomaly was attributed to forest fire activity, as corroborated by satellite imagery from the affected year.

4.5. Accuracy assessment of RSEI

In order to assess the reliability of RSEI, a comparative approach between the images of the years 2000, 2006, 2011, 2013, 2018 and 2023 was used. For this, a total of 73 random points were created throughout the study area. It was found that, a significant portion of agricultural land has been converted into **Built-up areas**, indicating rapid urban expansion and settlement growth. Some agricultural croplands also transitioned into **Open Forest** and **Plantation**, suggesting the transition of people from shifting agriculture to other land-use pattern such as plantation of commercial plants like rubber, teak, etc. as identified through image comparison. This also suggests that people in the lower parts of Nagaland are reducing shifting form of agriculture.

Table 14 Change in Land Use/Land Cover (LULC) classes of 73 random sample points between 2000 and 2023 in the study area.

2000 (Down)	2023 (Across)			
	Built-Up	Open Forest	Agriculture	Plantation
Agriculture	8	6	1	2
Barren Land	1	5	1	2
Built-up	24	0	0	0
Open Forest	7	11	4	1

The analysis indicates that although the overall RSEI exhibited a declining trend, the most substantial decrease was observed in areas where Agricultural land was converted to Built-up areas, with a strong relationship close to 1 ($R^2 = 0.784$). In contrast, Agricultural land that transitioned into Open Forest ($R^2 = 0.126$) or Plantation ($R^2 = 0.125$) showed only weak relationships, while Agricultural land that remained unchanged as Agriculture demonstrated a moderate relationship ($R^2 = 0.540$).

Similarly, transitions from Barren Land displayed varied outcomes: conversion to Open Forest ($R^2 = 0.442$) and Agriculture ($R^2 = 0.353$) reflected moderate relationships, while transformation into Plantation showed very little variation ($R^2 = 0.062$). Notably, Barren Land that was converted to Built-up areas exhibited a relatively strong decline in ecological quality ($R^2 = 0.511$).

For the Built-up class, areas that remained as Built-up showed a consistently high variation in the RSEI values ($R^2 = 0.772$), confirming a steady decline in ecological condition within settlement zones between 2000 and 2023. This pattern reflects ongoing rural–urban transformation and densification.

Conversely, the Open Forest class presented diverse patterns: conversion to Agriculture showed a moderate relationship ($R^2 = 0.495$), while conversion to Plantation showed negligible variation ($R^2 = 0.00008$). Open Forest that remained unchanged showed moderate stability ($R^2 = 0.426$), but conversion into Built-up areas resulted in a stronger decline in ecological condition ($R^2 = 0.727$). All these values indicate that change in land use strongly explains the decline in RSEI, showing urbanization as a key driver of ecological degradation.

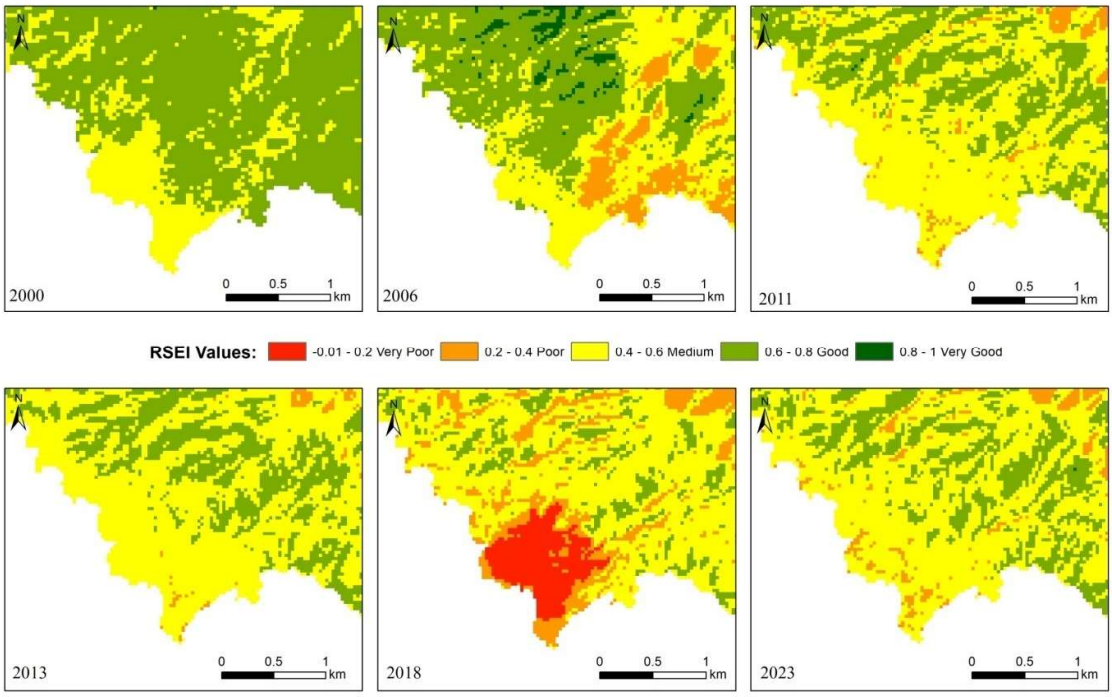

Figure 41 Time-Series RSEI showing the value changes for Dzukou Valley, Kohima District (2018 image showing post forest fire ecological condition of the valley burned by fire)

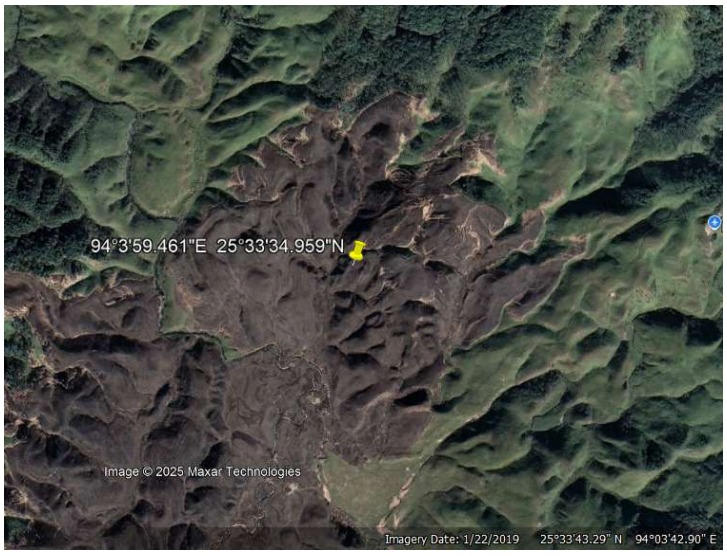

Figure 42 Google Earth Satellite Imagery of 22nd Jan 2019 showing the impact of forest fire that occurred in 26th November 2018.

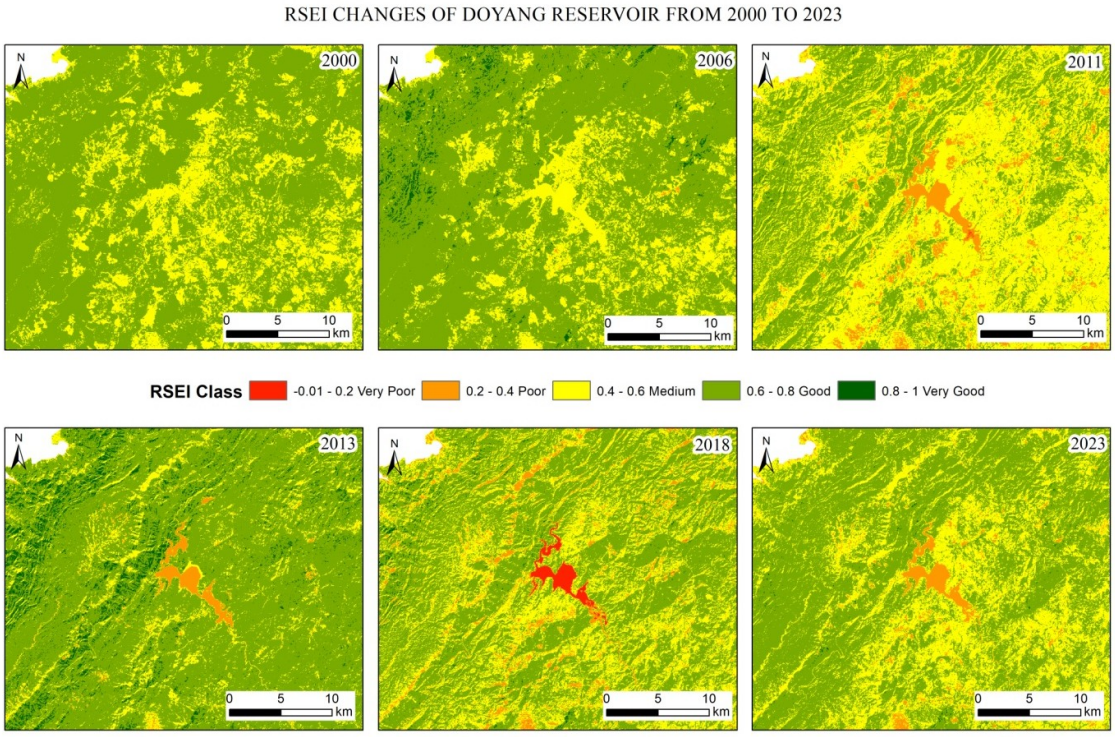

Figure 43 Time-Series RSEI showing the value changes for Doyang Reservoir, Wokha District.

Simultaneous field-work was also carried out for Doyang reservoir to assess water quality thereby conducting an ecological evaluation of Doyang Reservoir which is fed by perennial streams in Nagaland as indicated in the research done by Yhoshü & Kuho, 2025. Concurrently, the RSEI analysis showed that Doyang reservoir had significant ecological shifts throughout the study duration, which led to the examination of the reservoir status at the ground level. The seasonal variation in the Trophic State Index (TSI), derived from Secchi Depth measurements, revealed distinct shifts in nutrient dynamics and ecological productivity within the Doyang Reservoir. Pre-monsoon readings indicated a eutrophic state (mean TSI ≈ 61.52), suggesting elevated nutrient loading likely driven by intensified drainage inflow and sediment deposition. In contrast, post-monsoon conditions reflect a mesotrophic state (mean TSI ≈ 45.44), attributed to reduced hydrological input and sediment accumulation, thereby improving water clarity and lowering nutrient concentrations. These trophic transitions align with spatial patterns observed in the Remote Sensing

Ecological Index (RSEI) maps, which depict a temporal decline in ecological condition from 2000 to 2018, followed by partial recovery in 2023.

The convergence of high TSI values and low RSEI scores during pre-monsoon periods, particularly near the eastern inlet, underscores the ecological stress induced by nutrient-rich inflows. Conversely, the post-monsoon reversal, marked by improved RSEI classes and lower TSI values, reflects seasonal flushing and ecological resilience. These ecological fluctuations have direct implications for vegetation condition in the surrounding landscape. Elevated nutrient loads and sedimentation during the pre-monsoon phase can lead to increased turbidity and altered soil–water interactions, potentially inhibiting riparian and aquatic vegetation growth. Excessive nutrient enrichment may also favor opportunistic or invasive species, disrupting native plant assemblages and reducing overall biodiversity. In contrast, the post-monsoon decline in nutrient concentration and sediment deposition fosters improved water-soil balance, supporting the regeneration of native vegetation and enhancing ecological stability. The RSEI trends, which integrate greenness as a key component, reflect these vegetation responses, showing reduced vegetative vigor during periods of ecological stress and gradual recovery in years marked by improved trophic conditions. This multi-index assessment thus underscores the interconnectedness of water quality, nutrient dynamics, and vegetation health, offering a robust framework for monitoring ecosystem integrity and informing adaptive watershed management strategies in relation to the impact of climate change.

Interestingly, both the Dzukou Valley and Doyang Reservoir areas located within the districts of Kohima and Wokha, experienced notably reduced rainfall in 2018 compared to the preceding year. According to AWS/meteorological station data, annual precipitation in 2017 exceeded 2224 mm in Kohima and 2162 mm in Wokha, whereas in 2018, rainfall dropped to 1567 mm and 2085 mm, respectively. This decline in precipitation is reflected in the Remote Sensing Ecological Index (RSEI) values, which show a corresponding reduction in ecological quality across both sites. The overall RSEI pattern for the study area mirrors this meteorological shift,

indicating that lower rainfall levels were associated with diminished vegetation vigor, increased dryness, and reduced greenness, as captured through satellite-derived indicators. This correlation between ground-based precipitation data and RSEI-derived ecological stress underscores the sensitivity of these ecosystems to interannual climate variability and highlights the utility of RSEI as a proxy for monitoring climate-induced ecological change.

In 2013, an observable improvement in ecological conditions, reflected through elevated RSEI values, coincided with rainfall and temperature levels that were close to the 20-year climatological averages across most meteorological stations. While data from the Bhandari and Zunheboto stations were excluded due to inconsistencies and gaps in meteorological data records, the remaining datasets suggest that the overall climatic conditions remained relatively stable. This alignment suggests that ecological health in the study area is positively influenced by climatological normalcy, where consistent rainfall and temperature values support vegetation growth, soil moisture retention, and broader ecosystem stability. The correlation between RSEI and near-average meteorological parameters reinforces the utility of RSEI as a sensitive indicator of ecological response to climate variability.

4.6. Summary

Given the limitations of ground-based meteorological observations, particularly in regions where AWS stations suffer from data gaps, calibration inconsistencies, or limited temporal coverage, the integration of Remote Sensing (RS) and Geographic Information Systems (GIS) offers a robust methodological alternative. In this study, RS-derived indices such as RSEI were used to assess ecological conditions across diverse landscapes, compensating for unreliable or missing primary climatological data. The spatial continuity and temporal consistency of satellite datasets enabled cross-validation of ecological trends, especially in areas where station data were incomplete or unavailable. This approach not only enhances analytical reliability but also supports multi-scalar ecological monitoring, making it especially valuable for climate-sensitive regions like Nagaland, where field-based data infrastructure remains uneven.

In instances where forest fire events were either unreported or archived or overshadowed by more recent updates, satellite imagery proved instrumental in detecting and quantifying ecological damage. Despite the absence of reliable ground-based records, the post-fire Remote Sensing Ecological Index (RSEI) values clearly reflected degraded ecological conditions, capturing the spatial extent and severity of vegetation loss. This underscores the strength of RS-based monitoring, which can reveal disturbances that escape conventional reporting mechanisms and provide objective, spatially explicit evidence of environmental stress—particularly in remote or data-scarce regions.

CHAPTER 5

Chapter 5: Evaluation of the change in vegetation cover in response to climatological factors.

5.1. Harnessing Geospatial Technologies for Ecosystem Monitoring and Climate Adaptation

Recent advancements in Geographic Information System (GIS) methodologies, coupled with the expanding capabilities of remote sensing (RS), have transformed the landscape of environmental and geoscientific research. These technologies now play a pivotal role across a wide array of disciplines, including geological mapping, geomorphology, hydrogeology, geophysics, mining, civil and environmental engineering, land-use planning, hydrology, meteorology, and natural hazard assessment (Chaminé *et al.*, 2021).

Since the mid-1980s, RS platforms such as the Landsat mission have enabled continuous, large-scale monitoring of terrestrial ecosystems. These systems provide both quantitative and qualitative insights into changes in vegetation composition, soil characteristics, geomorphological features, hydrological dynamics, and patterns of urban expansion. Modern RS tools are capable of capturing ecosystem attributes ranging from structural and taxonomic traits to functional interactions and feedbacks, across spatial scales from local landscapes to global biomes (Lausch *et al.*, 2024).

In meteorology and climatology, the combined use of Remote Sensing (RS) and Geographic Information Systems (GIS) has significantly advanced our ability to monitor and analyze atmospheric processes. These technologies utilize data from satellite imagery, aerial surveys, and terrestrial sensors to generate spatially detailed information crucial for tackling complex environmental issues such as climate variability, extreme weather, resource distribution, and urban growth. Their integration enhances the development of early warning systems, supports climate simulations, and informs adaptive strategies, tools that are increasingly indispensable in navigating global environmental challenges (Roy & Bhardwaj, 2024).

The synergistic integration of RS and GIS has significantly broadened the scope and accuracy of environmental assessments. While RS delivers spatially rich datasets reflecting current ecological conditions, GIS facilitates their interpretation through

modeling, visualization, and spatial analysis. This integrated approach supports the monitoring of deforestation, land-use transitions, urban sprawl, habitat fragmentation, and pollution dynamics. In forestry, it enables the tracking of canopy cover and biodiversity trends; in agriculture, it underpins precision farming through assessments of soil health, crop vigor, and irrigation efficiency. Climate researchers increasingly depend on these tools to examine global climate systems, quantify greenhouse gas emissions, and evaluate ecosystem responses to climatic shifts, underscoring their indispensability in contemporary environmental science (Lausch *et al.*, 2024).

The capacity of RS technologies to generate high-resolution vegetation maps has become central to ecological monitoring and resource management. These maps offer critical insights into vegetation distribution, condition, and temporal dynamics. Recent innovations, including enhanced satellite sensors, UAVs, and improved spectral resolution in platforms like Landsat, Sentinel, and MODIS—have elevated the accuracy and scalability of environmental data collection (Matyukira & Mhangara, 2024). Such capabilities support multiscale analyses and inform decision-making in conservation planning, land-use governance, and sustainable resource allocation.

Additionally, integrating community perspectives into geospatial planning frameworks has emerged as a key strategy for climate adaptation. Studies show that local perceptions of climate impacts and green infrastructure are essential for shaping inclusive and effective adaptation policies. Embedding these insights into GIS-based planning ensures that interventions are not only technically sound but also socially equitable and contextually relevant (Canan Gungor & Osman Mohamed, 2025).

Geographic Information Systems (GIS) play a vital role in examining long-term climatic patterns, including shifts in temperature, rising sea levels, and variations in ice extent and vegetation cover. When paired with remote sensing (RS), these technologies enable comprehensive monitoring of climate indicators across both regional and global scales, thereby supporting evaluations of climate change impacts and informing adaptive strategies (Gabriele *et al.*, 2023).

RS satellites are instrumental in collecting continuous data on key climate variables such as sea surface temperature, ice distribution, vegetation dynamics, and atmospheric greenhouse gas levels. These datasets are essential for identifying climate trends, gauging the effects of global warming, and contributing to the implementation of international climate policies and agreements. GIS platforms enhance the analytical power of these observations by allowing researchers to visualize spatial patterns, perform geostatistical analyses, and model future climate scenarios. This integration supports evidence-based policymaking and the design of adaptive responses to climate-related challenges (Roy & Bhardwaj, 2024).

5.2. Vegetation cover response to climatological factors.

5.2.1 Global Context

Quantitative evaluation of vegetation resilience and resistance is essential for understanding how plant communities respond to climatic disturbances. Despite its importance, few studies have systematically explored the spatial and temporal dimensions of vegetation responses to key climate variables such as temperature, precipitation, and solar radiation (Sun & Zhang, 2024). Although ecosystem models are commonly employed to simulate vegetation dynamics at global scales, their ability to accurately reflect observed patterns of resilience and resistance remains uncertain.

Recent trends indicate a deceleration in the rates of temperature and precipitation change, resulting in increasingly complex vegetation responses. In some regions, elevated temperatures have prolonged the growing season, enhancing plant productivity. Conversely, in areas with limited water availability, rising temperatures can intensify evapotranspiration, deplete soil moisture, and hinder vegetation growth. Shifts in precipitation regimes, particularly in the timing, frequency, and duration of rainfall also exert significant influence. Extended droughts or altered monsoon cycles may reduce vegetation cover, while intense rainfall over short periods can trigger soil erosion, undermining ecosystem stability. The interplay between temperature and precipitation is particularly critical. In certain contexts, warmer conditions paired with adequate rainfall can stimulate vegetation expansion. In contrast, similar

temperature increases coupled with declining precipitation may exacerbate drought stress, leading to vegetation degradation. Therefore, identifying and interpreting the specific climatic drivers and their interactions is vital for forecasting vegetation dynamics and guiding ecosystem management under evolving climate scenarios (Sun & Zhang, 2024).

Climate extremes have significantly disrupted vegetation dynamics, raising concerns among ecologists, conservationists, and policymakers. These changes have intensified ecosystem vulnerability, now a central issue in ecological research. Understanding vegetation–climate interdependence is essential for characterizing vegetation response to climate change (VRC), including sensitivity in growth, productivity, and spatial distribution. Impacts vary by region and climate zone, with global consequences including species redistribution, water scarcity, reduced crop yields, and vegetation decline. Recent estimates attribute over 60,000 deaths and USD 1.2 trillion in losses, 1.6% of global GDP, to climate-induced vegetation shifts (Afuye *et al.*, 2021).

Over recent decades, remote sensing metrics such as the Normalized Difference Vegetation Index (NDVI) have revealed widespread increases in vegetation cover, with notable greening trends in regions like China and India. These changes are primarily driven by shifts in climate, particularly temperature and precipitation, and land-use modifications. Ongoing global warming is expected to further alter vegetation patterns, with cascading effects on Earth's systems. To anticipate future changes, it is crucial to examine how vegetation cover responds to climatic variability and extremes (Bao *et al.*, 2021).

Vegetation cover serves as a sensitive indicator of climatological variability, reflecting the impacts of global climate change through shifts in growth patterns, productivity, and distribution. These changes not only signal ecological stress but also contribute feedback effects that influence climate systems. Monitoring and mapping vegetation sensitivity to temperature and precipitation fluctuations is therefore essential for anticipating future dynamics and informing sustainable ecosystem management strategies (Han *et al.*, 2021).

5.2.2. Indian Context

Recent modelling efforts have highlighted the sensitivity of forest ecosystems in India to projected climate change, offering valuable insights into vegetation cover response under varying climatological scenarios. Using the Hadley Centre's Regional Climate Model (HadRM3) and the dynamic global vegetation model IBIS, Chaturvedi *et al.*, 2011 assessed vegetation shifts under A2 and B2 emission scenarios. Their findings indicate that by the end of the century, 39% and 34% of forest grids may undergo vegetation type changes under A2 and B2 scenarios, respectively. Forest-dominant states such as Chhattisgarh, Karnataka, and Andhra Pradesh show even higher projected shifts—up to 73%, 67%, and 62% of forested grids, respectively. These changes are accompanied by increases in Net Primary Productivity (NPP) and soil organic carbon (SOC), suggesting altered ecosystem functioning. A forest vulnerability index developed from observed forest density, biodiversity, and modeled vegetation shifts identifies the upper Himalayas, Western Ghats, and parts of central India as highly vulnerable, while Northeastern forests appear more resilient. This underscores the importance of region-specific adaptation strategies to mitigate climate-induced vegetation transformations and ecosystem risks (Chaturvedi *et al.*, 2011).

A multi-sensor remote sensing study in eastern India (2000–2022) assessed vegetation response to climate and human pressures using EVI, CHIRPS precipitation, MODIS LST, and other datasets. Elevation-dependent warming and shifting precipitation patterns significantly influenced vegetation cover, with precipitation showing a strong positive correlation to EVI (R^2 = 0.83). Human activities dominated vegetation change near Kolkata (87%), while climate factors were the main drivers in northern and southeastern highlands (70–85%). These findings highlight the need for region-specific land-use strategies (Banerjee *et al.*, 2024).

Vegetation regime shifts under climate change often follow gradual transitions rather than abrupt tipping points, progressing through bistable or metastable states. A recent study used satellite-derived vegetation maps and long-term precipitation data to

model moisture-driven hysteresis curves across India. Vegetation types such as forest, scrubland, grassland, and vegetation less exhibit distinct transition thresholds. For instance, forest-to-scrubland shifts occur under dry conditions (154–452 mm), while reverse transitions require wetter regimes (1080–1400 mm). Scrubland and grassland show reversible dynamics, forming hysteresis loops. These findings highlight the asymmetric energy required for forward and reverse transitions and propose a characteristic curve to visualize tipping zones and co-existence thresholds, offering critical insights into climate-induced vegetation responses (Das *et al.*, 2024).

A pan-India study assessed vegetation health under future climate scenarios using Shared Socioeconomic Pathways (SSPs), analyzing changes from 1981 to 2100 across seven vegetation types and four seasons. Using a Standardized Vegetation Index (SVI) and a bivariate copula model integrating hydroclimatic variables such as soil moisture, precipitation, solar radiation, and temperature, the study found that water-limited regions are more responsive to moisture availability, while energy-limited zones are influenced by temperature and radiation. Greenness has increased in most water-limited areas, but northeastern regions show stagnation or decline due to high convective activity. Future projections suggest monsoon-driven greening, with intensified browning in the northeast over time (Dash & Maity, 2025).

Existing literature underscores the complex and region-specific interactions between vegetation dynamics and climatological drivers, including temperature, precipitation, and hydroclimatic variability. Studies across India reveal that vegetation cover responds nonlinearly to climate change, with transitions often governed by hysteresis loops, tipping zones, and elevation-dependent sensitivities. Remote sensing analyses further demonstrate that vegetation greenness is modulated by both water and energy limitations, with spatial heterogeneity in response patterns across diverse ecological zones. These findings highlight the need for localized assessments, particularly in ecologically fragile and data-scarce regions such as Nagaland, where steep topography, monsoonal variability, and socio-environmental pressures converge. Building on these insights, this chapter aims to investigate vegetation cover response to climatological factors in Nagaland, offering a spatially explicit understanding of

vegetation sensitivity and resilience that can inform conservation planning and climate adaptation strategies in the Indo-Burma biodiversity hotspot.

5.3. Vegetation Cover Index (VCI)

The Vegetation Cover Index (VCI) derived from Landsat imagery, serves as a valuable tool for assessing drought impacts on vegetation across a given region. By tracking fluctuations in vegetation health and comparing them against long-term historical baselines, VCI enables the evaluation of both the duration and intensity of events of stress. This index is grounded in the Normalized Difference Vegetation Index (NDVI), utilizing historical NDVI data to infer soil moisture conditions (Dhawale & Paul, 2018). To facilitate interpretation, VCI values are normalized on a scale from 0 to 100, with lower values indicating more severe stress on vegetation (Kogan, 2003). VCI is calculated using the following formula:

$$VCI = \frac{NDVI - NDVImin}{NDVImax - NDVImin} \times 100$$

Where, NDVI is the Normalized Difference Vegetation Index; and,

NDVImin and NDVImax are the minimum and maximum NDVI Values respectively.

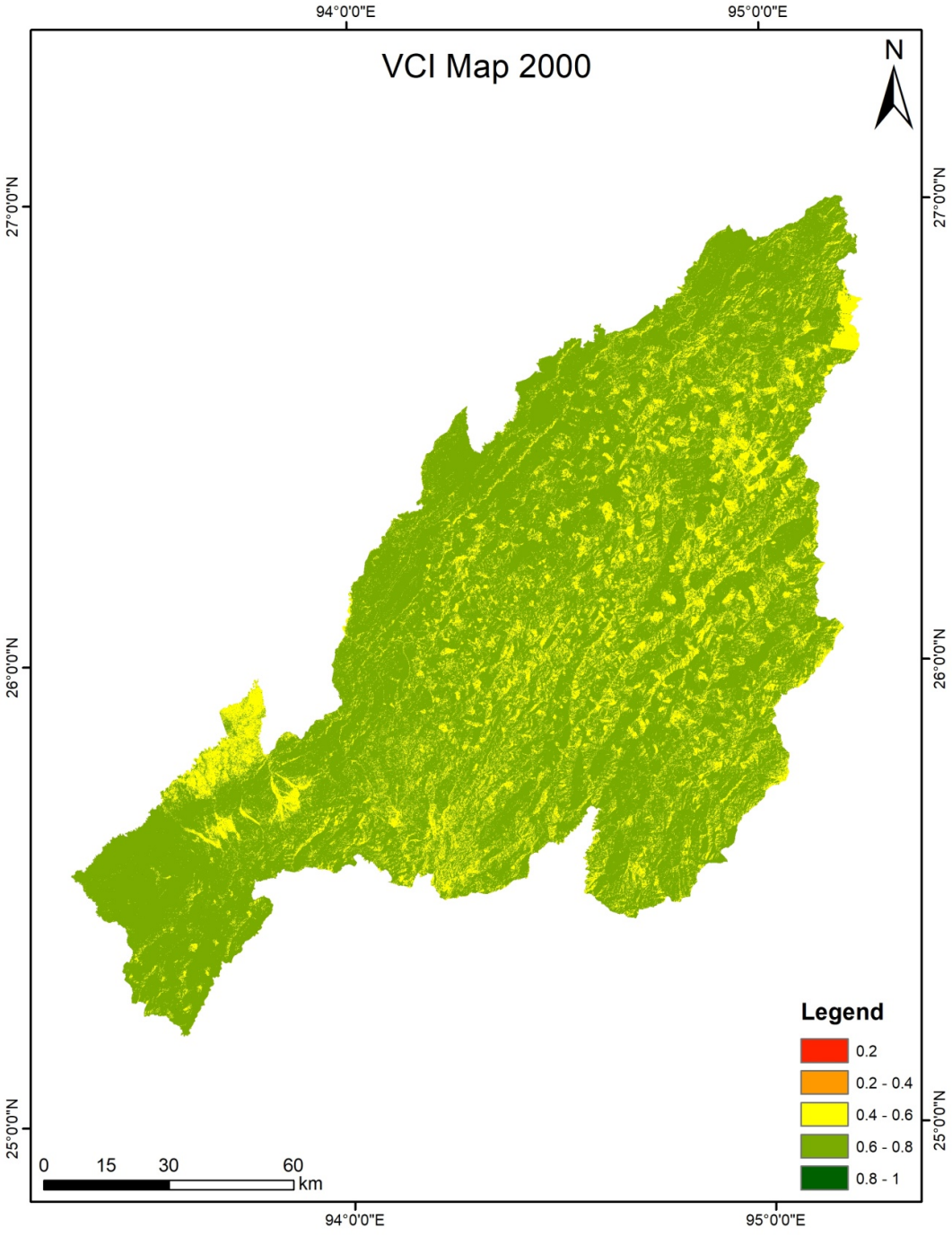

Figure 44 Map showing the distribution of VCI \ for the year 2000.

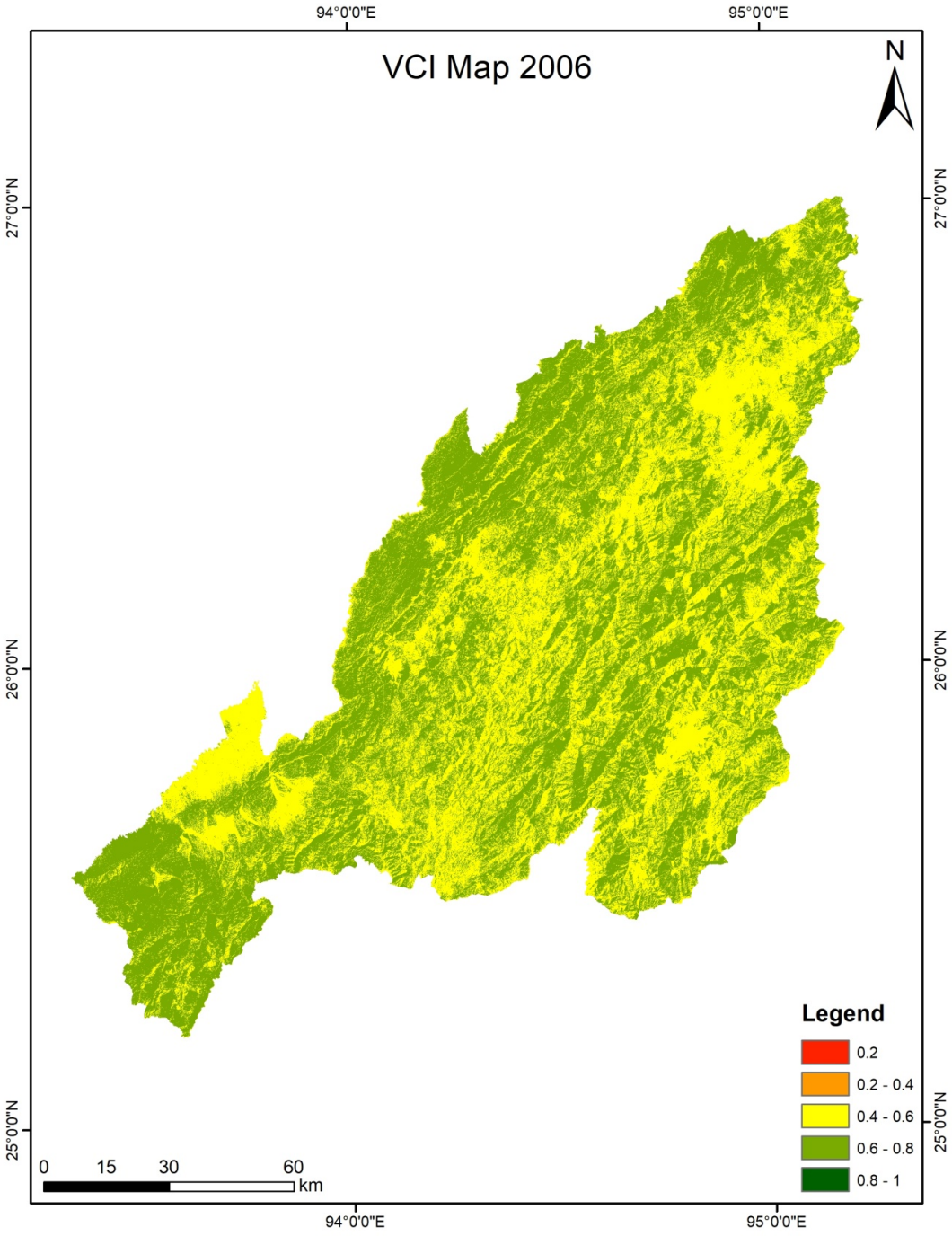

Figure 45 Map showing the distribution of VCI for the year 2006.

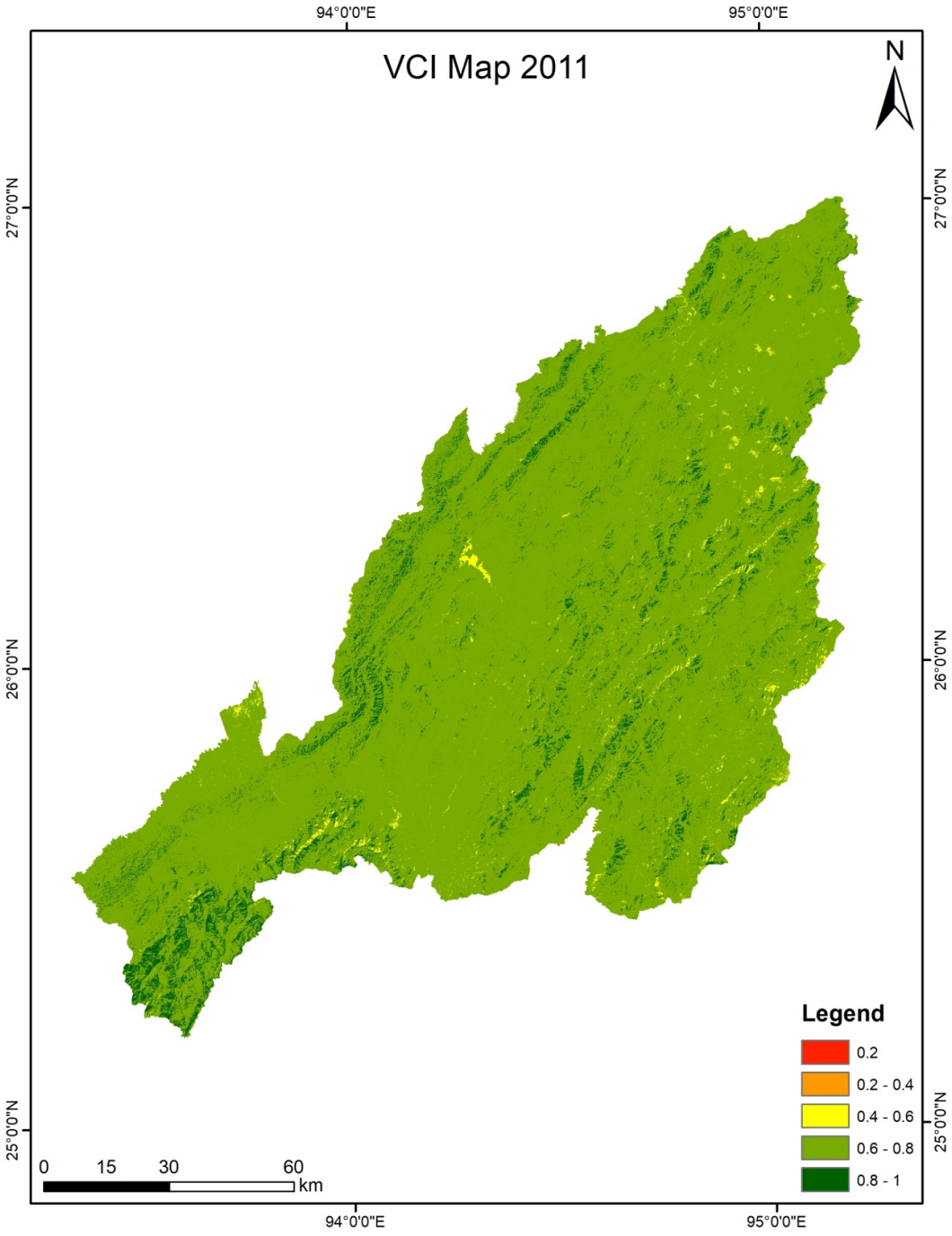

Figure 46 Map showing the distribution of VCI for the year 2011.

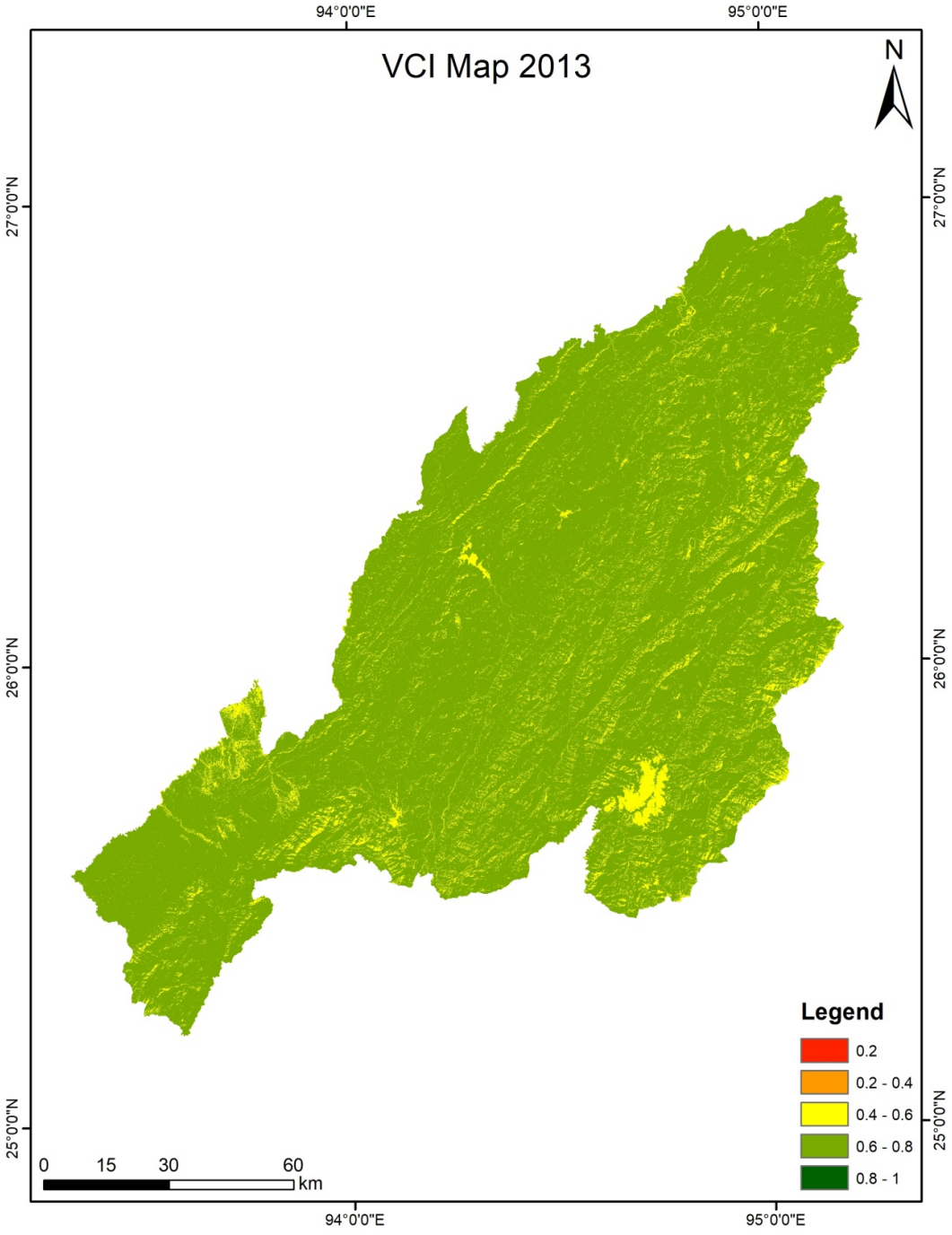

Figure 47 Map showing the distribution of VCI for the year 2013.

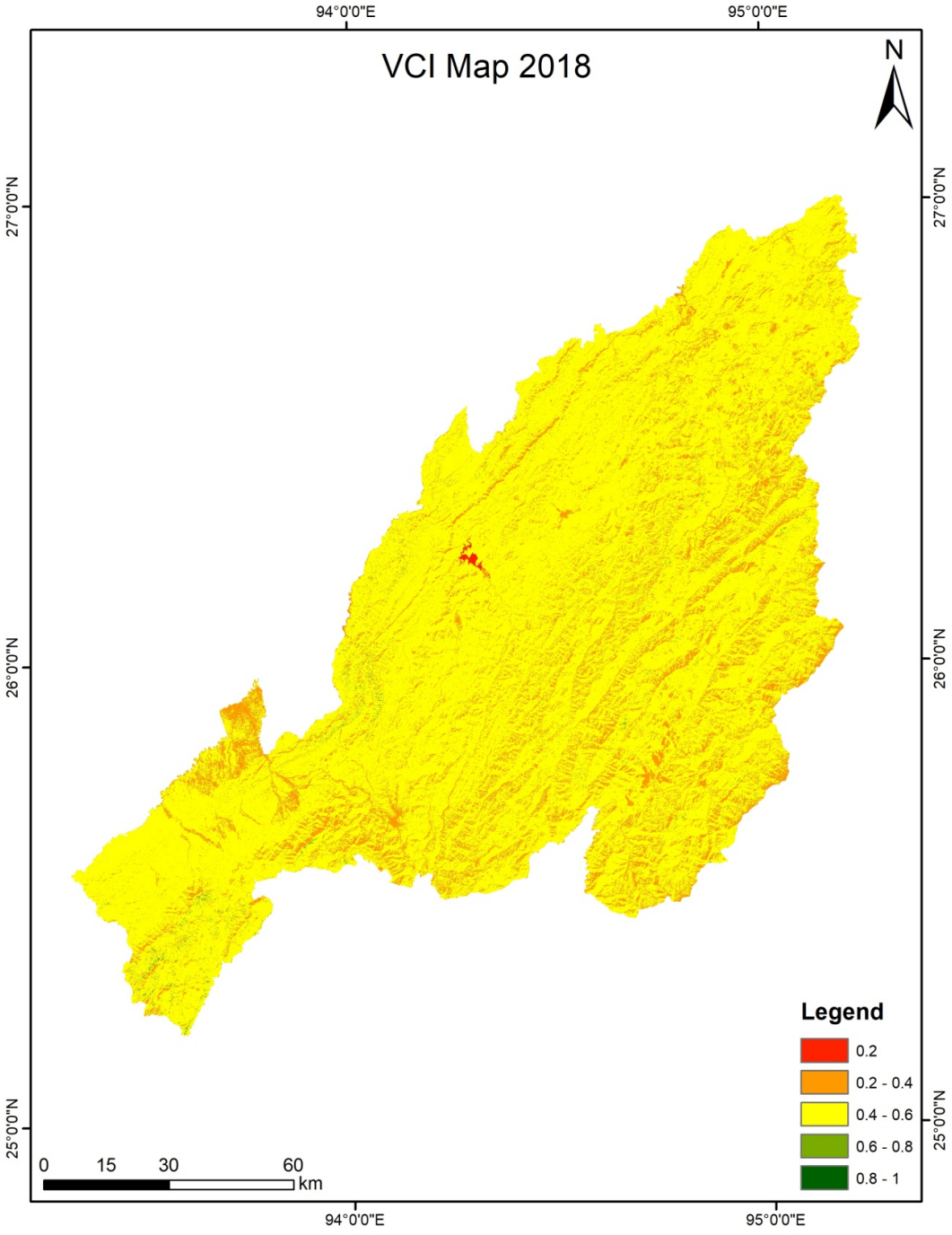

Figure 48 Map showing the distribution of VCI for the year 2018.

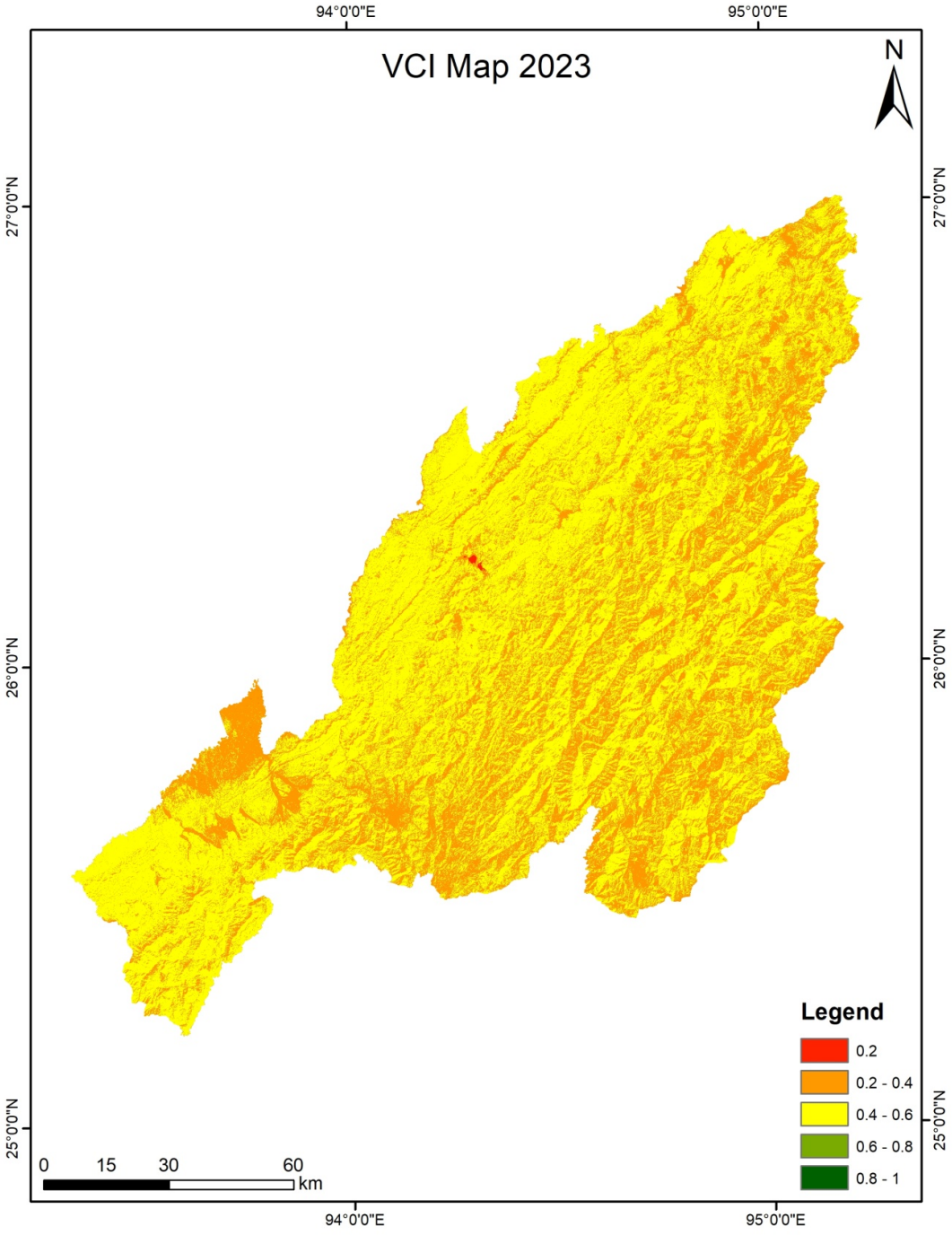

Figure 49 Map showing the distribution of VCI for the year 2023.

5.4. Temperature Condition Index (TCI)

The Temperature Condition Index (TCI) is designed to detect vegetation stress arising from elevated temperatures and excessive moisture levels. Drought conditions tend to intensify when high thermal stress coincides with inadequate soil moisture. TCI effectively captures vegetation health influenced by thermal anomalies by analyzing historical Land Surface Temperature (LST) data, which is derived from Brightness Temperature (BT) measurements for specific months and time periods. By comparing the minimum and maximum LST values across spatial domains, TCI helps identify areas experiencing vegetation drought. Persistently low TCI values indicate elevated temperatures and, when sustained over time, serve as indicators of severe stress on the vegetation (Dhawale & Paul, 2018; Zeng *et al.*, 2022). TCI is calculated using the following formula:

$$LST = \frac{LST - LSTmin}{LSTmax - LSTmin} \times 100$$

Where, LST is the Land Surface Temperature; and,

LSTmin and LSTmax are the minimum and maximum LST Values respectively.

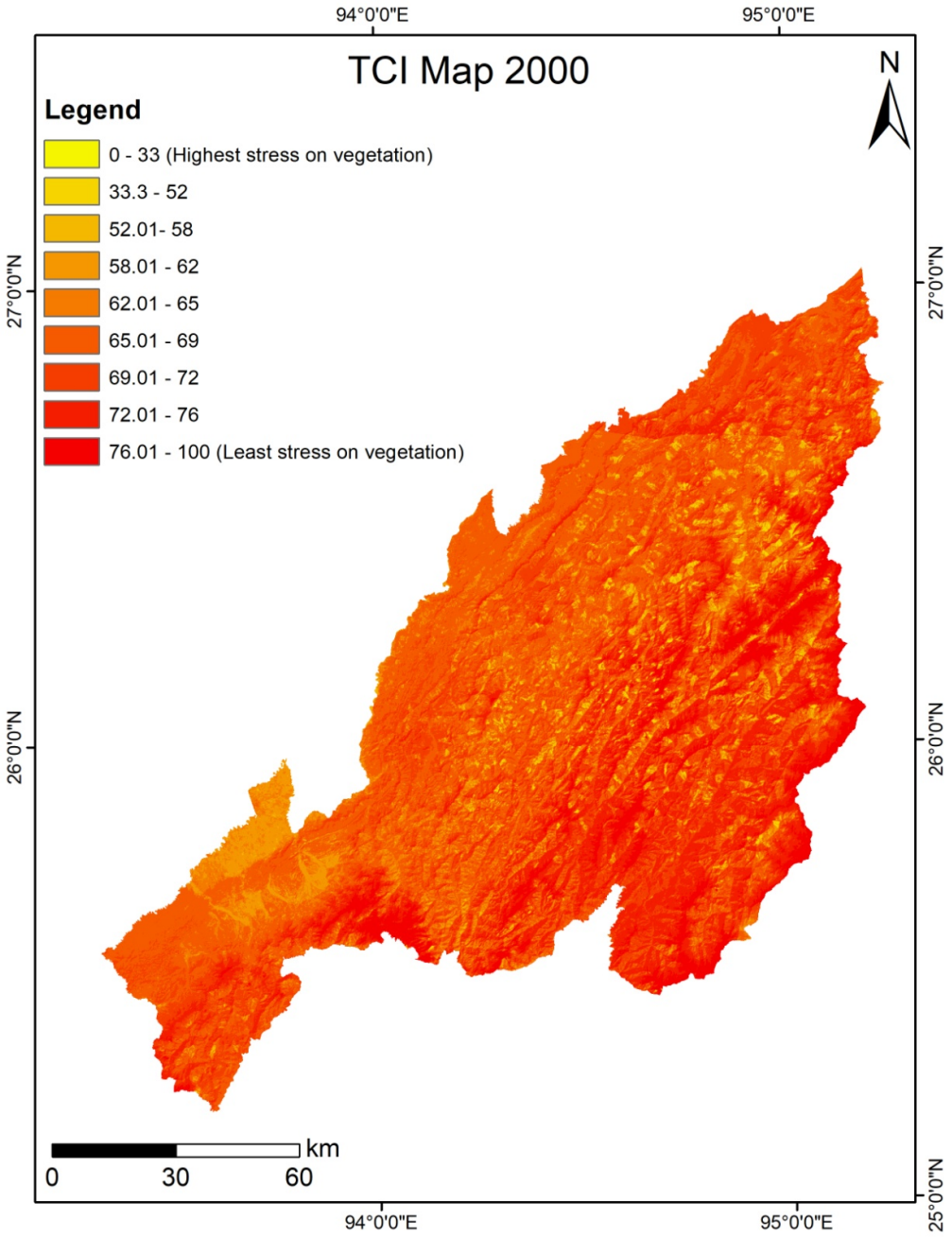

Figure 50 Map showing the distribution of TCI for the year 2000.

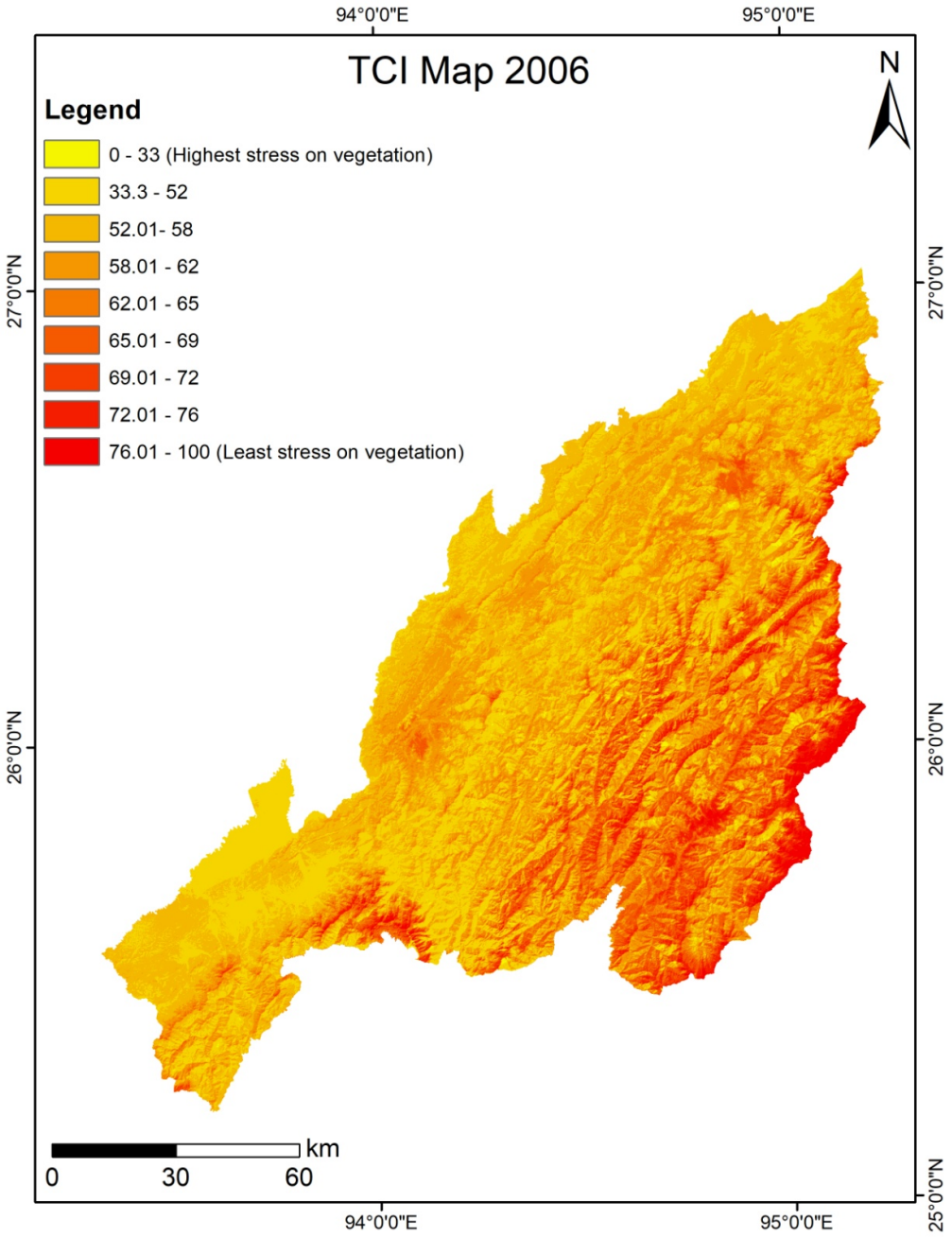

Figure 51 Map showing the distribution of TCI for the year 2006.

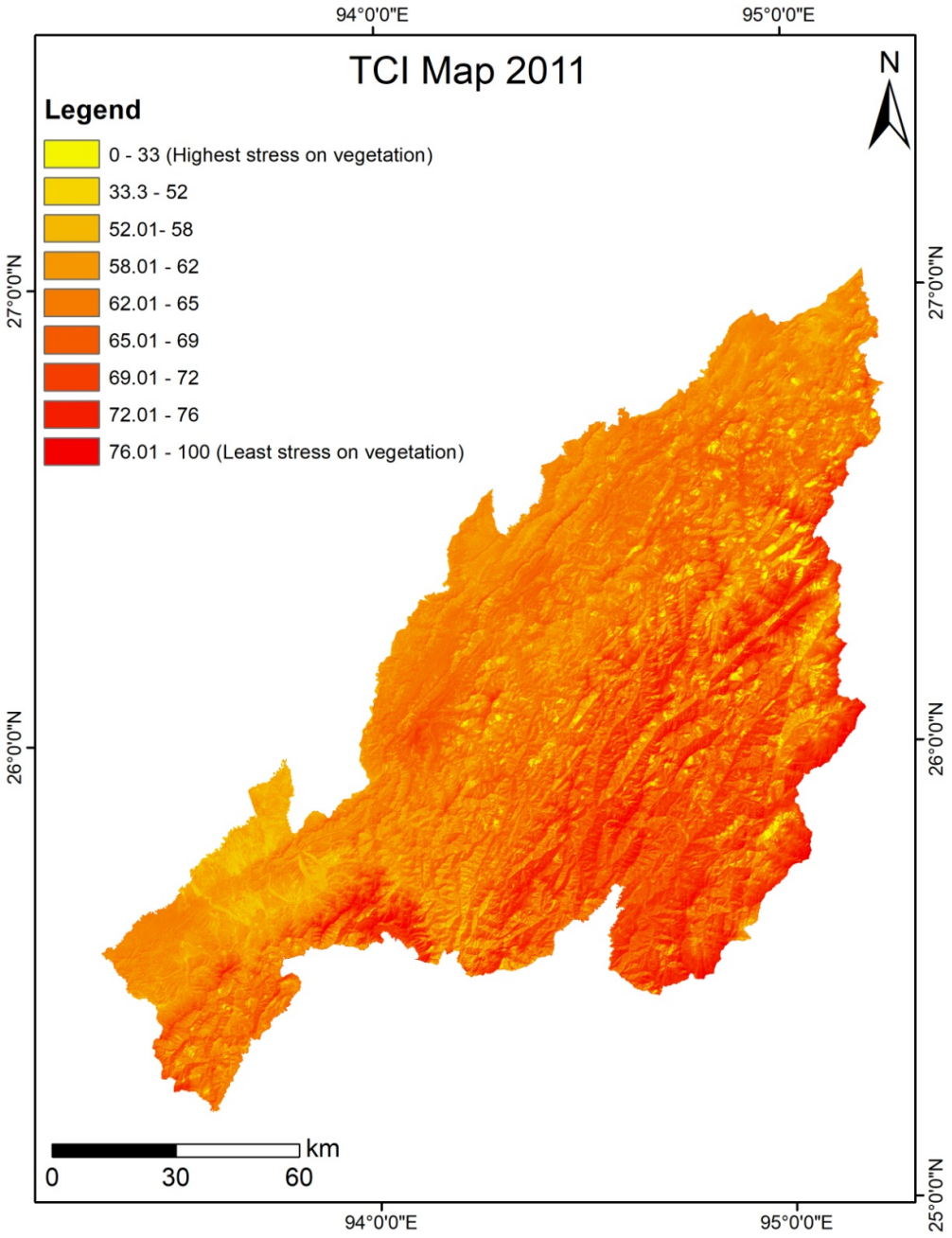

Figure 52 Map showing the distribution of TCI for the year 2011.

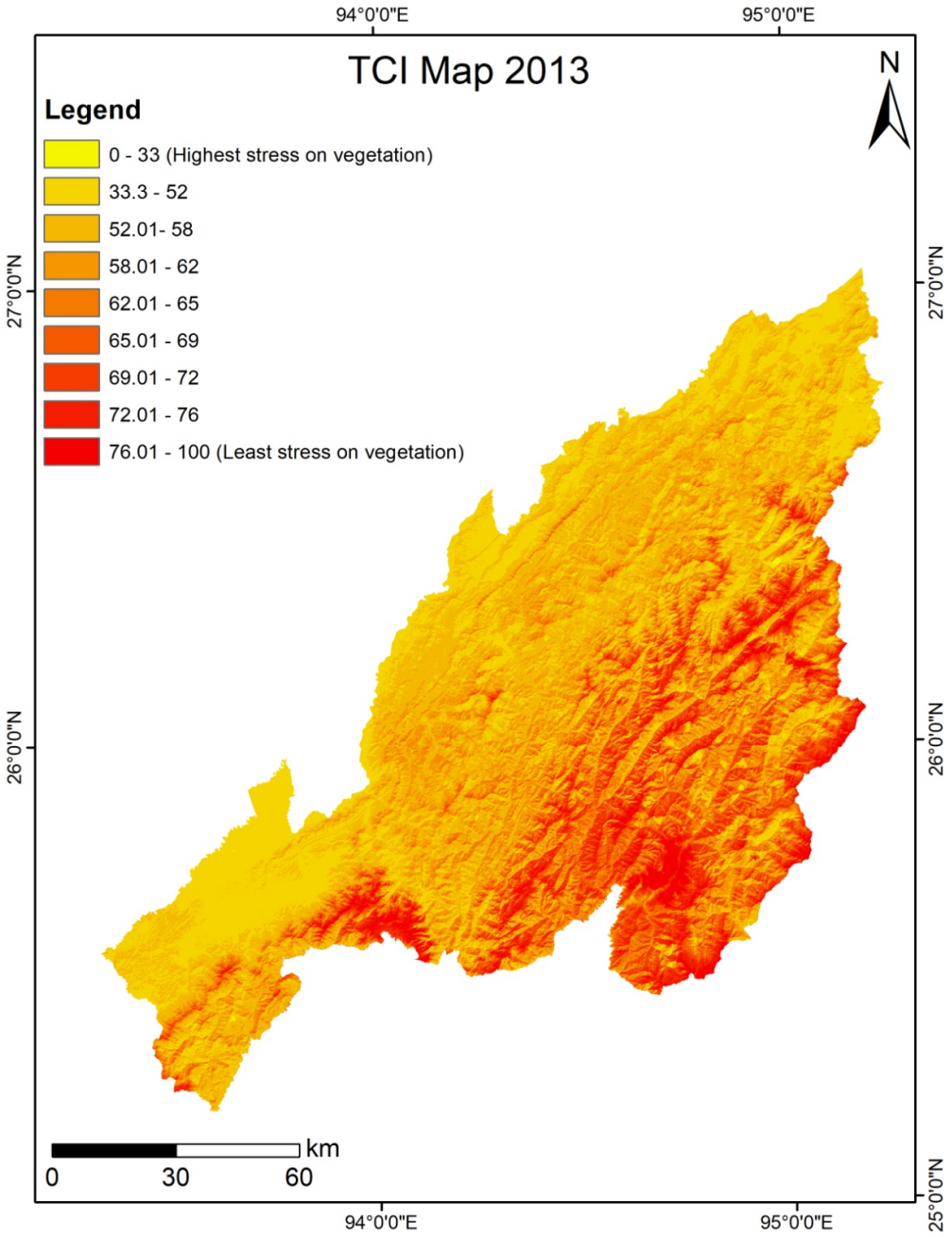

Figure 53 Map showing the distribution of TCI for the year 2013.

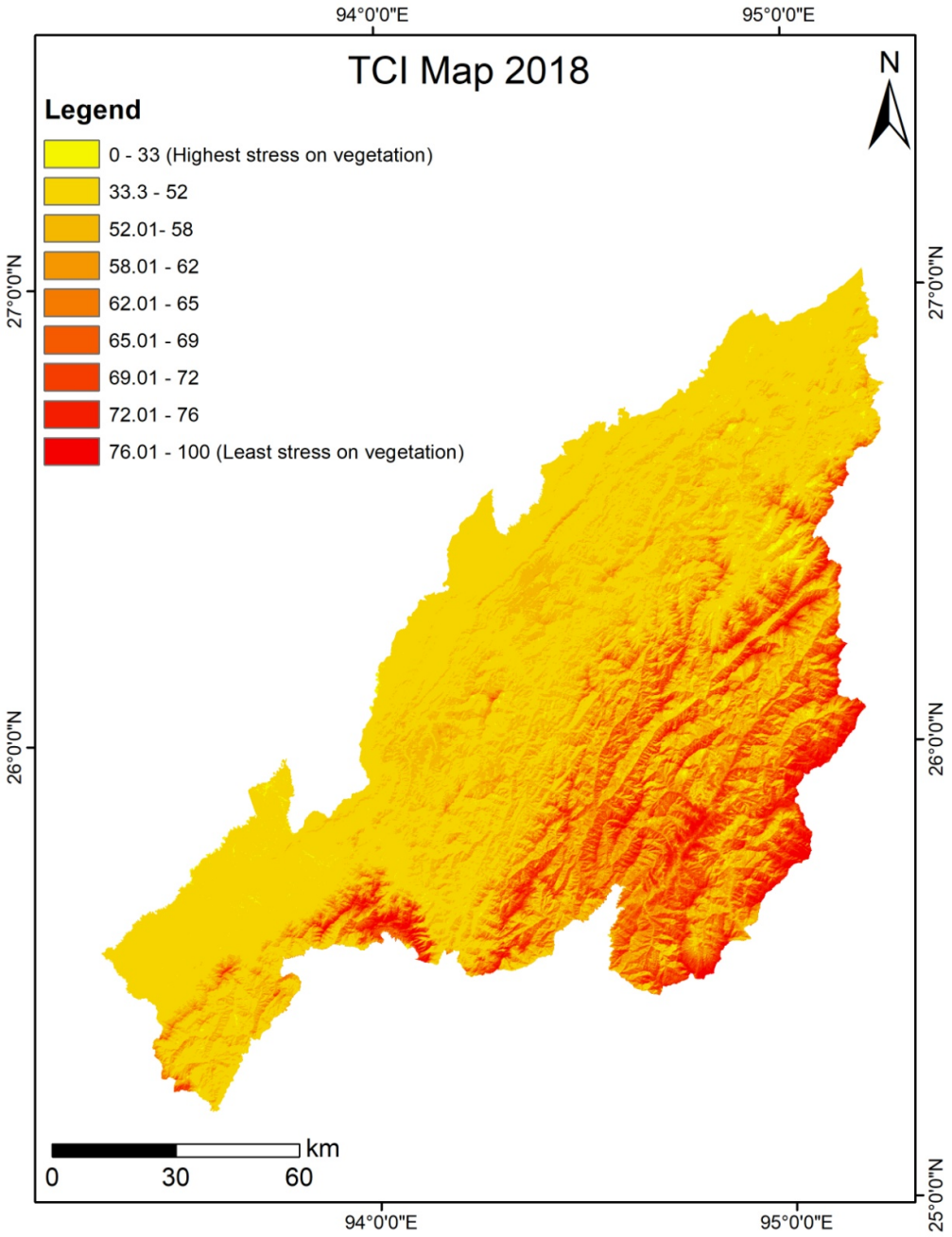

Figure 54 Map showing the distribution of TCI for the year 2018.

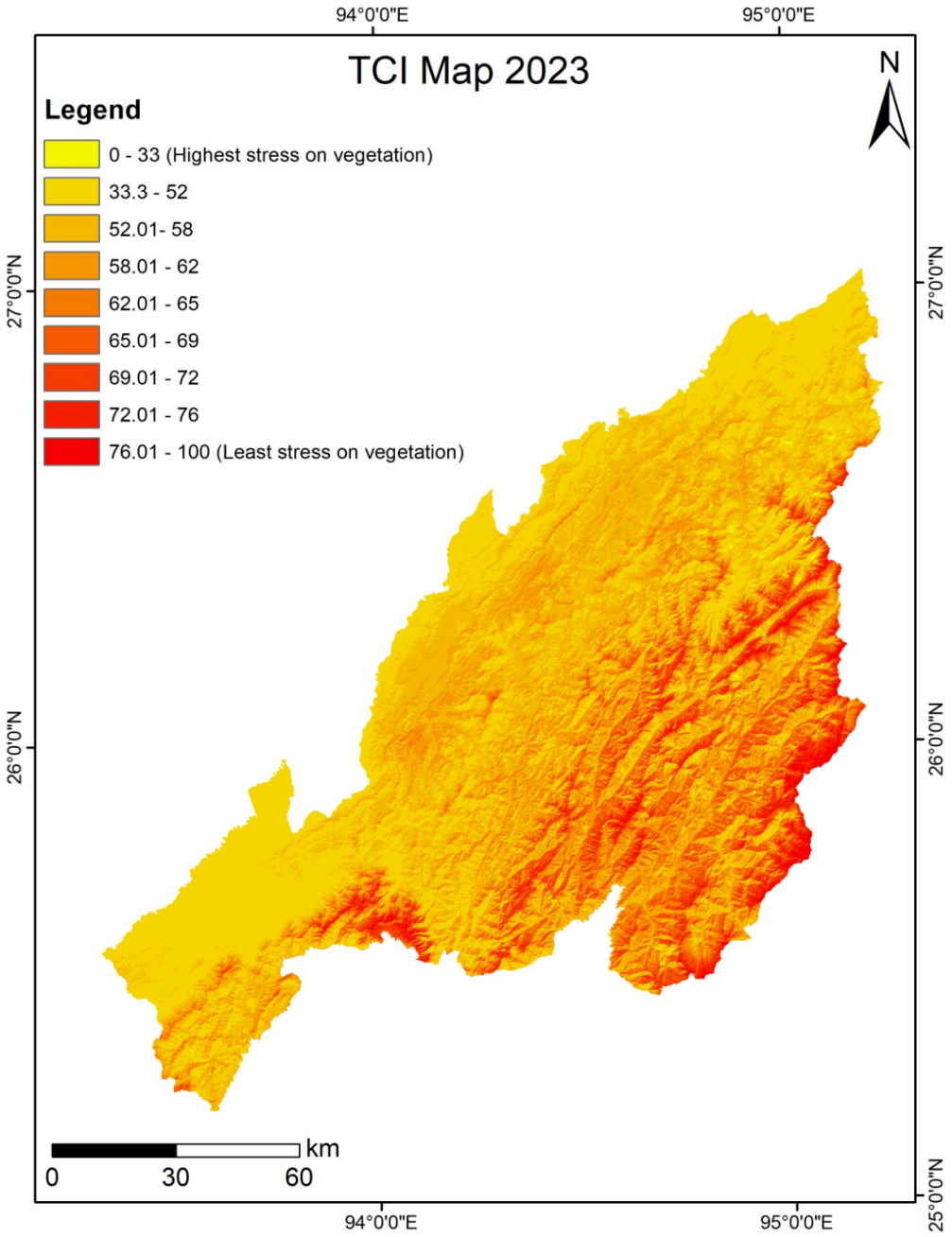

Figure 55 Map showing the distribution of TCI for the year 2023.

5.5. Vegetation Health Index (VHI)

The Vegetation Health Index (VHI) integrates both the Vegetation Condition Index (VCI) and the Temperature Condition Index (TCI) to provide a comprehensive assessment of vegetation health by accounting for soil moisture deficits and thermal stress. This composite index offers enhanced sensitivity in areas with substantial vegetation cover, outperforming individual indices in detecting drought-induced vegetation stress. By simultaneously evaluating moisture availability and temperature anomalies, VHI delivers a more robust and reliable measure of drought impact on vegetation dynamics (Dhawale & Paul, 2018; Jiang *et al.*, 2021; Burka *et al.*, 2024). VHI is calculated using the following formula:

$$VHI = 0.5* VCI+0.5 *TCI$$

Where, Vegetation Condition Index (VCI) and the Temperature Condition Index (TCI) are applied through the results extracted from the above equations of VCI and TCI respectively.

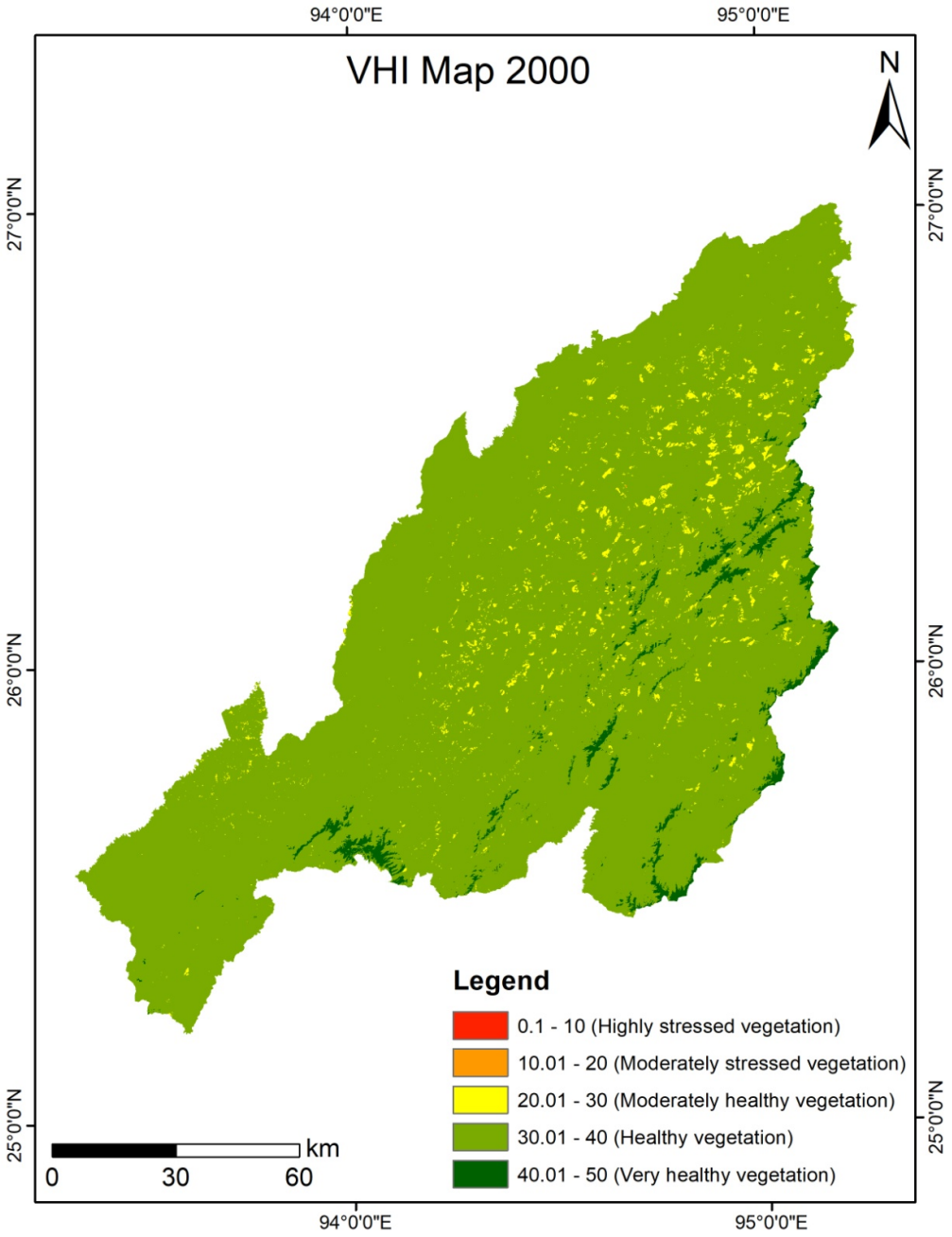

Figure 56 Map showing the distribution of VHI for the year 2000.

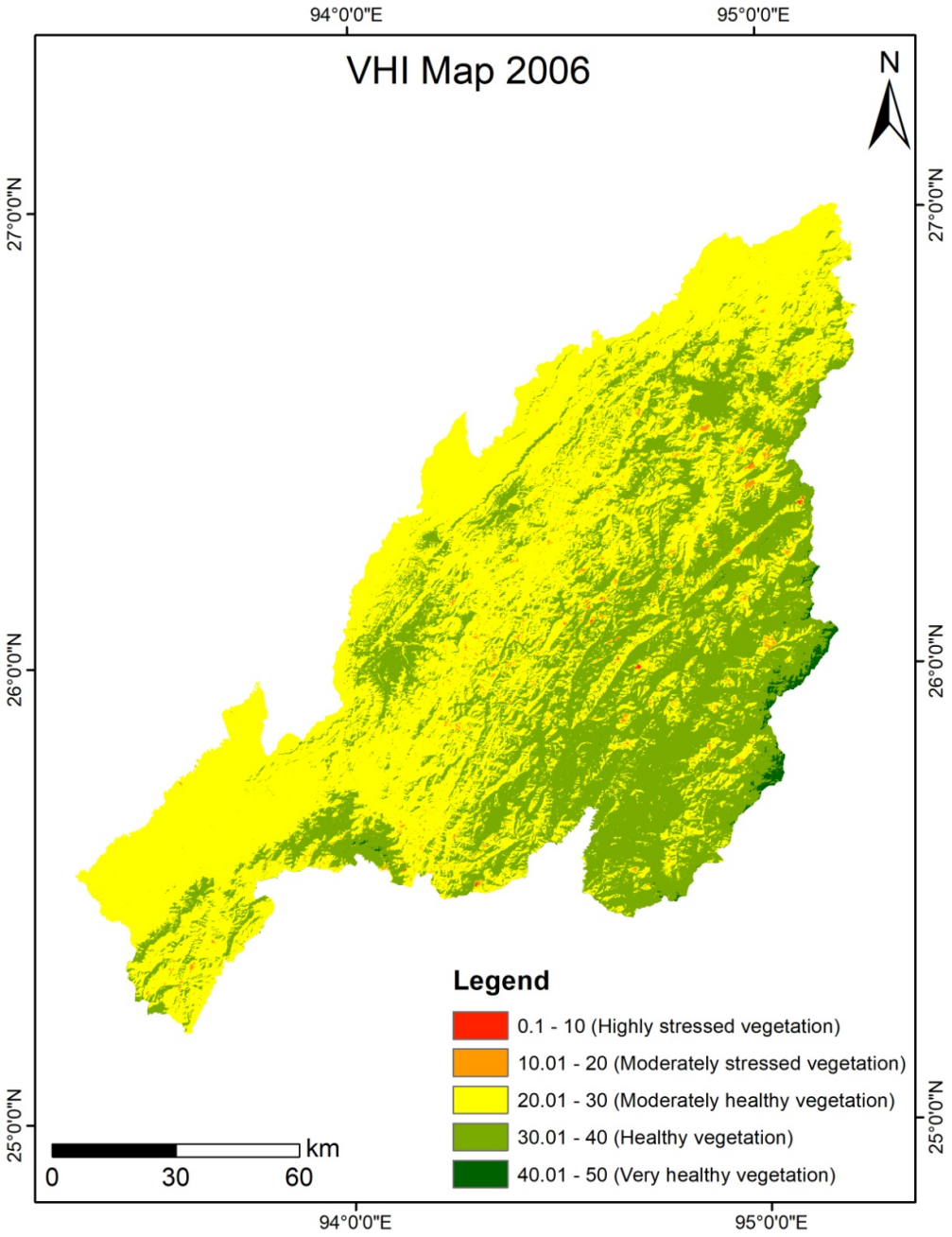

Figure 57 Map showing the distribution of VHI for the year 2006.

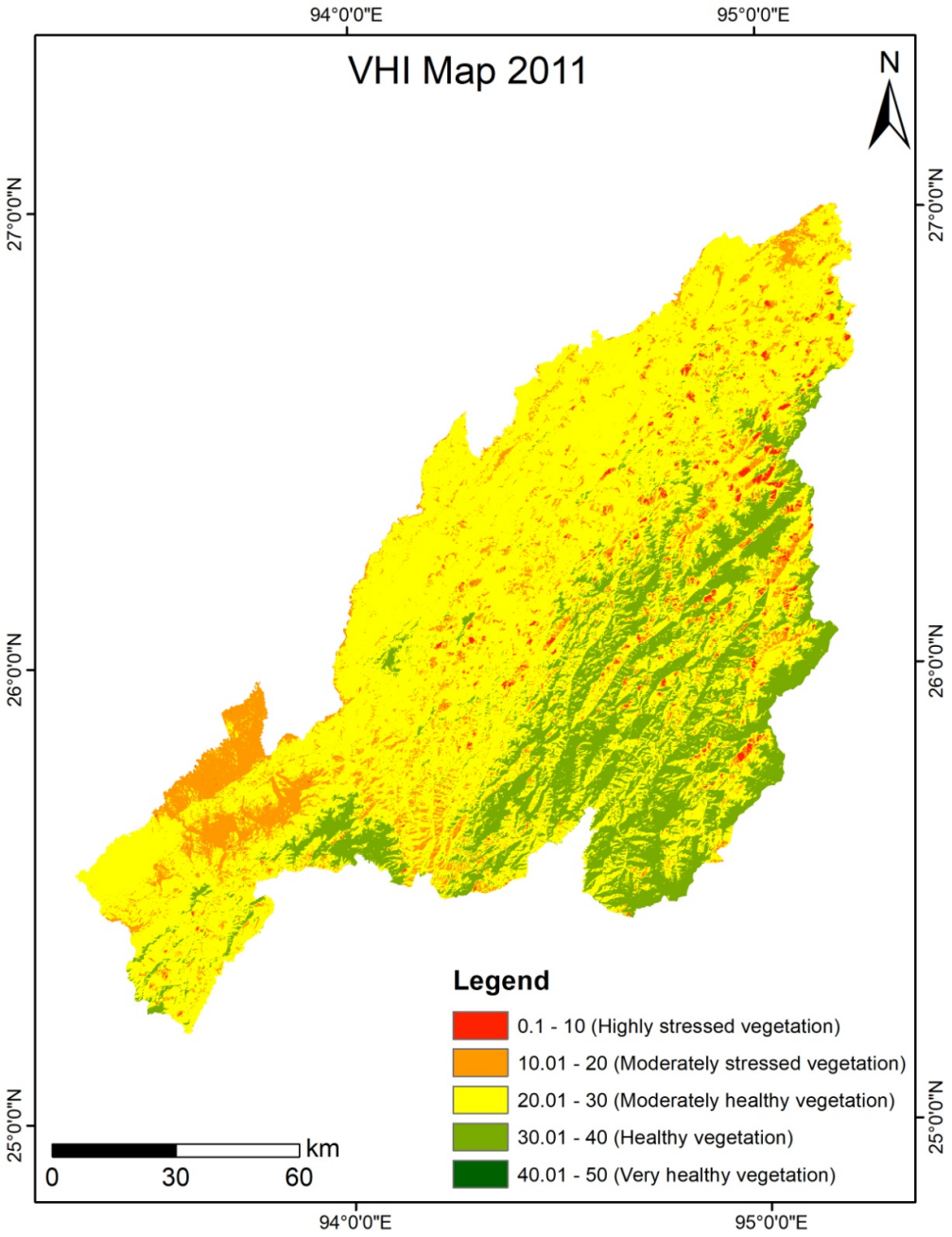

Figure 58 Map showing the distribution of VHI for the year 2011.

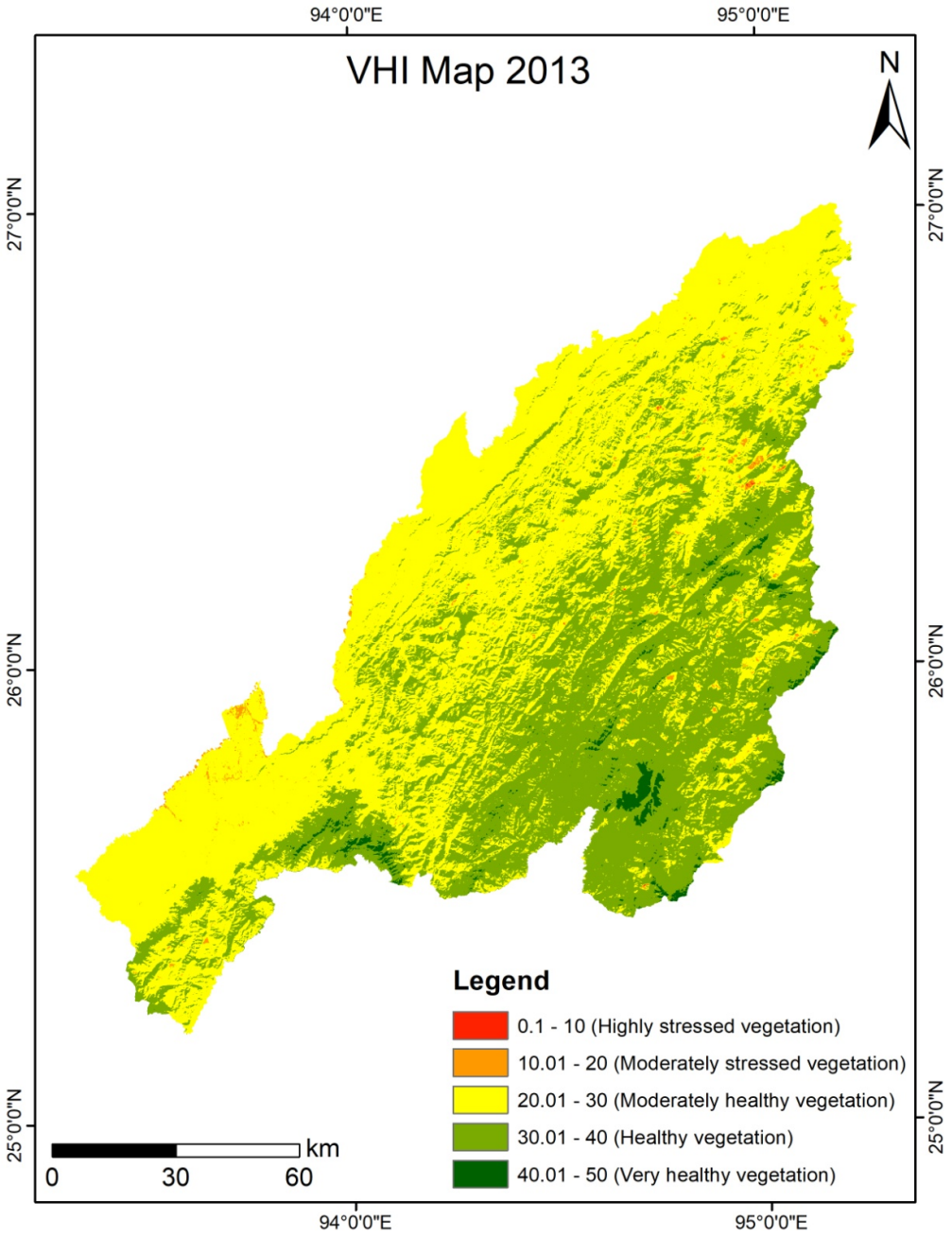

Figure 59 Map showing the distribution of VHI for the year 2013.

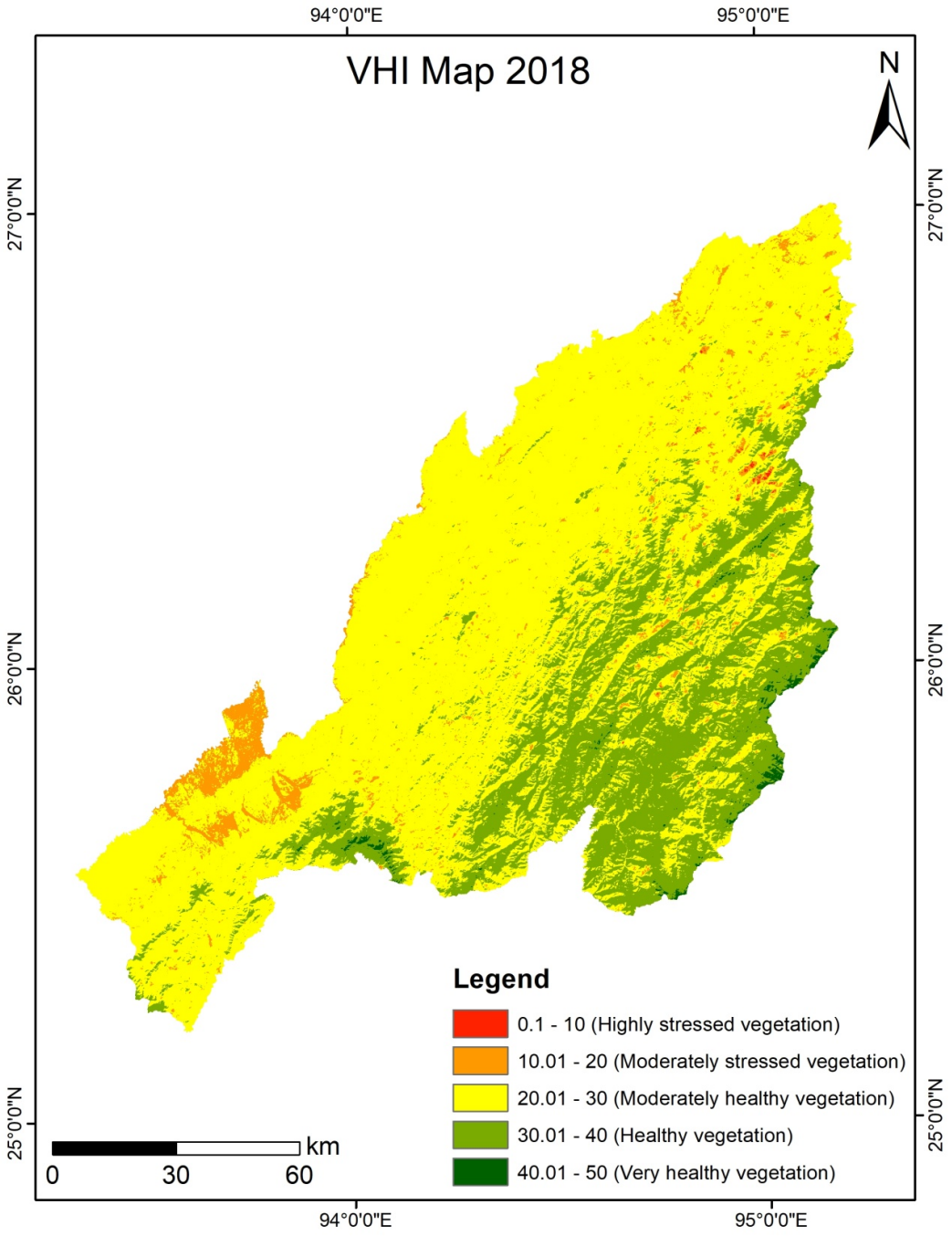

Figure 60 Map showing the distribution of VHI for the year 2018.

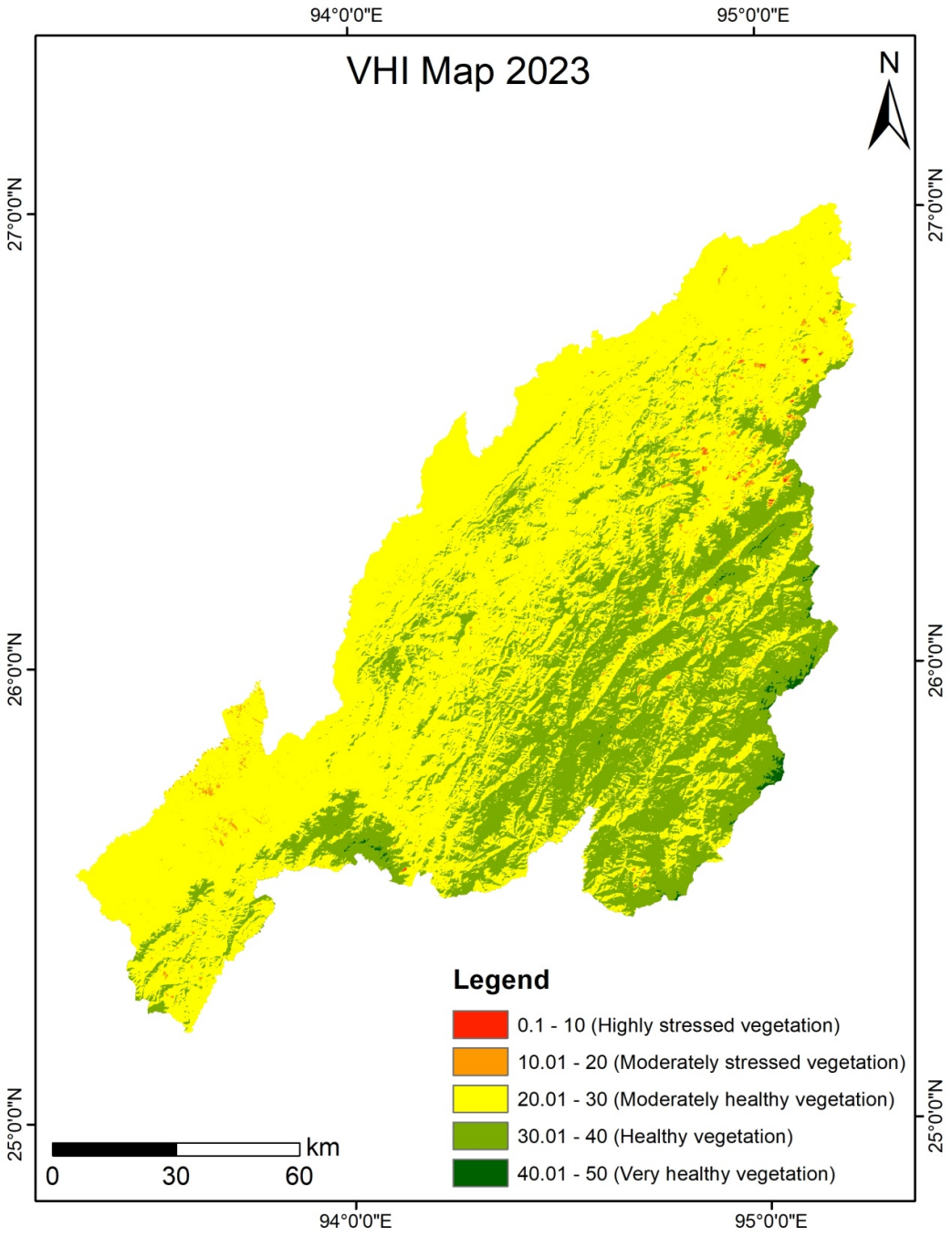

Figure 61 Map showing the distribution of VHI for the year 2023.

5.6. Trends shown through VCI and TCI

The temporal-spatial analysis of the vegetation indices through VCI for the study area indicate that the area has been undergoing stress over the study period of two-

decades from 2000-2023. The values “0-0.2” indicate “Highly stressed vegetation” represented by red color, “0.2- 0.4” indicate “Moderately stressed vegetation” represented by orange color, “0.4- 0.6” indicate “Moderately healthy vegetation” represented by yellow color, “0.6- 0.8” indicate “Healthy vegetation” represented by light green color, and “0.8- 1” indicate “Very healthy vegetation” represented by dark green color. This was done to better the visual interpretation of the study area on how the condition of the vegetation is improving or declining from 2000 till 2023.

Vegetation condition at the beginning of the decade (2000) was comparatively healthier than in 2006, with a notable recovery observed by 2011. In 2000, a larger proportion of the study area fell under the “Healthy vegetation” class, whereas by 2006, this shifted predominantly to the “Moderately healthy vegetation” category, indicating a decline in overall vegetation health. By 2011, the reappearance of the “Very healthy vegetation” class signaled a significant improvement, accompanied by a reduction in lower vegetation classes. This positive shift was evident even in urban zones, suggesting broader ecological recovery. However, the persistence of Jhum cultivation throughout the period contributed to localized vegetation degradation.

In contrast, the second half of the decade exhibited increasing vegetation stress. While the “Healthy vegetation” class was still present in 2013, it progressively diminished over time. By 2018, “Moderately healthy vegetation” became more widespread, and by 2023, the landscape was dominated by “Moderately stressed vegetation.” This deterioration was especially pronounced in urban and settlement areas, where vegetation was heavily impacted by anthropogenic pressures. Additionally, the expansion of barren zones, particularly in regions affected by mining activities, further underscored the intensifying ecological stress.

Similarly, for the Temperature Condition Index (TCI), the index values were reclassified and visualized using a color gradient, where brighter hues represented higher vegetation stress due to elevated temperatures or land surface temperature (LST), and darker tones indicated lower thermal stress on vegetation. The classification is as follows:

- 0–33 (Dark Red): Highest stress on vegetation

- 33.3–52 (Orange-Red)
- 52.01–58 (Orange)
- 58.01–62 (Yellow-Orange)
- 62.01–66 (Yellow)
- 66.01–72 (Light Yellow)
- 72.01–76 (Pale Yellow)
- 76.01–100 (Light Yellow): Least stress on vegetation

This gradation enabled nuanced interpretation of thermal stress across space and time. Across the temporal span, from 2000, 2006, 2011, 2013, 2018, to 2023, the maps reveal a progressive increase in temperature-induced vegetation stress. This trend suggests a consistent rise in thermal pressure on vegetation over time, likely driven by climatic warming, reduced canopy cover, and intensified land-use activities. Similar to VCI, the urban areas/settlement areas and the barren areas show a more pronounced temperature-induced vegetation stress throughout the study period.

5.7. Classification of Vegetation Health Index (VHI)

Lower values of the Temperature Condition Index (TCI) typically indicate that vegetation is experiencing heat-related stress, while higher values of the Vegetation Condition Index (VCI) reflect robust and healthy plant life. To gain a more holistic understanding of vegetation stress, the Vegetation Health Index (VHI) is employed, offering a more accurate assessment by integrating both temperature and vegetation conditions. In order to achieve this, VHI values were reclassified as indicated in the following attached table.

Table 15 Classification of Vegetation Health Index (VHI) from 2000 and 2023 in the study area.

Sl. No.	Class	Values
1	Highly stressed vegetation	<10
2	Moderately stressed vegetation	<20
3	Moderately healthy vegetation	<30
4	Healthy vegetation	<40
5	Very healthy vegetation	>40

The results indicated that vegetation health has been deteriorating over the past 2 decades. In 2000, the first decade started with “Moderately healthy vegetation” to “Very healthy vegetation” class. However, “Moderately stressed vegetation” appeared in 2006 which became more pronounced in 2011 leading to appearance of “Highly stressed vegetation”. In 2013, there was a mild improvement in the overall vegetation health with more prominent reappearance of “Very healthy vegetation” class with not much improvement in 2018. However, the 2023VHI values indicated that the condition was almost similar that of 2013 with improved vegetation health.

CHAPTER 6

Chapter 6: Summary and Conclusion

6.1. Summary of Major Findings

Over the study period from 2000 to 2023, Normalized Difference Vegetation Index (NDVI) analysis revealed a consistent decline in maximum NDVI values, indicating a reduction in overall vegetation health and density. This downward trend aligns with a noticeable decrease in the extent of healthy vegetation across the landscape. Statistical correlation analysis further supports this observation: NDVI exhibited a strong negative correlation with temperature ($r = –0.81$), suggesting that rising land surface temperatures are a significant driver of vegetation stress. Additionally, a weaker negative correlation was observed between NDVI and precipitation ($r = –0.19$), implying that rainfall variability may also contribute to vegetation decline, albeit to a lesser extent.

To strengthen the analysis, the Remote Sensing Ecological Index (RSEI) was integrated, offering a composite view of ecological condition by combining greenness, wetness, heat, and dryness indicators. RSEI results revealed a consistent decline in ecological quality over time, with lower index values concentrated in urbanizing and degraded zones. The synergy between RSEI, VCI, and TCI provided a robust multi-index framework for vegetation assessment, fulfilling Objective B. This integration enabled the identification of ecological hotspots and vulnerable zones, supporting targeted conservation planning.

With the progression of time and advancements in satellite technology, the availability of Landsat 8 significantly enhanced the accuracy and reliability of Remote Sensing Ecological Index (RSEI) estimations compared to earlier datasets from Landsat 5. Landsat 8's improved spectral resolution, particularly in the thermal infrared and shortwave infrared bands, allowed for more precise detection of ecological parameters such as surface temperature, vegetation greenness, and soil moisture. These enhancements contributed to more robust modeling of the RSEI components resulting in clearer spatial differentiation of ecological stress across the landscape. Consequently, RSEI outputs derived from Landsat 8 provided finer granularity and better sensitivity to subtle changes in ecological condition, especially

in transitional and peri-urban zones. This technological shift underscores the importance of sensor selection in long-term ecological monitoring and reinforces the value of integrating newer satellite platforms for multi-index analysis.

The study revealed distinct spatiotemporal patterns in vegetation health across the landscape, closely tied to rainfall variability and climatological stressors. Vegetation Condition Index (VCI) analysis from 2000 to 2023 showed a clear trajectory: the early part of the decade (2000–2011) experienced gradual improvement in vegetation condition, with 2011 marking the reappearance of "Very healthy vegetation" zones. This recovery correlated with relatively stable rainfall and reduced thermal stress. However, localized degradation persisted due to Jhum cultivation and transitional land-use pressures.

In contrast, the latter half of the study period (2013–2023) exhibited a marked decline in vegetation health. While 2013 retained patches of "Healthy vegetation," subsequent years showed a progressive shift toward "Moderately stressed" and "Highly stressed" categories. By 2023, stress was most pronounced in urban and peri-urban zones, where anthropogenic pressures, such as settlement expansion and mining, intensified vegetation loss. These findings underscore the growing vulnerability of vegetation cover to both climatic variability and land-use change, fulfilling Objective A.

Temperature Condition Index (TCI) maps further reinforced this trend. Reclassified using a detailed gradient from dark red (high stress) to pale yellow (low stress), the maps revealed increasing thermal pressure on vegetation over time. The 2000 TCI map showed relatively balanced stress distribution, but later years, especially 2018 and 2023, exhibited widespread thermal stress, particularly in southern and low-elevation zones. This pattern aligns with rising land surface temperatures and reduced canopy cover, highlighting the climatological influence on vegetation dynamics (Objective C).

Overall, the study successfully demonstrated the interplay between rainfall variation, temperature stress, and ecological degradation, offering valuable insights for adaptive land-use management and long-term ecological monitoring in the region.

6.2. Limitations of the Study

Despite the comprehensive integration of remotely sensed data and geospatial indices, several limitations were encountered during the course of this study:

- **Temporal Gaps and Data Availability**

The analysis relied on satellite datasets spanning from 2000 to 2023. However, certain years lacked consistent cloud-free imagery, particularly during monsoon months, which constrained the temporal resolution of vegetation assessments. This may have affected the accuracy of NDVI and RSEI estimations in cloud-prone zones.

- **Sensor Variability Across Time**

The transition from Landsat 5 to Landsat 8 introduced differences in spectral resolution and sensor calibration. While Landsat 8 provided improved estimations for RSEI due to its enhanced thermal and shortwave infrared bands, comparisons across time required careful normalization. Minor inconsistencies may persist due to sensor-specific limitations.

- **Limited Ground Truth Validation**

Although satellite-derived indices such as VCI, TCI, NDVI, and RSEI were used to infer vegetation condition, the study lacked extensive ground-based validation due to logistical constraints. This limits the ability to fully confirm ecological interpretations, especially in remote or inaccessible areas.

- **Simplified Climatic Correlation**

The correlation analysis between NDVI, temperature, and precipitation was based on available AWS data, which may not fully capture microclimatic variations across

diverse topographic zones, such as Nagaland where diverse climatic zones occur with differences in altitude. The observed negative correlation between NDVI and temperature (r = –0.81) and precipitation (r = –0.19) provides useful insights but should be interpreted with caution due to spatial averaging.

- **Anthropogenic Factors Not Fully Quantified**

While urban expansion, Jhum cultivation, and mining activities were identified as key drivers of vegetation stress, the study did not incorporate detailed socio-economic datasets or land-use change models. As a result, the direct attribution of vegetation degradation to human activities remains qualitative.

6.3. Suggestions for Future Research

Building on the findings and limitations of this study, several avenues for future research are recommended to deepen understanding of vegetation dynamics and ecological vulnerability in the region:

- **Integration of High-Resolution Satellite Data**

Future studies could incorporate higher-resolution datasets such as Sentinel-2 or PlanetScope to capture fine-scale vegetation changes, especially in fragmented landscapes, riparian zones, and peri-urban areas. This would enhance the detection of micro-level ecological stress and improve spatial precision in vulnerability mapping.

- **Expanded Ground Truthing and Field Validation**

Incorporating systematic field surveys and ecological sampling would strengthen the validation of remotely sensed indices such as NDVI, VCI, TCI, and RSEI. Ground-based observations of vegetation type, canopy structure, and soil moisture would help calibrate satellite-derived metrics and improve ecological interpretation.

- **Multi-Seasonal and Phenological Analysis**

Extending the analysis to include seasonal NDVI and RSEI trends could reveal vegetation responses to intra-annual climatic variability. Phenological studies would help identify shifts in growing seasons, flowering patterns, and crop cycles under changing climate regimes.

- **Socio-Ecological Linkages and Land-Use Modeling**

Future research could integrate socio-economic datasets (e.g., population density, land tenure, agricultural practices) with geospatial indices to model human–environment interactions. Land-use change modeling using tools like CA-Markov or CLUE-S could forecast future vegetation scenarios under different development trajectories.

REFERENCES

REFERENCES

Abderrazak, B., Morin, D., Bonn, F., & Huete, A. (1996). A review of vegetation indices. *Remote Sensing Reviews*, *13*, 95–120. https://doi.org/10.1080/02757259509532298

Afuye, G. A., Kalumba, A. M., & Orimoloye, I. R. (2021). Characterisation of Vegetation Response to Climate Change: A Review. *Sustainability*, *13*(13), 7265. https://doi.org/10.3390/su13137265

Al Balasmeh, O. I., & Karmaker, T. (2020). Effect of Temperature and Precipitation on the Vegetation Dynamics of High and Moderate Altitude Natural Forests in India. Journal of the Indian Society of Remote Sensing, 48(1), 121–144. https://doi.org/10.1007/s12524-019-01065-8.

Amer, Moamenla (2019). Gender and Climate change in Climate Change and Sustainable Development (Perspectives from North East India) (Ed.) Purbayon Publication.

Ayemi, Suli & Kar, Bimal. (2020). Patterns of Urbanization and Associated Infrastructure and Socio- Economic Development in Nagaland, India. Demography India. 49. 54-68.

Balasubramanian, A. (2013). Nagaland - At a glance [State profile and physiography]. (Video documentary script / state profile). University of Mysore.

Banerjee, A., Kang, S., Meadows, M. E., Xia, Z., Sengupta, D., & Kumar, V. (2023). Quantifying climate variability and regional anthropogenic influence on vegetation dynamics in northwest India. *Environmental Research*, *234*, 116541. https://doi.org/10.1016/j.envres.2023.116541

Banerjee, A., Kang, S., Meadows, M. E., Sajjad, W., Bahadur, A., Ul Moazzam, M. F., Xia, Z., Mango, J., Das, B., & Kirsten, K. L. (2024). Evaluating the relative influence of climate and human activities on recent vegetation

dynamics in West Bengal, India. *Environmental Research*, *250*, 118450. https://doi.org/10.1016/j.envres.2024.118450

Bao, Z., Zhang, J., Wang, G., Guan, T., Jin, J., Liu, Y., Li, M., & Ma, T. (2021). The sensitivity of vegetation cover to climate change in multiple climatic zones using machine learning algorithms. *Ecological Indicators*, *124*, 107443. https://doi.org/10.1016/j.ecolind.2021.107443

Baraj, B., Mishra, M., Sudarsan, D., Silva, R. M. da, & Santos, C. A. G. (2024). Climate change and resilience, adaptation, and sustainability of agriculture in India: A bibliometric review. *Heliyon*, *10*(8), e29586. https://doi.org/10.1016/j.heliyon.2024.e29586

Bhatt, D., Kundu, A., Mall, R., & Raju, K. P. (2020). Dynamics of Vegetation Response to Seasonal Rainfall in the Gomati River Basin (India) using Earth Observation Data Sets. Journal of Scientific Research, 64(01), 20–31. https://doi.org/10.37398/JSR.2020.640103.

Burka, A., Biazin, B., & Bewket, W. (2024). Spatial drought occurrences and distribution using VCI, TCI, VHI, and Google Earth Engine in Bilate River Watershed, Rift Valley of Ethiopia. *Geomatics, Natural Hazards and Risk*. https://www.tandfonline.com/doi/abs/10.1080/19475705.2024.2377672

Canan Gungor, H., & Osman Mohamed, A. (2025). Using Geographical Information Systems (Gis) For Climate Change Reduction And Adaptation: A Comprehensive Review. *International Journal of Ecosystems and Ecology Science (IJEES)*, *15*(2), 71–80. https://doi.org/10.31407/ijees15.210

Census of India (2011): Provisional Population Totals. Paper- 1 of 2011. Nagaland Series- 14.

Census of India (2011): Provisional Population Totals. Paper- 2, Volume 1of 2011. Rural- Urban distribution. Nagaland Series- 14.

Chaminé, H. I., Pereira, A. J. S. C., Teodoro, A. C., & Teixeira, J. (2021). Remote sensing and GIS applications in earth and environmental systems sciences. *SN Applied Sciences*, *3*(12), 870. https://doi.org/10.1007/s42452-021-04855-3

Changkakati, T. (2019). Temporal Response of NDVI to Climatic Attributes in North East India. International Journal of Engineering Research, International Journal of Engineering Research & Technology (IJERT) 8(08).

Changkija, Sapu (2019). Glimpses of Unique Biodiversity of North-East India in Climate Change and Sustainable Development (Perspectives from North East India) (Ed.) Purbayon Publication.

Chatterjee, S., Saikia, A., Dutta, P., Ghosh, D., & Goswami, A. K. (2006). Biodiversity Significance of North East India.

Chaturvedi, R. K., Gopalakrishnan, R., Jayaraman, M., Bala, G., Joshi, N. V., Sukumar, R., & Ravindranath, N. H. (2011). Impact of climate change on Indian forests: A dynamic vegetation modeling approach. *Mitigation and Adaptation Strategies for Global Change*, *16*(2), 119–142. https://doi.org/10.1007/s11027-010-9257-7

Chen, D. Impact of climate change on sensitive marine and extreme terrestrial ecosystems: Recent progresses and future challenges. *Ambio* **50**, 1141–1144 (2021). https://doi.org/10.1007/s13280-020-01446-1

Convention on Biological Diversity (CBD). (2011). The Strategic Plan for Biodiversity 2011–2020 and the Aichi Biodiversity Targets. CBD Decision X/2. United Nations.

Convention on Biological Diversity (CBD). (2020). Post-2020 Global Biodiversity Framework. CBD Decision 15/4. United Nations.

Das, P., Behera, M. D., Roy, P. S., & Barik, S. K. (2024). Predicting tipping points of vegetation resilience as a response to precipitation: Implications for understanding impacts of climate change in India. *Biodiversity and*

Conservation, *33*(12), 3441–3458. https://doi.org/10.1007/s10531-024-02804-1

Dash, S., & Maity, R. (2025). Association between hydroclimatic factors and vegetation health: Impact of climate change in the past and future. *Science of The Total Environment*, *964*, 178605. https://doi.org/10.1016/j.scitotenv.2025.178605

Dastour, H., & Hassan, Q. K. (2024). Quantifying the Influence of Climate Variables on Vegetation Through Remote Sensing and Multi-dimensional Data Analysis. *Earth Systems and Environment*, *8*(2), 165–180. https://doi.org/10.1007/s41748-024-00384-2

Debinski, D. M., Jakubauskas, M. E., & Kindscher, K. (2000). Montane Meadows as Indicators of Environmental Change. *Environmental Monitoring and Assessment*, *64*(1), 213–225. https://doi.org/10.1023/A:1006432030089

Dhawale, R., & Paul, S. K. (2018). A comparative analysis of drought indices on vegetation through remote sensing for Latur region of India. *The International Archives of the Photogrammetry, Remote Sensing and Spatial Information Sciences*, *XLII–5*, 403–407. ISPRS TC V Mid-term Symposium (Volume XLII-5) https://doi.org/10.5194/isprs-archives-XLII-5-403-2018

Dikici, M. (2022). Drought Analysis for the Seyhan Basin with Vegetation Indices and Comparison with Meteorological Different Indices. *Sustainability*, *14*(8), 4464. https://doi.org/10.3390/su14084464

Dietz, H., & Steinlein, T. (2002). Plant Cover: Ecological Implications and Methodical Approaches. In R. S. Ambasht & N. K. Ambasht (Eds.), Modern Trends in Applied Terrestrial Ecology (pp. 247–274). Springer US. https://doi.org/10.1007/978-1-4615-0223-4_13

Directorate of Economics & Statistics, Government of Nagaland. (2012). *Statistical handbook of Nagaland*. Kohima: Directorate of Economics & Statistics.

Directorate of Economics & Statistics, Government of Nagaland. (2024). *Statistical handbook of Nagaland*. Kohima: Directorate of Economics & Statistics.

Dunham, S., Fonstad, M. A., Anderson, S., & Czajkowski, K. P. (2005). Using Multi-temporal Satellite Imagery to Monitor the Response of Vegetation to Drought in the Great Lakes Region. GIScience & Remote Sensing, 42(3), 183–199. https://doi.org/10.2747/1548-1603.42.3.183

Edwin-Wosu, N. L., Mojuetan, T., Ndukwu, B. C., & Micheal, C. A. (2019). Geospatial technology, a satellite -based change detection agent: Imperative for analysis and management of vegetation resources in developing economy. Nigerian Journal of Botany, 32(1), Article 1. https://www.ajol.info/index.php/njbot/article/view/236111

Forest Survey of India. (2019). India state of forest report 2019. Ministry of Environment, Forest and Climate Change. https://fsi.nic.in/

Forest Survey of India. (2021). India state of forest report 2019. Ministry of Environment, Forest and Climate Change. https://fsi.nic.in/

Forest Survey of India. (2023). India state of forest report 2021. Ministry of Environment, Forest and Climate Change. https://fsi.nic.in/

Franklin, J., Serra-Diaz, J. M., Syphard, A. D., & Regan, H. M. (2016). Global change and terrestrial plant community dynamics. Proceedings of the National Academy of Sciences of the United States of America, 113(14), 3725–3734. https://doi.org/10.1073/pnas.1519911113

Gabriele, M., Brumana, R., Previtali, M., & Cazzani, A. (2023). A combined GIS and remote sensing approach for monitoring climate change-related land degradation to support landscape preservation and planning tools: The Basilicata case study. *Applied Geomatics*, *15*(3), 497–532. https://doi.org/10.1007/s12518-022-00437-z

Gandhi, G.M., Parthiban, S., Nagaraj, T. and Christy, A. (2015) Ndvi: Vegetation Change Detection Using Remote Sensing and Gis—A Case Study of Vellore District. Procedia Computer Science, 57, 1199-1210. https://doi.org/10.1016/j.procs.2015.07.415

Gopalakrishnan, R., Jayaraman, M., Bala, G., & Ravindranath, N. H. (2011). Climate change and Indian forests. *CURRENT SCIENCE*, *101*(3).

Guhathakurta, P., Sanap, S., Menon, P., Prasad, A. K., Sangwan, N., & Advani, S. C. (2020). *Observed rainfall variability and changes over Nagaland State* (Met Monograph No. ESSO/IMD/HS/Rainfall Variability/19 (2020)/43). India Meteorological Department, Ministry of Earth Sciences.

Gupta, S., & Gupta, R. (2024). The Impact Of Changing Climate On Natural Vegetation: A Comprehensive Analysis. *EPRA International Journal of Multidisciplinary Research (IJMR)*, *10*(2).

Hao H., Lian Z., Zhao J., *et al. (2022)* A Remote-Sensing Ecological Index Approach for Restoration Assessment of Rare-Earth Elements Mining. Retrieved October 9, 2023, from https://www.hindawi.com/journals/cin/2022/5335419/

Han, F., Yan, J., & Ling, H. (2021). Variance of vegetation coverage and its sensitivity to climatic factors in the Irtysh River basin. *PeerJ*, *9*, e11334. https://doi.org/10.7717/peerj.11334

Hansen, G., Stone, D., Auffhammer, M., Huggel, C., & Cramer, W. (2016). Links between climate change, land degradation, and migration in drylands. Environmental Science & Policy, 56, 221-227. doi: 10.1016/j.envsci.2015.11.016

Halder, S., & Bose, S. (2024). Comparative study on remote sensing-based indices for urban ecology assessment: A case study of 12 urban centers in the metropolitan area of eastern India. *Journal of Earth System Science*, *133*(2), 100. https://doi.org/10.1007/s12040-024-02321-3

Hame, T.; Salli, A.; Andersson, K.; Lohi, A. (1997). A new methodology for the estimation of biomass of conifer-dominated boreal forest using NOAA AVHRR data

Hosseini-Moghari, S.-M., Araghinejad, S., Tourian, M. J., Ebrahimi, K., & Döll, P. (2020). Quantifying the impacts of human water use and climate variations on recent drying of Lake Urmia basin: The value of different sets of spaceborne and in situ data for calibrating a global hydrological model. *Hydrology and Earth System Sciences*, *24*(4), 1939–1956. https://doi.org/10.5194/hess-24-1939-2020

Imchen, N. (2015). Integrated watershed management in Nagaland_a key to sustainable development [PhD Thesis, Nagaland University]. http://hdl.handle.net/10603/327072

India Meteorological Department. (2024). *Rainfall and temperature data (2000–2023)* [Data set]. Data Supply Portal, IMD Pune. https://dsp.imdpune.gov.in/

Intergovernmental Panel on Climate Change. (2013). Climate change 2013: The physical science basis. Contribution of Working Group I to the Fifth Assessment Report of the Intergovernmental Panel on Climate Change. Cambridge University Press.

Intergovernmental Panel on Climate Change. (2014). Climate change 2014: Impacts, vulnerability, and adaptation. Contribution of Working Group II to the Fifth Assessment Report of the Intergovernmental Panel on Climate Change. Cambridge University Press.

Jamir, C., Sharma, N., Sengupta, A., & Ravindranath, N. H. (2013). Farmers' vulnerability to climate variability in Dimapur district of Nagaland, India. *Regional Environmental Change*, *13*(1), 153–164. https://doi.org/10.1007/s10113-012-0324-3

Jamir, C., Kapoor, C., & Jagannath, P. (2023). Climate Change and Agroecosystems in the Hill and Mountain Regions of Northeast India. In S. A. Narula & S. P.

Raj (Eds.), *Sustainable Food Value Chain Development: Perspectives from Developing and Emerging Economies* (pp. 37–60). Springer Nature. https://doi.org/10.1007/978-981-19-6454-1_3

Jiang, R., Liang, J., Zhao, Y., Wang, H., Xie, J., Lu, X., & Li, F. (2021). Assessment of vegetation growth and drought conditions using satellite-based vegetation health indices in Jing-Jin-Ji region of China. Scientific Reports, 11(1), 13775. https://doi.org/10.1038/s41598-021-93328-z

Kalisa, W., Igbawua, T., Henchiri, M., Ali, S., Zhang, S., Bai, Y., & Zhang, J. (2019). *Assessment of climate impact on vegetation dynamics over East Africa from 1982 to 2015 | Scientific Reports*. https://www.nature.com/articles/s41598-019-53150-0

Kanwal, K. & Lodhi, Mahendra. (2018). Climate Change Impact On Plant Biodiversity Of Arunachal Himalaya: A Review. 33. 15-26.

Kefalas, G., Lattas, P., Xofis, P., Lorilla, R., Martinis, A., & Poirazidis, K. (2018). The use of vegetation indices and change detection techniques as a tool for monitoring ecosystem and biodiversity integrity. *International Journal of Sustainable Agricultural Management and Informatics*, *4*, 47. https://doi.org/10.1504/IJSAMI.2018.092411

Khetwani, S., & Singh, R. B. (2019). Geospatial Assessment Of Drought In Marathwada Region, India. 10(4), 17.

Krishnan, N. R., & Ct, M. F. (2016). A Geospatial Approach for Assessing and Monitoring the Drought Condition in Chittur Taluk, Palakkad District, Kerala. 03(09), 11.

Kumar, R., Jalem, K., Swain, S. K., Kanga, S., Singh, S. K., Meraj, G., Kumar, P., & Mandal, D. (2025). Geospatial analysis of climate-induced land cover changes and vegetation trends in western Jharkhand, India. *Environmental Monitoring and Assessment*, *197*(9), 1019. https://doi.org/10.1007/s10661-025-14452-1

Kumari, B., Tayyab, M., Shahfahad, Salman, Mallick, J., Khan, M. F., & Rahman, A. (2018). Satellite-Driven Land Surface Temperature (LST) Using Landsat 5, 7 (TM/ETM+ SLC) and Landsat 8 (OLI/TIRS) Data and Its Association with Built-Up and Green Cover Over Urban Delhi, India. *Remote Sensing in Earth Systems Sciences*, 1(3), 63–78. https://doi.org/10.1007/s41976-018-0004-2

Lausch, A., Selsam, P., Pause, M., & Bumberger, J. (2024). Monitoring vegetation- and geodiversity with remote sensing and traits. *Philosophical Transactions of the Royal Society A: Mathematical, Physical and Engineering Sciences*, *382*(2269), 20230058. https://doi.org/10.1098/rsta.2023.0058

Lele, S., & Krishnaswamy, J. (2019). *Climate Change and India's Forests*. https://academic.oup.com/book/35227/chapter/299755542

Li, Y., Zhao, Z., Wang, L., Li, G., Chang, L., & Li, Y. (2021). Vegetation Changes in Response to Climatic Factors and Human Activities in Jilin Province, China, 2000–2019. *Sustainability*, *13*(16), 8956. https://doi.org/10.3390/su13168956

Li, P. (2022). Research on Ecoenvironmental Quality Evaluation System Based on Big Data Analysis. Computational Intelligence and Neuroscience, 2022, 1–14. https://doi.org/10.1155/2022/5191223

Li, L., Xin, X., Zhao, J., Yang, A., Wu, S., Zhang, H., & Yu, S. (2023). Remote Sensing Monitoring and Assessment of Global Vegetation Status and Changes during 2016–2020. *Sensors (Basel, Switzerland)*, *23*(20), 8452. https://doi.org/10.3390/s23208452

Liang, T., Tian, F., Zou, L., Jin, H., Tagesson, T., Rumpf, S., He, T., Liang, S., & Fensholt, R. (2024). Global assessment of vegetation patterns along topographic gradients. *International Journal of Digital Earth*, *17*(1), 2404232. https://doi.org/10.1080/17538947.2024.2404232

Lotha, T. N., Ritse, V., Nakro, V., Ketiyala, Imkongyanger, Hazarika, N., Jamir, L., & Rudithongru, L. (2024). Climate Change Impact and Traditional Adaptation Practices in Northeast India: A Review. *Current World Environment*, *Volume 19*(Issue 2). https://www.cwejournal.org/vol2no2/pclimate-change-impact-and-traditional-adaptation-practices-in-northeast-india-a-reviewp

Lu, D. (2006). The potential and challenge of remote sensing-based biomass estimation. *International Journal of Remote Sensing*, *27*(7), 1297–1328. https://doi.org/10.1080/01431160500486732

Lunetta, R. S., Knight, J. F., Ediriwickrema, J., Lyon, J. G., & Worthy, L. D. (2006). Land-cover change detection using multi-temporal MODIS NDVI data. *Remote Sensing of Environment*, 105(2), 142–154.

Mace, G. M., Norris, K., & Fitter, A. H. (2018). Nature's dangerous decline: Why biodiversity loss matters. Science, 346(6209), 1080-1081. https://doi.org/10.1126/science.1257542

Maharana, P., Agnihotri, R., & Dimri, A. P. (2021). Changing Indian monsoon rainfall patterns under the recent warming period 2001–2018. *Climate Dynamics*, *57*(9), 2581–2593. https://doi.org/10.1007/s00382-021-05823-8

Maity, S., Das, S., Pattanayak, J. M., Bera, B., & Shit, P. K. (2022). Assessment of ecological environment quality in Kolkata urban agglomeration, India. Urban Ecosystems, 25(4), 1137–1154. https://doi.org/10.1007/s11252-022-01220-z

Maity, Sukamal. (2022). Assessment of Spatio-temporal Variation of Urban Eco-Environmental Quality based on Remote Sensing Ecological Index (RSEI) in Delhi Urban Agglomeration, India. 13. 15.

Mao, A. A., & Gogoi, R. (2010). Fire-induced invasion of an endemic plant species alters forest structure and diversity: A study from north-east India. *Current Science*. https://www.semanticscholar.org/paper/Fire-induced-invasion-of-an-

endemic-plant-species-a-Mao-Gogoi/a6b66f2768d9cb5d34e4092680e2c72101526cf1

Mann, M. E., Rahmstorf, S., Kornhuber, K., Steinman, B. A., Miller, S. K., & Coumou, D. (2017). Influence of anthropogenic climate change on planetary wave resonance and extreme weather events. Scientific Reports, 7, 1-10. doi: 10.1038/s41598-017-11492-2

Martemjen & Lanusashi Longkumar (2019). Identification of Different Biodiversity Belt in Nagaland: A Geographical Perspective in Climate Change and Sustainable Development (Perspectives from North East India) (Ed.) Purbayon Publication.

Matyukira, C., & Mhangara, P. (2024). Advances in vegetation mapping through remote sensing and machine learning techniques: A scientometric review. *European Journal of Remote Sensing*, *57*(1), 2422330. https://doi.org/10.1080/22797254.2024.2422330

Meru, L. B., & Pandey, R. (2024). Climate change ecological vulnerability and hotspot analysis of Himalayan forests in North-Eastern region, India. *Environmental and Sustainability Indicators*, *24*, 100472. https://doi.org/10.1016/j.indic.2024.100472

Mishra, G., & Francaviglia, R. (2021). Land uses, altitude and texture effects on soil parameters: A comparative study in two districts of Nagaland, Northeast India. Agriculture, 11(2), 171. https://doi.org/10.3390/agriculture11020171.

Motohka, T., Nasahara, K. N., Oguma, H., & Tsuchida, S. (2010). Applicability of Green-Red Vegetation Index for Remote Sensing of Vegetation Phenology. Remote Sensing, 2(10), 2369–2387. https://doi.org/10.3390/rs2102369

Murry, N., & Das, S. (2021). Zabo Farming System- A Sustainable Farming based on Traditional Knowledge for Natural Resource Management Practiced by Tribal in Nagaland, India. *International Journal of Agriculture Environment and Biotechnology*.

Nabizada, A. F., Rousta, I., Dalvi, M., Olafsson, H., Siedliska, A., Baranowski, P., Tkaczyk, P., & Krzyszczak, J. (2022). A Remotely Sensed Study of the Impact of Meteorological Parameters on Vegetation for the Eastern Basins of Afghanistan. *Earth Sciences*. https://doi.org/10.20944/preprints202207.0257.v1

Nagaland State Disaster Management Authority. (2019). *Nagaland State Disaster Management Plan* (Physiography section). Government of Nagaland. nsdma.nagaland.gov.in

Nagendra, H., Lucas, R., Honrado, J. P., Jongman, R. H. G., Tarantino, C., Adamo, M., & Mairota, P. (2013). Remote sensing for conservation monitoring: Assessing protected areas, habitat extent, habitat condition, species diversity, and threats. *Ecological Indicators*, *33*, 45–59. https://doi.org/10.1016/j.ecolind.2012.09.014

Newbold, T., Hudson, L. N., Arnell, A. P., Contu, S., De Palma, A., Ferrier, S., … & Scharlemann, J. P. (2015). Global effects of land use on local terrestrial biodiversity. Nature, 520(7545), 45-50. https://doi.org/10.1038/nature14324

Niu, Xiaonan & Li, Y.. (2020). Remote Sensing Evaluation of Ecological Environment of Anqing City Based on Remote Sensing Ecological Index. Isprs - International Archives of the Photogrammetry, Remote Sensing and Spatial Information Sciences. XLIII-B3-2020. 733-737. 10.5194/isprs-archives-XLIII-B3-2020-733-2020.

Nongbri, B., Feroze, S. M., Singh, R., & Devarani, L. (2019). *Factors softening drought vulnerability of farm households in Nagaland*. 7.

Palmate, S. S., Pandey, A., Kumar, D., Pandey, R. P., & Mishra, S. K. (2017). Climate change impact on forest cover and vegetation in Betwa Basin, India. Applied Water Science, 7(1), 103–114. https://doi.org/10.1007/s13201-014-0222-6

Parida, B. R., & Oinam, B. (2015). Unprecedented drought in North East India compared to Western India. *CURRENT SCIENCE*, *109*(11), 6.

Parida, B. R., Pandey, A. C., & Patel, N. R. (2020). Greening and Browning Trends of Vegetation in India and Their Responses to Climatic and Non-Climatic Drivers. Climate, 8(8), 92. https://doi.org/10.3390/cli8080092

Pan, K., Moens, M., Marshall, L., Cieraad, E., Snoo, G. R. de, & Biesmeijer, K. (2021). Importance of natural land cover for plant species' conservation: A nationwide study in The Netherlands. PLoS ONE, 16(11), e0259255. https://doi.org/10.1371/journal.pone.0259255

Pe'er, G., Martín-López, B., Garon, M., Mühlhauser, R., & Sutherland, W. J. (2014). The role of monitoring in achieving global biodiversity targets. Nature, 510(7503), 8-11. https://doi.org/10.1038/nature13509

Pei, F., Zhou, Y., & Xia, Y. (2021). Application of Normalized Difference Vegetation Index (NDVI) for the Detection of Extreme Precipitation Change. Forests, 12(5), 594. https://doi.org/10.3390/f12050594

Philip, A., R.J, R., & V.K, J. (2024). Dynamic monitoring and analysis of ecological quality based on RSEI: A case study of Akkulam-Veli Lake Basin of Thiruvananthapuram City, Kerala, India. *Geology, Ecology, and Landscapes*, *0*(0), 1–21. https://doi.org/10.1080/24749508.2024.2359772

Pradhan Mantri Krishi Sinchayee Yojana (PMKSY). (2017). *Introduction — general information of the state* (state profile; elevation and physiography data). Government of India.

Ramachandra T V, Uttam Kumar and Anindita Dasgupta, 2016, Time-series MODIS NDVI based Vegetation Change Analysis with Land Surface Temperature and Rainfall in Western Ghats, India, ENVIS Technical Report 100, Sahyadri Conservation Series 53, Energy & Wetlands Research Group, CES, Indian Institute of Science, Bangalore 560012.

Rawat, M. S. (2014). Integrated Watershed Management: An Alternative Approach for Sustainable Development in Nagaland. *Journal of Agriculture and Life Sciences*, *1*(1).

Revised Nagaland State Biodiversity Strategy and Action Plan. (2022). https://nsbb.nagaland.gov.in/wp-content/uploads/2023/10/Revised-Nagaland-State-Biodiversity-Strategy-Action-Plan.pdf

Ritse, V., Basumatary, H., Kulnu, A. S., Dutta, G., Phukan, M. M., & Hazarika, N. (2020). Monitoring land use land cover changes in the Eastern Himalayan landscape of Nagaland, Northeast India. *Environmental Monitoring and Assessment*, *192*(11), 711. https://doi.org/10.1007/s10661-020-08674-8

Rouse, J.W.; Haas, R.H.; Schell, J.A.; Deering, D.W (1973). Monitoring vegetation systems in the Great Plains with ERTS. In Proceedings of the Third ERTS Symposium, NASA SP-351, Washington, DC, USA, 10–14 December; pp. 309–317.

Rousta, I., Mansourmoghaddam, M., Olafsson, H., Krzyszczak, J., Baranowski, P., Zhang, H., & Tkaczyk, P. (2022). Analysis of the recent trends in vegetation dynamics and its relationship with climatological factors using remote sensing data for Caspian Sea watersheds in Iran. International Agrophysics, 36(3), 139–153. https://doi.org/10.31545/intagr/150020

Roy, D. P., & Bhardwaj, D. S. (2024). *Remote Sensing and GIS Applications for Weather and Climate Monitoring*.

Sánchez-Bayo, F., & Wyckhuys, K. A. G. (2019). Worldwide decline of the entomofauna: A review of its drivers. Biological Conservation, 232, 8-27. https://doi.org/10.1016/j.biocon.2019.01.020

Sahany, S., Mishra, S. K., Pathak, R., & Rajagopalan, B. (2018). Spatiotemporal Variability of Seasonality of Rainfall Over India. Geophysical Research Letters, 45(14), 7140–7147. https://doi.org/10.1029/2018GL077932.

Saitluanga, B. L., Lalchhandama, G., & Rinawma, P. (2021). Climate Change and Variability in the Northeastern Himalayan Region of India. *Landscape & Environment*, *15*(2), 53–64. https://doi.org/10.21120/LE/15/2/5

Saitluanga, B. L., Lalchhandama, G., & Rinawma, P. (2021). Analysis of Climate Variability and Agricultural Productivity in Mizoram, Northeast India. *Acta Geographica Debrecina Landscape & Environment Series, 15*(2), 53-64. https://doi.org/10.21120/LE/15/2/5

Sarma P.K. (2019) Climate Change and Sustainable Development: With Special Focus on North East India. Climate Change and Sustainable Development (Perspectives from North East India), pages 104-116

Seddon, A. W. R., Macias-Fauria, M., Long, P. R., Benz, D., & Willis, K. J. (2016). Sensitivity of global terrestrial ecosystems to climate variability. *Nature*, *531*(7593), 229–232. https://doi.org/10.1038/nature16986

Shan, W., Jin, X., Ren, J., Wang, Y., Xu, Z., Fan, Y., Gu, Z., Hong, C., Lin, J., & Zhou, Y. (2019). Ecological environment quality assessment based on remote sensing data for land consolidation. Journal of Cleaner Production, 239, 118126. https://doi.org/10.1016/j.jclepro.2019.118126

Shokirov, S., Abdurahmanov, I., Mamatkulov, Z., Abdurahmanov, Z., Zarifboev, D., Oymatov, R., Kovács, Z., Csabai, J., Shiping, Y., & Khakberdiev, O. (2025). Leveraging Vegetation Indices and Random Forest for Soil Nutrient Monitoring in Winter Wheat. *Journal of the Indian Society of Remote Sensing*, *53*(11), 3711–3721. https://doi.org/10.1007/s12524-025-02198-9

Sinha, S., & Modak, S. (2023). *Analyzing the Spatio-temporal Forest Aboveground Biomass Dynamics in Dimapur, Nagaland, India Using Integrated Geospatial Techniques. Research & Reviews: Journal of Space Science & Technology*, 12(1), 21–32.

Soubry, I., Doan, T., Chu, T., & Guo, X. (2021). A Systematic Review on the Integration of Remote Sensing and GIS to Forest and Grassland Ecosystem

Health Attributes, Indicators, and Measures. Remote Sensing, 13(16), Article 16. https://doi.org/10.3390/rs13163262

Sparrow, B. D., Edwards, W., Munroe, S. E. M., Wardle, G. M., Guerin, G. R., Bastin, J.-F., Morris, B., Christensen, R., Phinn, S., & Lowe, A. J. (2020). Effective ecosystem monitoring requires a multi-scaled approach. Biological Reviews, 95(6), 1706–1719. https://doi.org/10.1111/brv.12636

Su, Z., He, Y., Dong, X., & Wang, L. (2017). Drought Monitoring and Assessment Using Remote Sensing. In V. Lakshmi (Ed.), *Remote Sensing of Hydrological Extremes* (pp. 151–172). Springer International Publishing. https://doi.org/10.1007/978-3-319-43744-6_8

Sun, Y., Li, J., Yu, Y., & Zeng, W. (2022). Ecological Assessment Based on Remote Sensing Ecological Index: A Case Study of the "Three-Lake" Basin in Yuxi City, Yunnan Province, China. *Sustainability*, *14*(18), 11554. https://doi.org/10.3390/su141811554

Sun, Y., & Zhang, J. (2024). A Review of the Impact Factors Driving Vegetation Cover Change. *International Journal of Agriculture and Food Sciences Research*, *1*(3), 39–42. https://doi.org/10.62051/ijafsr.v1n3.06

Talukdar, N.C. & Thakuria, K. (2015). Microbial diversity of Indian Himalayan Regions: Jhum Agroecosystem of North East Himalaya. Envis Newslatter on Himalayan Ecology. Vol. 12 (4).

Tittensor, D. P., Walpole, M., Hill, S. L., Boyce, D. G., Britten, G. L., & Scharlemann, J. P. (2014). A global assessment of biodiversity loss. Science, 344(6187), 1289-1297. https://doi.org/10.1126/science.1246752

Tiwari, B. & Singh, Om Prakash. (2002). State Level Biodiversity Strategy and Action Plan of Nagaland 2. 10.13140/RG.2.2.14775.34726.

Tordoff, A. W., Baltzer, M. C., Fellowes, J. R., Pilgrim, J. D., & Langhammer, P. F. (2012). Key Biodiversity Areas in the Indo-Burma Hotspot: Process, Progress and Future Directions. *Journal of Threatened Taxa*, 2779–2787. https://doi.org/10.11609/JoTT.o3000.2779-87

TV, R., Kumar, U., & Dasgupta, A. (2016). Time-series MODIS NDVI based Vegetation Change Analysis with Land Surface Temperature and Rainfall in Western Ghats, India. https://wgbis.ces.iisc.ernet.in/biodiversity/pubs/ETR/ETR100/section3.html

United Nations. (2015). Transforming our world: The 2030 Agenda for Sustainable Development. Retrieved from https://sustainabledevelopment.un.org/post2015/transformingourworld/publication

United Nations Framework Convention on Climate Change. (2015). The Paris Agreement. Retrieved from https://unfccc.int/sites/default/files/resource/parisagreement_publication.pdf

United Nations Office for Disaster Risk Reduction. (2015). The human cost of weather-related disasters. Retrieved from https://www.undrr.org/publication/human-cost-weather-related-disasters-1995-2015

Verencar, A., et al. (2021). *Tectono-magmatic evolution of Tethyan oceanic fragments and related ophiolitic assemblages: implications for the Naga Hills geology.* [Geoscience research article]. ScienceDirect / Journal.

Verma, P., & Sahu, S. lal. (2021). Climate Change And Indian Plant Species: Impacts And Adaptation Strategies. *19*(8).

Vidican, R., Mălinaș, A., Ranta, O., Moldovan, C., Marian, O., Ghețe, A., Ghișe, C. R., Popovici, F., & Cătunescu, G. M. (2023). Using Remote Sensing Vegetation Indices for the Discrimination and Monitoring of Agricultural

Crops: A Critical Review. *Agronomy*, *13*(12), 3040. https://doi.org/10.3390/agronomy13123040

Vishvendra Raj Singh, B., Agarwal, V., & Sanwal, V. (2024). Climatic shifts and vegetation response in Western India: A four-decade retrospective through GIS and multi-variable analysis. Oxford Open Climate Change, 4(1), kgae020. https://doi.org/10.1093/oxfclm/kgae020

World Health Organization (2023).. A Framework for the Quantification and Economic Valuation of Health Outcomes Originating from Health and Non-Health Climate Change Mitigation and Adaptation Action (1st ed).

Xu. (2013). A remote sensing index for assessment of regional ecological changes. China Environmental Science, 33(5), 889–897. https://doi.org/10.0000/j.zghjkx.1000-6923.20133313253

Xu, H., Wang, Y., Guan, H., Shi, T., & Hu, X. (2019). Detecting Ecological Changes with a Remote Sensing Based Ecological Index (RSEI) Produced Time Series and Change Vector Analysis. Remote Sensing, 11(20), 2345. https://doi.org/10.3390/rs11202345

Yaden, Sangyu & Pongener, Temjensangla (2019). Participation of Local Community to Conserve and Promote Biodiversity in Climate Change and Sustainable Development (Perspectives from North East India) (Ed.) Purbayon Publication.

Yan, K., Gao, S., Yan, G., Ma, X., Chen, X., Zhu, P., Li, J., Gao, S., Gastellu-Etchegorry, J.-P., Myneni, R. B., & Wang, Q. (2025). A global systematic review of the remote sensing vegetation indices. *International Journal of Applied Earth Observation and Geoinformation*, *139*, 104560. https://doi.org/10.1016/j.jag.2025.104560

Yin, T., Zhai, Y., Zhang, Y., Yang, W., Dong, J., Liu, X., Fan, P., You, C., Yu, L., Gao, Q., Wang, H., Zheng, P., & Wang, R. (2023). Impacts of climate change and human activities on vegetation coverage variation in mountainous and

hilly areas in Central South of Shandong Province based on tree-ring. *Frontiers in Plant Science*, *14*, 1158221. https://doi.org/10.3389/fpls.2023.1158221

Yhoshü, K., & Krishnaiah, Y. V. (2020). Assessing landslide vulnerability in Kohima city, Nagaland: A geospatial approach. National Geographical Journal of India, 66(3), 274–287. https://doi.org/10.48008/ngji.1747

Yhoshü, K., & Kuho, T. A. (2025). Secchi Disk Estimation for Trophic State Index in Barail range Doyang Reservoir Nagaland. *International Journal of Lakes and Rivers*, *Volume 18, Number 1 (2025)*(ISSN 0973-4570), 33–42.

Zeng, J., Zhang, R., Qu, Y., Bento, V. A., Zhou, T., Yuehuan Lin, Wu, X., Qi, J., Shui, W., & Qianfeng Wang. (2022). Improving the drought monitoring capability of VHI at the global scale via ensemble indices for various vegetation types from 2001 to 2018. *Weather and Climate Extremes*, *35*, 100412. https://doi.org/10.1016/j.wace.2022.100412

Zeng, J., Zhou, T., Qu, Y. *et al.* (2023). An improved global vegetation health index dataset in detecting vegetation drought. Scientific Data 10, 338. https://doi.org/10.1038/s41597-023-02255-3

Zhu, Q., Guo, J.-X., Guo, X., Xu, Z., Ding, H., & Han, Y. (2019). Spatial variation of ecological environment quality and its influencing factors in Poyang Lake area, Jiangxi, China. Ying Yong Sheng Tai Xue Bao, The Journal of Applied Ecology, *30*(12), 4108–4116. https://doi.org/10.13287/j.1001-9332.201912.035

Zingkhai, Hormila. (2017). Forest and livelihood: the Naga traditional practice of prudent use of forest resources for a sustainable livelihood. People: International Journal of Social Sciences. 1. 912-926. 10.20319/pijss.2015.s21.912926.

APPENDIX

APPENDIX

Python 3.1 codes for downloading and converting gridded IMD data to .csv format.

```
import imdlib as imd

import numpy as np

import pandas as pd

"""

# install imdlib python library

# you should be connected to internet for downloading the data

#-9999 value is for no data in saved csv file

# This code will download the imd data first and then convert the data to csv file

if you have data already downloaded then create folder named rain/tmax/tmin inside any folder and copy yearly data files in the respective folder and rename yearly data file as year name i.e 1951.GRD 1952.GRD etc and comment the line imd.get_data(variable,start_yr) and run the code it will convert the binary .GRD data into csv file

"""

start_yr = 2000 # give starting year from which you want to download/convert data: 1901 ownwards for rainfall, 1951 for tmax and tmin

end_yr = 2023 # give ending year upto which you want to download/convert data

variable = 'rain' # give variable name (rain for rainfall, tmax or tmin for min or max temperature)

file_format = 'yearwise' # other option (None), which will assume deafult imd naming convention
```

```
imd.get_data(variable, start_yr, end_yr, fn_format='yearwise', file_dir='D:/IMD_Data/') # download IMD data: just change path as per your requirement

file_dir = 'D:/IMD_Data/' # this path should be same as mentioned in previous line

data = imd.open_data(variable, start_yr, end_yr,'yearwise', file_dir) # this will open the data downloaded and saved in the location mentioned in previous line

if variable == 'rain':
    grid_size = 0.25 # grid spacing in deg
    y_count = 129 # no of grids in y direction
    x_count = 135 # no of grids in x direction
    x = 66.5 # starting longitude taken from control file (.ctl)
    y = 6.5 # starting latitude taken from control file (.ctl)
elif variable == 'tmax' or variable == 'tmin':
    grid_size = 1 # grid spacing in deg
    y_count = 31 # no of grids in y direction
    x_count = 31 # no of grids in x direction
    x = 67.5 # starting longitude taken from control file (.ctl)
    y = 7.5 # starting latitude taken from control file (.ctl)
#print(grid_size,x_count, y_count, x, y)

data

data.shape

np_array = data.data

#print(np_array[0,0,0])

#xr_objecct = data.get_xarray()
```

```
#type(xr_objecct)

#xr_objecct.mean('time').plot()

years_no = (end_yr - start_yr) + 1

#print(years_no)

day = 0

for yr in range(0,years_no):

    f= open ("D:/IMD_Data/csv/"+str(start_yr+yr)+"_"+str(variable) + ".csv",'w') # just change the path where you want to save csv file

    if ((start_yr+yr) % 4 == 0) and ((start_yr+yr) % 100 != 0):  # check for leap year

        days = 366

        count = yr + days

    elif ((start_yr+yr) % 4 == 0) and ((start_yr+yr) % 100 == 0) and ((start_yr+yr) % 400 == 0):

        days = 366

        count = yr + days

    else:

        days = 365

        count = yr + days

    day = day + days

    f.write("X,Y,")

    for d in range(0, days):

        f.write(str(d+1))

        f.write(",")

    f.write("\n")
```

```
    #print(np_array[364,0,0])
    for j in range(0, y_count):
        for i in range(0, x_count):
            f.write(str((i * grid_size) + x))
            f.write(",")
            f.write(str((j * grid_size) + y))
            f.write(",")
            time = 0
            for k in range(day-days, day):
                val = np_array[k,i,j]
                if val == 99.9000015258789 or val == -999:
                    f.write(str(-9999))
                    f.write(",")
                else:
                    f.write(str(val))
                    f.write(",")
            f.write("\n")
    print("File for " + str(start_yr + yr) + "_" + str(variable) + " is saved")
print("CSV conversion successful !")
```

PHOTOGRAPHS

Photo Plate 1 Paddy Field in Shilloi Lake, Meluri District. Photos taken for validation of LULC.

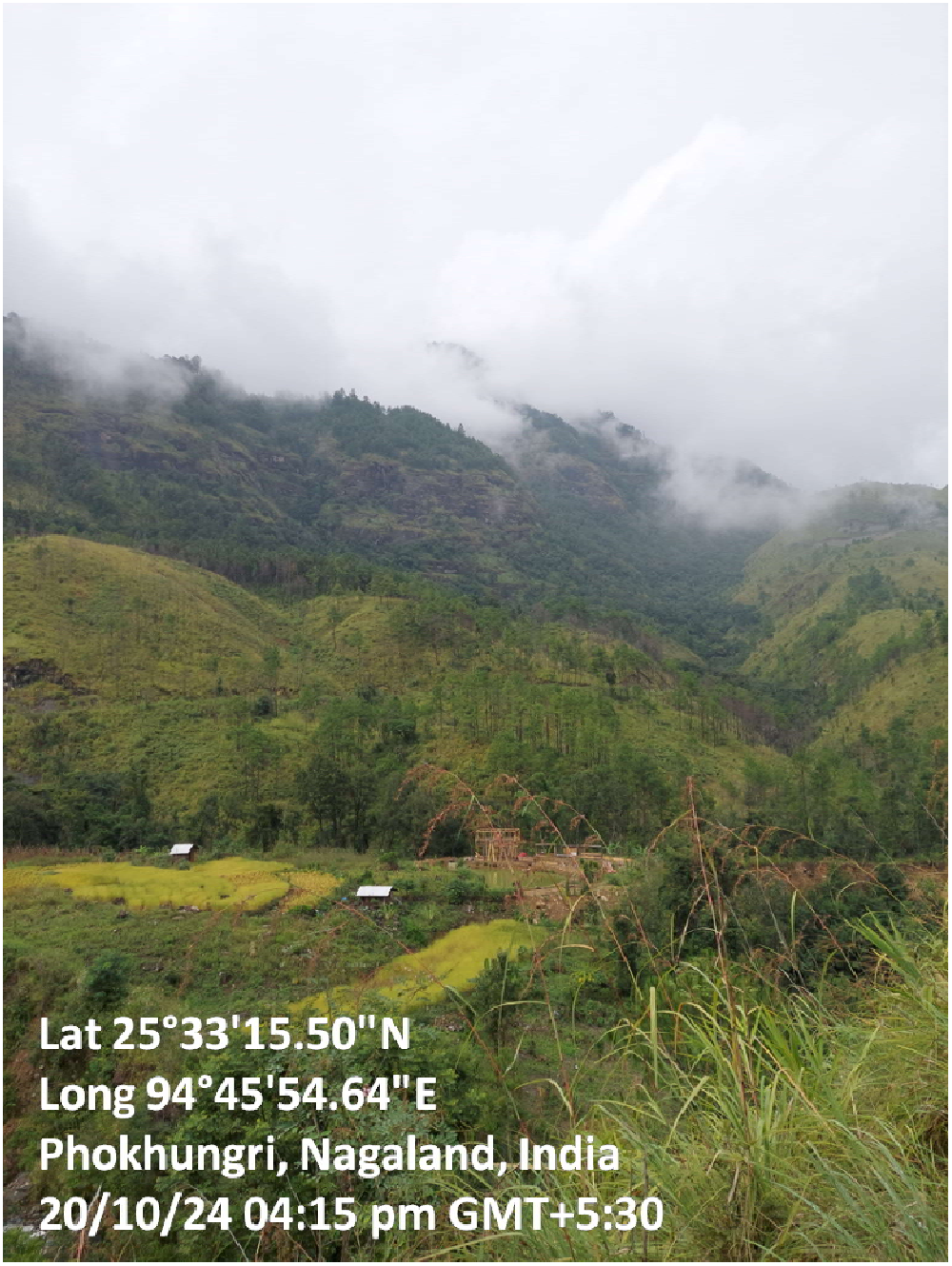

Photo Plate 2 Pine Forest, Agricultural Fields and Rock Outcrops in Phokhungri, Meluri District. Photos taken for validation of LULC.

Photo Plate 3 Moderately Dense Forest in Tuensang District. Photos taken for validation of LULC.

Photo Plate 4 Fishery Pond in Kohima District. Photos taken for validation of LULC.

Photo Plate 5 Dima Raja Pond (waterbody) in Purana Bazaar, Dimapur District. Photos taken for validation of LULC.

Photo Plate 6 Moderately Dense Forest in Kohima District. Photos taken for validation of LULC.

Photo Plate 7 Open Forest in Kohima District. Photos taken for validation of LULC.

Photo Plate 8 Moderately Dense Forest in Kohima District. Photos taken for validation of LULC.

Photo Plate 9 Field photos taken during collection of field data for water quality and vegetation quality.